Aus dem Institut für Virologie
des Fachbereichs Veterinärmedizin
der Freien Universität Berlin

Engineering and characterization of avian coronavirus mutants expressing reporter proteins from the replicase gene

Inaugural-Dissertation
zur Erlangung des Grades eines
PhD of Biomedical Sciences
an der Freien Universität Berlin

vorgelegt von
Na Xing
aus Shanxi, Volksrepublik China

Berlin 2022
Journal-Nr.: 4376

Gedruckt mit Genehmigung
des Fachbereichs Veterinärmedizin
der Freien Universität Berlin

Dekan: Univ.-Prof. Dr. Uwe Rösler
Erster Gutachter: Univ.-Prof. Dr. Klaus Osterrieder
Zweiter Gutachter: PD Dr. Michael Veit
Dritter Gutachter: PD Dr. Sandra Blome

Deskriptoren (nach CAB-Thesaurus): avian coronavirus, genetic engineering, gene expression, genetic regulation, viral replication, reporter proteins, mutants, genetic resources, cell culture, next generation sequencing.

Tag der Promotion: 21.11.2022

Table of contents

List of figures

List of tables

Abbreviation

aa	Animo acids
BSA	Bovine serum albumin
CEF	Chicken embryo fibroblast
CPE	Cytopathic effect
DMEM	Dulbecco’s Modified Eagle Medium
DMSO	Dimethyl sulfoxide
DNA	Deoxyribonucleic acid
dNTP	Deoxynucleotide triphosphate
dpi	Days post infection
E. coli	Escherichia coli
EGFP	Enhanced green fluorescent protein
FBS	Fetal bovine serum
h	Hour
HRP	Horseradish peroxidase
IBV	Infectious bronchitis virus
kb	Kilobases
L	Liter
MOI	Multiplicity of infection
mRNA	Messenger RNA
nt	Nucleotide
P/S	Penicillin/streptomycin
PBS	Phosphate saline buffer
PCR	Polymerase chain reaction
PFU	Plaque forming unit
RNA	Ribonucleic acid
SDS	Sodium dodecyl sulfate
SPF	Specific-pathogen-free
UTR	Untranslated regions
WB	Western blot
WT	Wild type

1 Introduction

1.1 History of infectious bronchitis virus (IBV)

IBV is the causative agent of infectious bronchitis (IB), a highly contagious respiratory disease in chickens that poses a serious threat to the poultry industry's development and causes enormous economic losses worldwide. IBV is the first member of the *Coronavirinae* family to be discovered. Schalk and Hawn first reported IBV in the 1930s in the United States, which causes respiratory infection primarily in young chickens with rapid spread and high mortality rates (Schalk 1931). It was discovered five years later that this infectious disease was caused by a novel virus called Infectious Bronchitis Virus (Beach and Schalm 1936). After that, cases of infection with various IBV serotypes and genotypes have been reported worldwide (Jackwood et al. 1997; Wit et al. 2011).

1.2 Taxonomy of IBV

1.2.1 Classification of the order *Nidovirales*

Because a 3' co-terminal nested set of subgenomic mRNAs is created during viral infection, the name of the order *Nidovirales* is derived from the Latin word "*nidus,*" which means "nest." The *Coronaviridae*, *Roniviridae, Mesoniviridae,* and *Arteriviridae* families make up the order *Nidovirales.* The two subfamilies *Coronavirinae* and *Torovirinae* have been added to the classification of the *Coronaviridae.* There are four genera in the *Coronaviridae* subfamily, including alpha-, beta-, and *gammacoronaviruses* with crown-like or coronal spike proteins on the virus surface (L et al. 1968; Carstens and Ball 2009). This classification is determined by serological and genetic characteristics.

1.2.2 Subfamily *Coronavirinae*

There are numerous viruses in the subfamily *Coronavirinae* that can infect both humans and animals. Coronaviruses are viruses with an envelope and a single-stranded positive-sense RNA. Their main distinguishing feature is their large genomes, which range in size from 26 to 32 kb. Furthermore, nucleoproteins surrounded the genomic RNA, which had a cap and a poly(A) tail at the 5' and 3' ends. (Senanayake and Brian 1999).

IBV is a member of the order *Nidovirales,* family *Coronaviridae,* subfamily *Coronavirinae*, and genus *Gammacoronavirus,* with a capped and polyadenylated genomic RNA of approximately 27.6kb in size (Boursnell et al. 1987; Cavanagh 2003; González et al. 2003).

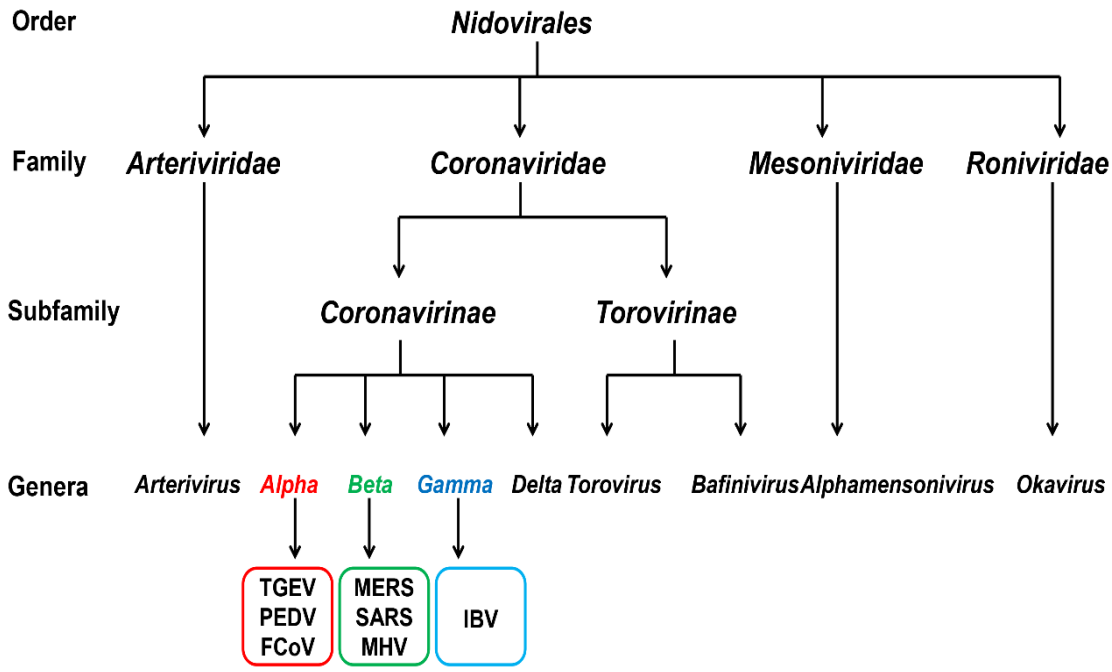

Figure 1: Classification of the order *Nidovirales.*

The order *Nidovirales* is composed of four families, including *Arteriviridae, Coronaviridae, Mesoniviridae,* and *Roniviridae*. The *Coronaviridae* are classified into two subfamilies, the *Coronavirinae* and the *Torovirinae.* In the Coronavirinae, there are four genera, including *Alpha-*, *Beta-*, *Gamma-*, and *Deltacoronaviruses.* The IBV belongs to *Gammacoronavirus,* subfamily *Coronavirinae,* family *Coronaviridae,* and order *Nidovirales.*

1.3 Viral morphology and genome organization

The IBV particle has a diameter of 120 nm and is spherical to pleomorphic in shape under the electron microscope. IBV virions have club-shaped projections or spikes (20 nm in length) emanating from their surface, which is one of their distinguishing features.

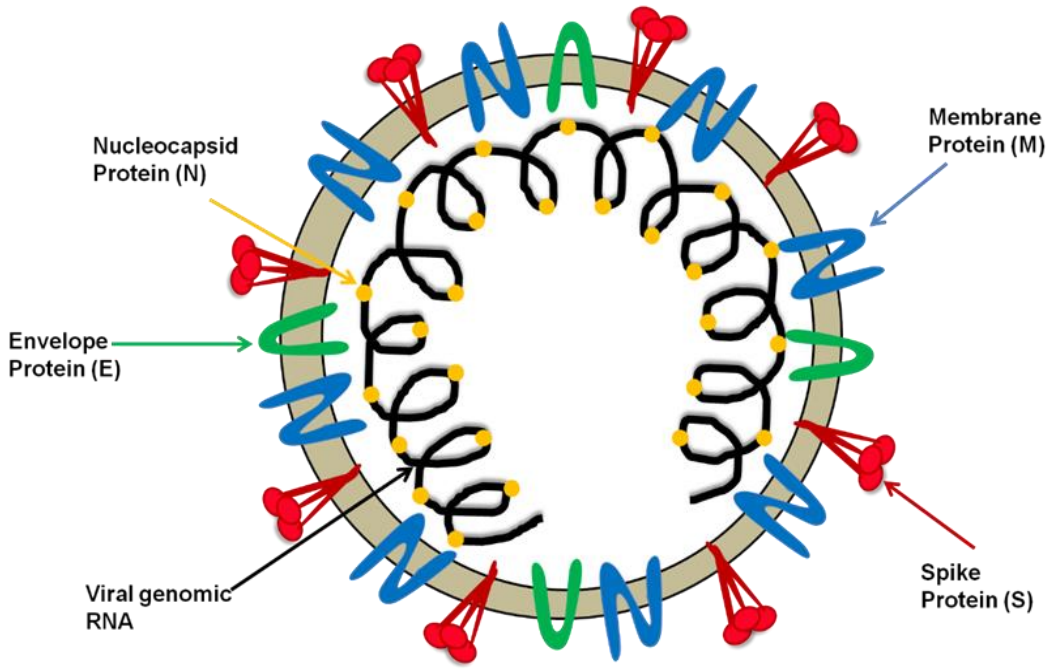

Figure 2: Schematic structure of an IBV virion.

The nucleocapsid proteins are bound to IBV genomic RNA, forming the core of the virus particle. The helical nucleocapsid is surrounded by a lipid membrane, in which three different structural proteins are embedded: the spike protein (S), the envelope protein (E), and the membrane protein (M).

IBV has a 27.6 kb genome with a 5' m7GpppN-cap and a 3' polyA tail. There are untranslated regions (UTRs) at the 5' and 3' ends known as the 5' UTR and 3' UTR (Senanayake and Brian 1999; Ziebuhr et al. 2000; Mo et al. 2012). ORF1a and ORF1b make up the first two-thirds of the genome, encoding two large and important polyproteins (pp1a and pp1ab) via a ribosomal frameshift mechanism (Boursnell et al. 1987; Brierley et al. 1987). The remaining region, located close to the 3'UTR, encodes structural proteins in the following order: spike (S1 and S2), envelope (E), membrane (M), and nucleocapsid (N). Aside from the polymerase and structural protein genes, two accessory genes, ORF3 and ORF5, have been discovered, encoding proteins 3a/3b and 5a/5b, respectively (Lai and Cavanagh 1997; Pasternak et al. 2006). A 3' co-terminal nested set of subgenomic mRNAs with an identical 5' leader sequence is also produced during IBV replication. However, only the 5' proximal ORF of each subgenomic RNA is translated (Sawicki et al. 2007).

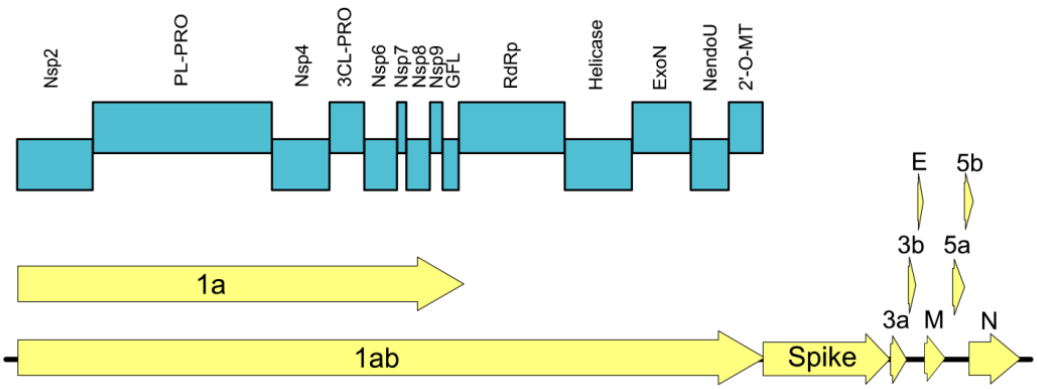

Figure 3: The genome organization of IBV.

Two-thirds of the IBV genome encodes pp1a and pp1ab through the -1 frameshift mechanism. The two large polyproteins are post-translationally cleaved by papain-like protease and 3CL-protease into fourteen non-structural proteins, such as RNA-dependent RNA polymerase (RdRp), helicase, exonuclease, and RNA methyltransferase. The structural proteins, including spike protein, membrane protein, envelope protein, and nucleocapsid protein, are located proximal to the 3' untranslated region (UTR). The accessory proteins 3a, 3b, 5a, and 5b are interspersed among IBV structural protein genes.

1.4 Viral proteins

1.4.1 Replicase proteins

ORF1a and ORF1b comprise nearly two-thirds of the IBV genome. The two ORFs are translated into two large polyproteins, pp1a and pp1ab, which are then post-translationally cleaved by proteinases into fourteen non-structural proteins (nsp2-nsp16), which include RNA-dependent RNA polymerase (RdRp), 3CL-protease, papain-like proteinase, helicase, exonuclease, and RNA methyltransferase (Ziebuhr et al. 2000; Hemert et al. 2008). Although the function of some nsps is unknown, they play an important role in viral replication.

It is well known that nsp1 is only found in *alpha-* and *beta-coronaviruses*. Nsp1 has been related to virulence in some studies (Jimenez-Guardeño et al. 2014; Lokugamage et al. 2015; Zhang et al. 2015; Shen et al. 2017; Shen et al. 2019). The nsp1 protein could inhibit host cell protein expression, ensuring virus replication and RNA synthesis. Furthermore, it is hypothesized that nsp1 inhibits the production of IFNs, interfering with the host immune system and allowing the virus to evade the host immune response (Zhang et al. 2016).

Coronaviruses like SARS-CoV and MHV can be recovered even when nsp2 is deleted from the viral genome, indicating that nsp2 proteins are not required for virus replication in cell culture (Graham et al. 2005). Amino acids 1-120 of nsp2 have strong potential for activating NF-κB while controlling inflammation (Wang et al. 2018).

It has been demonstrated that nsp3, with a molecular mass of approximately 200 kDa, is the largest replicase protein and involved in the formation of the replication/transcription complex (RTC). Nsp3 is made up of multi-functional domains, including papain-like proteases, ubiquitin-like domains, and ADP-ribose-phosphatase (ADRP) domains (Lei et al. 2018). The nsp3 gene is thought to be connected to virulence. Recombinant viruses, such as MHV and SARS-CoV, have a reduced nsp3 function, resulting in virus attenuation (Fehr et al. 2014; Fehr et al. 2016). Additionally, it has been reported that nsp3 inhibits the production of IFN-α, allowing it to evade the host immune response (Mielech et al. 2015; Wang et al. 2019).

Nsp4 is a membrane protein with four transmembrane spanning domains (TMs). It is important in cellular membrane rearrangement because it allows RTCs to anchor on double-membrane vesicles (DVMs) (Gorbalenya et al. 1989). Recombinant viruses with TM domains 1-3 deletion have lower replication ability in cell culture, indicating that nsp4 is required during virus replication (Sparks et al. 2007; Sakai et al. 2017).

Nsp5 is also known as $3CL^{pro}$. It proteolytically cleaves pp1a and pp1ab into several non-structural proteins in collaboration with PL^{pro}. It could be a target for antiviral drug development (Tomar et al. 2015; Jo et al. 2019). Nsp5 is thought to be involved in virus replication. It has been verified in many coronaviruses that nsp5 inhibits IFN production by cleaving NF-κB essential modulator (NEMO) and STAT2 (Wang et al. 2015; Zhu et al. 2017; Chen et al. 2019).

Nsp6 inhibits autophagosome expansion during autophagy, the cellular response to starvation (Cottam et al. 2014). Researchers used the MHV reverse genetics system to create mutants with deletions in the coding regions of nsp7-nsp10 and tested their replication properties. The results showed that the virus could be recovered from the infectious clones by deleting any regions encoding nsp7 to nsp10 (Deming et al. 2006). During PEDV infection, two non-structural proteins, nsp7 and nsp8, were related to the suppression of interferon production (Zhang et al. 2016).

Nsp10 is composed of 148 amino acids that form two zinc finger domains. Nsp10 activates respective enzyme activities by interacting with 3'-5' exoribonuclease and 2'-O-methyltransferase, making it a key regulator of virus replication function (Bouvet et al. 2014). Furthermore, researchers discovered that a nsp10 mutant with a disruption in the interaction between nsp10 and nsp14 results in decreased replication fidelity (Smith et al. 2015).

Nsp14 of coronaviruses has 3’ to 5’ exoribonuclease (ExoN) activity, which ensures virus replication fidelity through its proofreading function. ExoN activity is abolished by the mutations D89A and E91A in MHV nsp14. The recombinant viruses remained stable after 250 serial passages without reversing the mutation sites. Multiple amino acid changes were discovered in the region of RdRp and nsp14, indicating that other replicase proteins could compensate for the ExoN function during virus replication (Graepel et al. 2017). In addition, ExoN is thought to be critical for virulence. Coronaviruses without ExoN activity were attenuated in animals

relative to the WT virus, but they can still trigger a protective immune response against WT virus infection (Graham et al. 2012). Furthermore, ExoN plays an important role in immune response regulation. For example, it inhibits the expression of IFN-β, tumor necrosis factor (TNF), and interferon-stimulated genes (Becares et al. 2015; Case et al. 2018). Nsp15 is a virulence factor known as nidoviral uridylate-specific endoribonuclease (NendoU). Inactivation of NendoU activity of nsp15 could lead to attenuation in mice with only mild disease (Deng et al. 2017; Deng et al. 2019). The coronavirus-encoded Nsp16 is associated with 2'-O-methyltransferase (MTase), which becomes a potential target for virus attenuation (Yong et al. 2019). It has been reported that inhibiting 2'-O-methyltransferase activity increases the expression of type I IFN in infected cells, indicating it is essential for negatively regulating the immune response (Hou et al. 2019; Yong et al. 2019).

1.4.2 Spike (S) glycoprotein

The S protein of IBV, which is found on the viral envelope's surface, is a highly glycosylated membrane glycoprotein with a club-like projection. The synthesized S glycoprotein is a single polypeptide chain with a molecular weight of 180 kDa (Delmas and Laude 1990). The S protein is found to be a determinant of cell tropism and is cleaved by a furin-like protease into two non-covalently associated subunits, S1 and S2. The S1 subunit (535 amino acids, 90 kDa) has two functional domains, the signal sequence (SS) and receptor binding domain (RBD), which are involved in inducing neutralizing antibodies, recognition, and binding to receptors on host cells, while the S2 subunit (627 amino acids, 84 kDa) is responsible for fusion of IBV with susceptible cells (Koch et al. 1990; Koch and Kant 1990; Schultze et al. 1992; Ignjatovic and Galli 1994; Johnson et al. 2003). The S2 subunit contains putative fusion peptides, two heptad repeats (HR1 and HR2) that facilitate protein oligomerization and entry into host cells, a transmembrane region (TR) that is involved in anchoring S protein to the viral membrane, and a cytoplasmic tail (Luo and Weiss 1998).

1.4.3 Envelope (Small membrane) protein (E)

The IBV E protein, which is translated from sgmRNA3, is a small integral membrane protein that is required for virus assembly (Maeda et al. 1999). It has been demonstrated that only a small portion of E protein is incorporated into virus particles (Smith et al. 1990; Liu and Inglis 1991). The E protein domains of IBV are composed of a transmembrane region with a hydrophobic domain at the N-terminus and a cytoplasmic tail domain at the C-terminus. The latter is essential in mediating E protein targeting the Golgi complex (Corse and Machamer 2003). During virus replication, the interaction of the E protein with the M protein enhances the formation and budding of virus particles (Fischer et al. 1998; Lim and Liu 2001).

1.4.4 Membrane protein (M)

The M protein, which is embedded in the lipid bilayer of virions, is the most abundant structural protein in IBV. Inside virus particles, the M protein is glycosylated and consists of a short N-

terminal domain, triple-spanning transmembrane domains, and a large C-terminal domain (Godet et al. 1992). The first membrane-spanning domain contains Golgi targeting information, which is necessary for retaining a plasma membrane protein in the Golgi complex (Machamer et al. 1990; Tseng et al. 2010). It has been suggested that the M protein plays a central role in virus assembly and morphogenesis through its interaction with other structural proteins, such as S, E, and N (Vennema et al. 1996; Hogue and Machamer 2007).

1.4.5 Nucleocapsid protein (N)

The N protein, which is translated from sgmRNA6, is a phosphoprotein with 409 amino acids. This protein serves multiple functions. It binds to IBV genomic RNA and forms a helical ribonucleoprotein (RNP). Apart from interacting with the viral genome, it also interacts with the M protein during virion assembly (Hurst et al. 2005). In addition, it has been reported that the N protein may have some enhanced effect on subgenomic RNA transcription and virus replication.

1.4.6 Accessory proteins

In addition to replicase and structural proteins, IBV encodes four non-structural proteins (3a, 3b, 5a, and 5b), which are encoded from ORF3 and ORF5 (Casais et al. 2005; Hodgson et al. 2005). These non-structural genes are interspersed among the structural genes. Gene 3 contains two ORFs (ORF3a and ORF3b), which, respectively, encode the 3a and 3b proteins. It is also known that gene 3 is functionally tricistronic, with highly conserved regions in its nucleotide sequence (Mo et al. 2012). Gene 5 is bicistronic and encodes two accessory proteins, 5a and 5b.

The function of these accessory proteins is unclear and needs further investigation. It has been reported that when either gene 3 or gene 5 are deleted, IBV can still replicate on cells but results in attenuated virulence *in vivo*, implying that these proteins may be the determinant of viral pathogenicity (Casais et al. 2005).

1.5 Transmission, replication, and pathogenesis

IBV, a highly infectious respiratory virus, spreads horizontally throughout the flock via aerosol droplets or ingestion. The main source of viral infection is contact with infected chickens' feces and nasal excretions. IBV transmission rates differ based on virulence, immunity, and chicken age. Susceptible chickens can develop mild to severe clinical signs within 36-48 hours post-infection. The virus can also be transmitted from one flock to another via contaminated drinking water, food, and feces. IBV can persist in feces for a long time, potentially serving as a source of reinfection (Cook 1968; Alexander et al. 1978). Indirect transmission occurs via contaminated vehicles, workers, and equipment (Cumming 1970).

The attachment of virus particles to the receptor on host cells, mediated by the S1 subunit, is the first step in the IBV replication cycle (Koch and Kant 1990; Luo and Weiss 1998). This binding process induces conformational changes in spike protein, leading to the fusion of the

virion with the cell membrane via the S2 subunit (Zelus et al. 2003). Upon virions entering the host cell through the endocytic mechanism, viral genomic RNA is released from the nucleocapsid into the cytosol and functions as mRNA to translate replicase proteins. Two major polyproteins (pp1a and pp1ab) are generated through ribosomal frameshift and then cleaved by encoded proteases (Gorbalenya 2001). Other than genomic RNA, subgenomic RNAs are synthesized and serve as mRNA to produce viral structural and non-structural proteins. Assembly of these proteins occurs in the ER-Golgi intermediate compartment (ERGIC) (Klumperman et al. 1994). The newly synthesized genomic RNA, together with the N protein, forms the nucleocapsid and is incorporated into virions. Then the complete viral particles bud through the membrane of the Golgi apparatus and are released from the host cell by exocytic mechanisms.

In a natural IBV infection, the virus replicates initially in the upper respiratory tracts, though some IBV strains have tissue tropism. The IBV then spreads to other organs through viremia and continues to replicate in epithelial cells of the kidney, oviduct, testis, and gastrointestinal tract (Albassam et al. 1986; Ignjatovic et al. 2002; Raj and Jones 2007; Hewson et al. 2014).

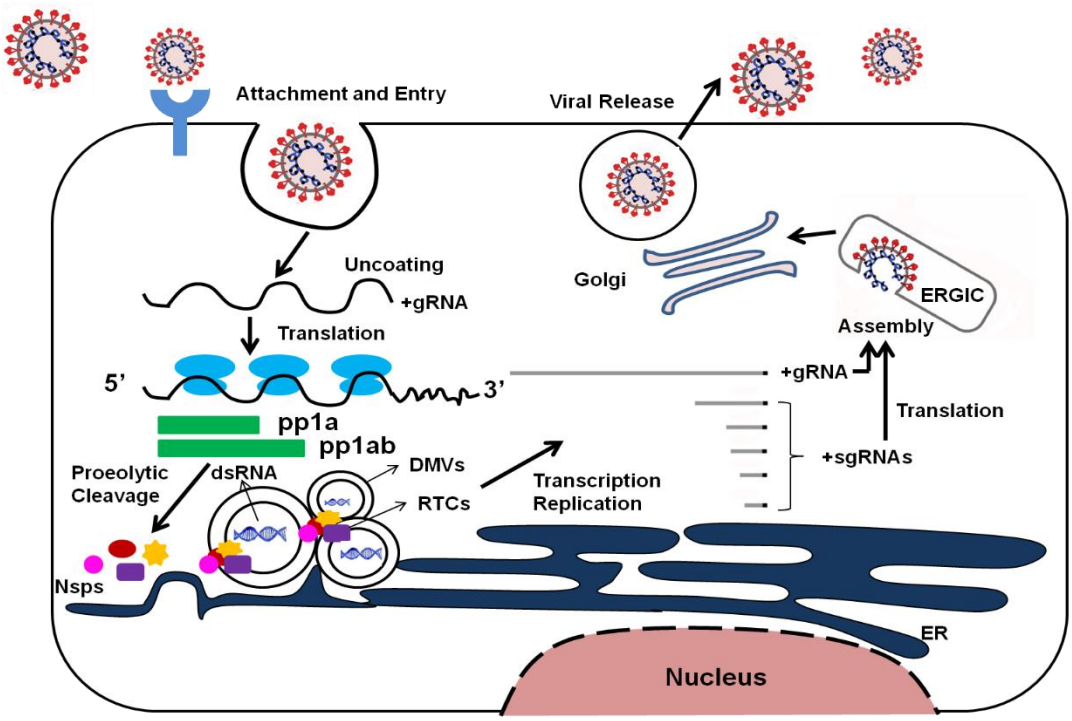

Figure 4: The replication cycle of IBV.

The IBV particles bind to the receptor and enter the host cells through membrane fusion mediated by the S protein. After release and uncoating, the IBV genomic RNA acts as an mRNA for the translation of two large polyproteins, pp1a and pp1ab, which are post-translationally processed into individual nonstructural proteins (nsps) and form the replication/transcription complex (RTC). The replication and

transcription occur in virus-induced double-membrane vesicles (DMVs), which ultimately integrate to form elaborate webs of convoluted membranes (CMs). The structural and nonstructural proteins are expressed from sgRNAs, followed by an assembly at ERGIC. The N protein is bound to the newly synthesized genomic RNA to form the nucleocapsid and is incorporated into virions. Finally, the mature virus particles are released from host cells by exocytosis.

According to the replication sites that IBV favors, clinical outcomes are divided into four types: respiratory infection, nephritis, reproductive system infection, and alimentary tract infection.

The respiratory tract is the primary replication site of IBV, especially the trachea (Ignjatovic et al. 2002). The virus attacks ciliated and mucus-secreting cells, causing mild to severe respiratory signs, such as nasal discharge, tracheal rales, coughing, and gasping within 36-48 hours, combined with other signs such as decreased food intake, reduction in body weight, and depression (Patterson and Bingham 1976). In this case, infected chickens become more vulnerable to secondary infection with pathogenic bacteria (Hopkins and Yoder 1982).

Some IBV strains, referred to as "nephropathogenic," could cause nephritis, mainly in broiler-type chickens. In this case, swollen and pale kidneys filled with urate crystals could be observed in the affected chickens. The high titer of IBV is not well correlated to the severity of kidney lesions. Furthermore, the nephropathogenic strains appear to cause only mild respiratory signs and damage, but they are always accompanied by a high mortality rate, especially in young chickens (Lambrechts et al. 1993; Seo and Collisson 1997; Cook et al. 2001; Li and Yang 2001).

During an IBV outbreak, IBV may replicate in the oviduct epithelium (Sevoian and Levine 1957). Infected chickens are clinically characterized by reduced egg production and poor quality. In contrast to normal eggs, those produced by infected layers have rough, soft shells, watery yolks, and irregular shapes (Muneer et al. 1987). In testicular tissues of male chickens, IBV can be detected, but it does not cause any lesions there.

IBV persists in the alimentary tracts of affected young chickens, but it rarely shows clinical signs.

1.6 IBV serotypes and strain variation

Currently, there are plenty of IBV serotypes that have been recognized and are circulating worldwide (Darbyshire et al. 1979; Ignjatovic and McWaters 1991; Cavanagh 2001; Farsang et al. 2002; Liu and Kong 2004; Cavanagh et al. 2005; Jr et al. 2005; Cook et al. 2010). The serotype classification of IBV is mainly based on the variation in the S1 subunit. It has been known that the S1 region is highly variable, and its differences at the amino acid sequence level can reach 20%-50%, which leads to the emergence of multiple variants and poor vaccine protection. The genetic diversity of IBV is due in part to the replication mechanism utilized by

most RNA viruses. During viral replication, the RNA-dependent RNA polymerase (RdRp) with poor proofreading ability is prone to making mistakes, which could introduce mutations into the IBV genome. When they occur in the key position of the IBV genomic RNA, they can result in the emergence of a new strain. In addition, the unique template switching mechanism also contributes to variation in the IBV genome. Other than the high mutation rate, high frequency of genetic recombination among different IBV strains is not uncommon, which creates a new chimeric strain (Kusters et al. 1990; Cavanagh et al. 1992; Wang et al. 1993; Jia et al. 1995; KOTTIER et al. 1995; Wang et al. 1997; Lee and Jackwood 2000; Estevez et al. 2003; Chen et al. 2010; Jackwood et al. 2010; Kuo et al. 2010; Mardani et al. 2010; Thor et al. 2011).

The isolated pathogenic strain M41 grows in embryonated eggs and chicken embryo kidney cells (CEKC). The attenuated strain Beaudette, on the other hand, was created by serial passage in embryonated eggs from its parental strain M41. It has been adapted to replicate not only in CEKC but also in many animal cells, such as Vero cells, DF-1 cells, and BHK-21 cells. Comparing the amino acid sequences of both strains, they share approximately 95% similarity. It is worth mentioning that the strain M41 can cause clinical respiratory signs in chickens and can grow in multiple tissues, whereas the strain Beaudette does not cause any symptoms.

1.7 Vaccination against infectious bronchitis disease

Due to the widespread prevalence of IBV, vaccination, and the well-coordinated balancing of biosafety, hygiene measures should be implemented to reduce the economic losses and impact on the poultry industry. Currently, two types of IBV vaccines (live, attenuated and inactive vaccines) are commonly used for IBV immunization in flocks.

1.7.1 Live attenuated Vaccines

Live attenuated vaccines are usually used in broilers and booster vaccination for breeders. This type of vaccine was produced by serial passage in embryonated eggs and is administered to day-old broilers through coarse spray, drinking water, and nasal or eye drops (Cavanagh 2003). Live attenuated vaccines used in the field may differ among countries or areas. It is known that commercially available IBV live vaccines are usually used in combination with vaccines against other viruses, such as infectious bursal disease virus (IBDV) and Marek's disease virus (MDV) (Vagnozzi et al. 2010). Although live vaccines are less expensive and could be applied by mass vaccination against more than one poultry disease, they still have some limitations. Some studies have shown that the application of attenuated vaccines is likely to cause virulence reversion, leading to pathological effects and even severe outbreaks of IBV (Tarpey et al. 2006). Moreover, recombination happens frequently between vaccine strains and pathogenic field strains, resulting in the emergence of a new serotype (McKinley et al. 2008; Lee et al. 2010). It should also be noted that the vaccine's efficacy could be interfered with by maternal antibodies.

The widely used live vaccines include H120, Mb5, IB 4/91, and Primo QX. The attenuated vaccine H120 originated from a Massachusetts-like IBV strain after 120 passages. Since the resulting viruses have adapted to grow on the embryo, they lose the ability to cause significant clinical signs in chicks. However, they can still induce an immune response to protect young chicks against IBV infection. The vaccine Ma5 is also based on the Massachusetts strain and can be used in the initial vaccination plan to help chicks gain broad protection against IBV. The vaccine IB 4/91 is specific for protection against the 4/91 serotype. Chicks immunized with vaccine IB 4/91 in combination with Ma5 and the IB multi-vaccine could gain broad protection. The newly developed Primo QX vaccine has been applied in broilers, layers, and even breeders, which prevents them from newly prevalent QX strain infection. Because vaccines against one serotype or strain sometimes cannot provide adequate cross-protection, in practice, two or more serotypes or strains are combined to broaden protection. However, the vaccine contains different serotypes or stains that must be used with caution because new types may emerge and become prevalent in some areas.

1.7.2 Inactivated or killed vaccines

In practice, inactivated or killed vaccines are applied to breeders and layers between the ages 13 and 18 weeks. Since inactivated vaccines lose the ability to replicate, virulence reversion does not occur, and tissue damage has not been observed in this case. Unlike live vaccines, killed vaccines can produce antibodies, but T-cell mediated immune responses are not involved (Collisson et al. 2000; Ladman et al. 2002). Exploiting the potential of killed vaccines requires priming with live vaccines properly, optimal combination with a large dose of adjuvant, and frequent booster vaccinations, which increases the cost of vaccine development and limits its large-scale application.

1.7.3 Novel IBV vaccines

1.7.3.1 Viral vector recombinant vaccine

Over the past years, extensive research has been conducted to develop a novel and effective IBV recombinant vaccine based on a viral vector. These vaccines are developed by inserting the genes of interest rather than the complete genome into a viral vector, which could induce an appropriate immune response and protect chickens from IBV infection. There have been attempts to create a recombinant system in which the S1 or S2 portion of IBV has been incorporated into a viral backbone (Johnson et al. 2003; Toro et al. 2014). These vaccine candidates have been shown to protect chickens from homologous and heterologous challenges at varying levels. However, this type of vaccine still has some limitations, which prevent it from being approved and eventually reaching the market. These vaccines should be administered to chicks individually in order to induce an adequate immune response, which becomes the main reason why vaccines do not meet the application requirement.

1.7.3.2 Subunit and peptide-based vaccine

The subunit vaccine is created using a portion of the viral protein required to stimulate the immune response. The peptide-based vaccine is defined as a vaccine that contains only minimal antigenic epitopes (Jackwood 1999; YANG et al. 2009). The synthetic peptide-based vaccine has several advantages over the full-length IBV genome, including the fact that it is noninfectious and has a low risk of side effects. However, it should be used in combination with an adjuvant to trigger an appropriate immune response. Currently, the commercially available and safe adjuvant is mainly based on aluminum, which can potentially induce humoral immune responses but appears to stimulate cellular immunity with low efficiency.

1.7.3.3 Plasmid DNA vaccine

This technology is based on the construction of immunogenic protein(s) of interest to a DNA vector rather than a live viral vector. Until now, there are no licensed DNA vaccines commercially available in the poultry industry, but they have shown potential to control IB. The plasmid DNA vaccine has many benefits, such as its potency in stimulating both antibody and T-cells immune responses. In addition, the DNA vaccine is relatively easier to manufacture within a short period on a large scale, which makes it more attractive to be applied in handling emerging IBV threats. Another advantage of this vaccine is its stability and safety. In order to enhance the immune response generated by these vaccines, some genes encoding immune factors, such as cytokines, and granulocyte-macrophage stimulating factors (GM-CSF), have been added to the plasmid system (Tang et al. 2008; Tan et al. 2009). However, to achieve high efficacy, this vaccine must be administered by intramuscular injection, which limits its application in a commercial setting.

1.7.3.4 Reverse genetics vaccine

This is a new and promising technology based on a reverse genetics system, which can be employed to manipulate target genes of a virus, including point mutation, gene insertion, or deletion (Britton et al. 2005; Casais et al. 2005; Cavanagh et al. 2007; Britton et al. 2012).

With this technology, the complete genome of IBV has been cloned and modified, followed by transfection into a suitable cell line where the IBV genome replicates, and viral proteins are synthesized and assembled to finally produce virus particles with full function. The recombinant IBV vaccine based on reverse genetics is promising, making it a major focus of research related to IBV. The vaccine has several advantages compared to other vaccine candidates. Firstly, the recombinant IBVs are fully functional, which means they have the same ability for replication and infection as real viruses. Since all the proteins of IBV have been presented to the immune system, the response could be stimulated by spike proteins and other immunogenic proteins (Bentley et al. 2013a). Secondly, some genes associated with virulence can be modified and engineered, which makes it possible to change the pathogenicity of IBV instead of serial passage on embryonated eggs to achieve attenuation (Casais et al. 2003).

Additionally, the reverse genetics vaccine is feasible to apply in the poultry industry because, once the vaccine is created, it can be produced at high speed and maintained in embryonated eggs for propagation (Cavanagh 2007). Nevertheless, there remains one major hurdle, which is the approval of its use as a novel vaccine. Further studies and surveillance need to be conducted before these vaccines are licensed.

1.8 Prevention and control of IB

To prevent the spread of IB, creating a clean environment with good ventilation, optimal temperature, and moisture is of great importance. To minimize the risk of introducing viruses, proper management practices should be considered. For example, it is advisable to strictly control the access to the house and keep visitors, even birds, from entering; separate equipment and footwear at each site; and set a footbath at the entrance to the house. Additionally, hygienic measures are also required for the control of IB. The organic wastes must be removed from the sites, and chicken houses should be cleaned using water under high pressure. Since IBV is susceptible to almost all disinfectants, using suitable disinfectants at optimal concentrations will help reduce the infectivity of other pathogens, including viruses and bacteria.

1.9 IBV propagation system

To date, three different systems for IBV propagation have been developed, including embryonated chicken eggs (ECE), chick kidney cells (CKC), and tracheal organ culture (TOC). The propagation systems of different IBV stains may differ due to their tropism. For example, the cell-adapted strain Beaudette can grow on various primary and secondary cells, such as chicken embryo fibroblasts, BHK-21, and Vero cells. However, the strain M41 only propagates in embryonated eggs and chick kidney cells. Several studies suggest that after 5 days post-inoculation through the allantoic route, embryos showed characteristic lesions in all inoculated eggs, including curling and dwarfing. In the CKC culture system, a slight detachment of cells from the cell plate was observed after 48 h post-infection. After 72 h post-infection, CPE showed complete sloughing of cells and plaque formation. The TOCs are considered an ideal system for studying IB because the changes observed in the tracheal ring are almost the same as those of a natural IBV infection in living chickens. It has been reported that ciliary movement becomes slow but persists after 4 days post-infection. On day 5 after infection, ciliary movement completely ceased (Chomiak et al. 1958; Lukert 1965; Lukert 1966; DuBose 1967; Coria 1969; Cunningham et al. 1972; Coria and Ritchie 1973).

1.10 Coronavirus reverse genetics system

It is known that the first step to establishing a reverse genetics system for coronaviruses is to convert their RNA genome into cDNA, which could act as a template for generating infectious RNA. In the second step, the generated infectious RNA functions as mRNA for transcriptional

machinery in host cells to recognize and synthesize proteins essential for genome replication. The reverse genetics system for coronaviruses was first developed by a researcher called Masters. Instead of recovery of the virus from full-length cDNA, this system is based on target RNA recombination, a technology that allows modification of the viral genome. However, the replicase region of the coronavirus is large, which makes it difficult to be modified. Another reverse genetics system in which infectious RNA generated from full-length cDNA is capable of larger RNA, ranging from 15 to 20 kb. Despite this, several groups found that cDNA derived from coronaviruses is extremely unstable in bacteria. To overcome this problem, researchers have devised some ingenious strategies without assembling the full-length cDNA in bacteria. One approach is *in vitro* ligation, which allows the assembly of viral DNA fragments using DNA ligase to seal the nicks instead of bacteria. Additionally, utilizing the yeast system to construct the full-length cDNA is also successful (Thao et al. 2020). Another strategy is introducing short introns into virus-derived cDNA, which enables them to propagate stably in *E. coli* (Rice et al. 1987; Polo et al. 1997; Yamshchikov et al. 2001).

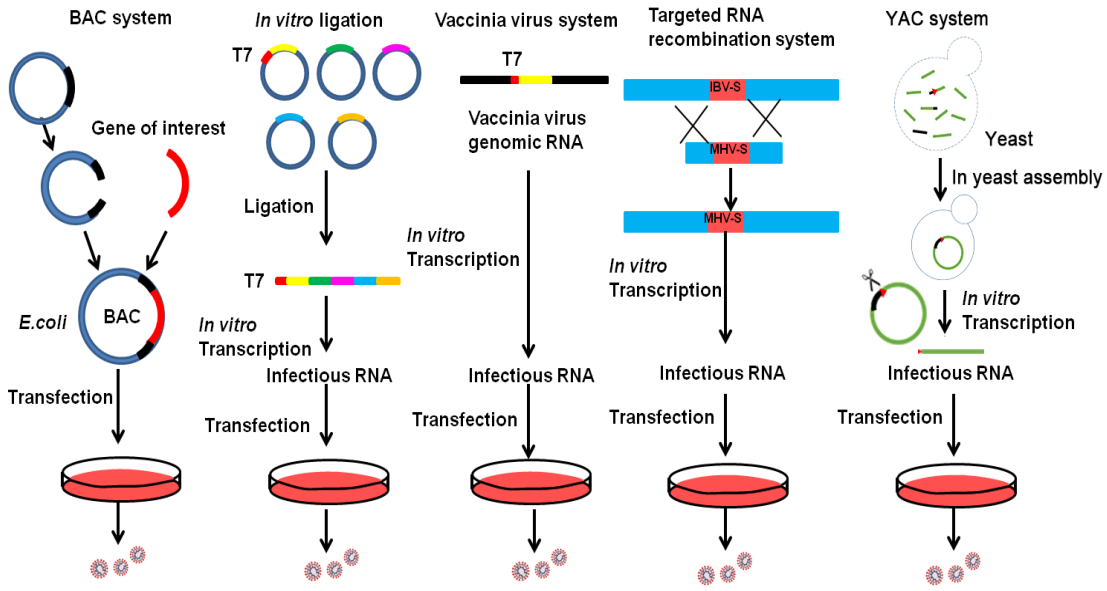

Figure 5: Coronavirus reverse genetics systems.

1.10.1 Targeted RNA recombination

The first reverse genetics system to allow specific manipulation of the coronavirus genome was targeted RNA recombination (Masters 1999; Masters and Rottier 2005). This method enables us to manipulate genes at the most 3'-proximal part of the genome. Recombination between a synthetic donor RNA and a recipient parent virus produces a modified gRNA in this system. The virus progeny bearing the desired gene modification was then selected based on phenotypic properties, such as temperature sensitivity and cell tropism. However, it has some

limitations, such as the ability to modify genes in the replicase region.

1.10.2 *In vitro* ligation of subgenomic fragments

The second reverse genetics system developed for coronaviruses was based on assembling full-length virus-derived cDNA *in vitro* without the need for propagation in *E. coli*. In this system, the viral genome was divided into several fragments. Each fragment was amplified by RT-PCR using extracted RNA from infected cells as a template to generate a series of contiguous cDNAs flanked by engineered unique restriction sites at both the 5´ and 3´ ends. Then these sequential cDNAs were systematically ligated together *in vitro*, yielding a full-length cDNA with a prokaryotic T7 or S6 promoter placed upstream of the 5´ ends. Infectious RNA was produced *in vitro* and electroporated with additional mRNA of the N gene into susceptible cells for efficient recovery of infectious viruses (Yount et al. 2000).

1.10.3 Vaccinia virus-based (VV) clones

The vaccinia virus-based reverse genetics system is an improvement over the ligation-based *in vitro* system (Casais et al. 2001; Thiel et al. 2001). The first step of this system is similar to *in vitro* assembly, which requires multiple-step ligation of continuous cDNAs containing unique restriction sites, followed by constructing the generated full-length cDNA of the virus into a VV vector. The full-length virus-derived cDNA acts as the template for *in vitro* transcription using T7 RNA polymerase to generate infectious viral RNA, which is transfected into susceptible cells to recover the virus. Alternatively, infectious RNA can be produced by utilizing the T7 RNA polymerase-based system, in which T7 RNA polymerase is expressed from recombinant fowlpox virus (rFPV-T7) (Britton et al. 1996).

1.10.4 Reverse genetics system based on bacterial artificial chromosomes (BAC) and yeast artificial chromosomes (YAC)

The reverse genetics systems of coronaviruses based on BACs or YACs are the most advanced approach. The BAC-based system involves the assembly of the full-length of viral genome in a bacterial artificial chromosome (BAC), such as pBeloBAC, a low-copy plasmid, in which the replication is under strict control, resulting in one or two copies in one cell. In the BAC system, the complete viral genome is controlled by the immediate-early promoter of human cytomegalovirus (CMV), allowing the efficient generation of viral RNA transcripts from the infectious clone in eukaryotic cells. Additionally, coronavirus BACs contain a poly (A) tail, ensuring authentic viral genomic ends are formed. The self-cleaving sequence of the hepatitis delta virus (HDV) ribozyme and bovine growth hormone termination and polyadenylation signals are located downstream of the coronavirus genome with the poly(A) sequence. Until now, the infectious BAC clones were developed for TGEV, SARS-CoV, MERS-CoV, and PEDV (Almazán et al. 2000; Jengarn et al. 2015; Fehr 2019; Chiem et al. 2020).

The most recent reverse genetics system for cloning and manipulating coronavirus genomes is based on transformation-associated recombination (TAR) cloning in yeast (Thao et al. 2020).

Here, the entire cDNA of the coronavirus genome is assembled by homologous recombination of overlapping subgenomic fragments in yeast, generating a YAC or YAC/BAC, which can subsequently be transferred into *E. coli* and further manipulated by bacterial genetics

1.10.5 Reverse genetics system for IBV

The main feature of coronaviruses is their largest viral RNA genome compared with other RNA viruses. Apart from this, as one of the numbers of the genus *Gammacoronavirus,* IBV contains several sequences located in the replicase gene, showing instability in bacteria, which has hampered the development of a reverse genetics system for IBV.

Paul Britton's group from England generated a reverse genetics system for IBV, considered the first recovery system for group III coronaviruses (Casais et al. 2001). This system is based on the assembly of IBV full-length cDNA downstream of a T7 RNA polymerase promoter by *in vitro* ligation, followed by direct cloning into a VV vector. The production of T7 RNA polymerase was achieved by infecting susceptible cells with a recombinant fowlpox virus expressing T7 RNA polymerase in advance. Then the cells were transfected with the linearized recombinant vaccinia virus DNA that is digested by specific restriction enzymes and the plasmid containing the N gene to successfully generate infectious IBV RNA. The results have demonstrated that the vaccinia virus-based reverse genetics system also applies to IBV, allowing us to produce genetically modified IBV using this system.

Additionally, the vaccinia virus vector containing full-length IBV-derived cDNA is believed to be a potential vector for developing vaccines against IBV and even other poultry pathogens. Based on the established reverse genetics system for the strain Beaudette, the research groups replaced the spike gene of Beaudette with that of M41 to further study the role of spike protein in determing cell tropism. They found that the chimera with spike of M41 on the background of Beaudette is only able to grow in chicken kidney cells but loses the ability to grow in BHK-21 and Vero cells, demonstrating that Spike protein is the determinant of cell tropism (Casais et al. 2003). To investigate which subunits of Spike glycoprotein are responsible for Beaudette replicating in Vero and BHK-21 cells, several chimeras composed of either the S1 subunit from M41 and the S2 subunit from Beaudette or the S1 subunit derived from Beaudette and the S2 subunit from M41 were generated with the genomic background of Beaudette. They found that the S2 subunit, other than the S1 subunit, is involved in extending cellular tropism (Bickerton et al. 2018). Interestingly, the recombinant virus (BeauR-M41(S)) has the same cellular tropism as the pathogenic strain M41, but it remains attenuated. To give insight into whether structural genes or accessory genes are the determinants of pathogenicity, a chimeric virus was produced with the replicase gene from the virulent strain Beaudette, but the rest of the parts, including structural and accessory genes, were derived from the virulent strain M41. Relevant studies showed that the recombinant virus can still restore virulence, suggesting that the region associated with the loss of pathogenicity does not reside in structural

and accessory genes but in replicase genes (Armesto et al. 2009).

Another reverse genetics system for the IBV strain H120 was successfully developed. Unlike the cell-adapted strain Beaudette, H120 is an attenuated, live vaccine strain. In this method, thirteen continuous cDNA spanning the complete genome of H120 were generated and ligated together *in vitro* using restriction enzymes Bsa I and BsmB, generating the full-length H120 cDNA with T7 RNA polymerase promoter at the 5′ ends and PolyAs at the 3′ end, followed by transcription into an infectious RNA genome. Then, the transcripts derived from full-length H120 cDNA and the N gene were transfected into BHK-21 cells. After 2 days post-transfection, the cell supernatant was collected and inoculated into 10-day-old embryonated chicken eggs (ECE) to recover the H120 virus. After five passages on ECE, the rescued viruses were successfully recovered with the same HA titers, growth kinetics, and ECID50 as their parental strain (Zhou et al. 2013).

A reverse genetics system for the strain H52, named after the 52nd serial passage of the Massachusetts-like IBV strain in embryonated chicken eggs, was established using targeted RNA recombination (Beurden et al. 2017). The viruses were successfully rescued in two steps. In the first step, recombination between IBV genomic RNA and a synthetic RNA transcribed from a donor plasmid p-mIBV occurs, resulting in an interspecies chimeric murinized IBV (mIBV), in which the gene region coding spike ectodomain was replaced by that of murine hepatitis virus (MHV). Through the selection on murine cells (LR7), only the recombinant murinized intermediate (mIBV) is capable of propagation. Then the mIBV was chosen to be the recipient for another recombination event with synthetic RNA transcribed from a donor plasmid p-IBV with the 3’ end of the IBV genome to produce a recombinant IBV (rIBV) comprising the spike gene of IBV, followed by the rescue and selection in embryonated chicken eggs.

Analysis of the characteristics of the rIBV and its parental strain H52 demonstrated that they are comparable to each other *in ovo* and *in vivo* kinetics. This established system allows us to manipulate the genome of a non-attenuated strain, which cannot replicate in continuous cell lines, especially the region placed at the 3’ end of the IBV genome, which includes structural and accessory genes. This system not only has the potential to develop promising live-attenuated vaccines, but it also provides us with a valuable research tool for IBV biology.

2. Aim of the study

Avian coronavirus, formerly known as infectious bronchitis virus (IBV), is the causative agent of highly contagious infectious bronchitis, which leads to substantial economic losses in the poultry industry worldwide.

Reverse genetics systems are handy tools in virology, as they simplify the functional dissection of viral genomes and accelerate the development of viral vaccines and antiviral strategies. Systems based on bacterial artificial chromosomes (BAC) are perhaps the most useful reverse genetics systems for coronavirus research because they have several advantages over other existing methods. Even the notoriously unstable coronavirus sequences are stable in BACs, where they can be rapidly modified by well-established and easily controlled mutagenesis techniques of bacterial genome engineering. Infectious clones of many different coronaviruses have been established using BACs, but until recently, no BAC-based system was available for any avian coronavirus. It has been questioned whether a genome of IBV can be cloned into a BAC vector, as IBV-derived sequences are genetically unstable in existing cloning vectors, including BACs.

Thus, the first goal of our study is to establish a stable and reliable reverse genetics system for the IBV strain Beaudette-FUB, the most intensively studied IBV strain. The second objective of this study is to insert the EGFP ORF into 11 putative cleavage sites of the main IBV protease, $3CL^{pro}$, thereby constructing several recombinant replicase-EGFP mutant viruses. Their growth properties and genetic stability were determined after 20 serial passages in cell culture. I selected one mutant reporter virus that exhibited identical growth kinetics compared to the parental Beaduette virus and stably expressed EGFP and applied it to antiviral drug screening. In addition, the colocalization of viral RNA-dependent RNA polymerase (RdRp) and double-stranded RNA (dsRNA) with EGFP during viral infection was studied.

3. Materials and methods

3.1 Materials

3.1.1 Buffers and solutions

Name	Composition
1% Agarose gel	1% w/v Agarose TAE buffer 0.5 µg /ml Ethidium bromide
Blocking buffer for IF	3% BSA in PBS
Buffer P1 (Resuspension buffer)	50 mM Tris HCL, pH 8.0 10 mM EDTA 100 µg/ml RNAse
Buffer P2 (Lysis buffer)	200 mM NaOH 1% w/v SDS
Buffer P3 (Neutralization buffer)	3 M Potassium Acetate, pH 5.5
LB medium (1 L)	10 g Tryptone 5 g Yeast extract 10 g NaCl
LB agar (1 L)	
SOC medium (1 L)	20 g Tryptone 5 g Yeast Extract 0.6 g NaCl 0.2 g KCl 20 mM, Glucose, pH 7.0
LB agar (1 L)	10 g Tryptone 5 g Yeast extract 10 g NaCl 15 g Agar

Tris-acetate-EDTA buffer (TAE)	40 mM Tris 1 mM $Na_2EDTA \cdot 2H_2O$ 20 mM Acetic acid 99%, pH 8.0
Fixation solution for immunofluorescence (IF)	4% paraformaldehyde (PFA) in PBS
Plaque assay overlay medium	0.6% Avicel 5% FCS 1% penicillin/streptomycin 1x EMEM
Phosphate buffered saline (PBS)	1.8 mM KH2PO4 10 mM Na2HPO4 137mM NaCl 2.7 mM KCl, pH 7.3
PBST	0.1% Tween-20 in PBS
Stacking-gel	5%(w/v) acrylamide/bisacrylamide 0.1% (w/v) SDS 125 mM Tris·HCl (pH 6.8) 0.075% (w/v) APS 0.15% (v/v) TEMED
Separating-gel	12%(w/v) acrylamide/bisacrylamide 0.1% (w/v) SDS 375 mM Tris·HCl (pH 8.8) 0.05% (w/v) APS 0.1% (v/v) TEMED

3.1.2 Cell culture medium and supplement

Name	Manufacturer/Compisition
Dulbecco's Modified Eagle Medium (DMEM)	PAN-Biotech GmbH, Aidenbach
Minimum essential Medium Eagle (MEM)	PAN-Biotech GmbH, Aidenbach
Fetal bovine serum (FBS)	PAN-Biotech GmbH, Aidenbach

Sodium Pyruvate	PAN-Biotech GmbH, Aidenbach
L-Glutamine	PAN-Biotech GmbH, Aidenbach
Trypsin-EDTA	PAN-Biotech GmbH, Aidenbach

3.1.3 Reagents

Name	Manufacture
Acetic acid	VWR, Darmstadt
Agar	Carl-Roth, Karlsruhe
Agarose	Carl-Roth, Karlsruhe
Arabinose L (+)	Carl-Roth, Karlsruhe
Avicel	FMC BioPolymer, Sandvika
BSA (albumin bovine fraction V)	Applichem, Darmstadt
Bromophenol blue	Carl-Roth, Karlsruhe
Calcium chloride	Applichem, Darmstadt
Chloroform	Merck, Darmstadt
Dimethyl sulphoxide (DMSO)	Merck, Darmstadt
dNTP Mix (10 mM total)	Bioline, Luckenwalde
EIDD-2801(Molnapiravir)	MedChem Express
Ethanol	VWR, Darmstadt
Ethidium bromide 1%	Carl-Roth, Karlsruhe
Ethylenediaminetetraacetic acid (EDTA)	Applichem, Darmstadt
Formaldehyde 37%	Applichem, Darmstadt
GC376	BPS Bioscience, California
Glucose (α-D (+) glucose monohydrate)	Merck, Darmstadt
Glycerol	Applichem, Darmstadt
Isopropyl alcohol (2-propanol)	Applichem, Darmstadt
Lipofectamine® 2000 Transfection Reagent	Thermo Scientific
Magnesium chloride	Merck, Darmstadt
Opti-MEM	Thermo Fisher Scientific, Darmstadt
Paraformaldehyde	Sigma-Aldrich, St. Louis
Phenol/Chloroform	Applichem, Darmstadt
Phenol	Roth, Karlsruhe
Potassium acetate	Applichem, Darmstad
Random hexamers	Thermo Fisher, Darmstadt

Sodium chloride (NaCl)	Carl Roth, Karlsruhe
Sodium dodecyl sulphate (SDS)	Sigma-Aldrich, St. Louis
Tris	Applichem, Darmstadt
Tris hydrochloride	Applichem, Darmstadt
Triton X-100	Thermo Fisher Scientific, Darmstadt
DEPC-treated water	Carl Roth, Karlsruhe

3.1.4 Consumables

Name	Manufacturer
Cell culture plate (6-well, 24-well)	Sarstedt, Nümbrecht
Cell culture dish (100 mm)	Sarstedt, Nümbrecht
Cell scrapers	Sarstedt, Nümbrecht
Cell strainers	BD Falcon, San Jose
Cryotubes (1.8 ml)	Nunc, Kamstrupvej
Electroporation cuvettes	Biodeal, Markkleeberg
Eppendorf tubes (1.5 ml and 2 ml)	Sarstedt, Nümbrecht
Falcon (15 ml and 50 ml)	Sarstedt, Nümbrecht
Falcon bacteria (13 ml)	Sarstedt, Nümbrecht
Pipette tips (P1000, 200, 100 and 10)	VWR, Darmstadt
Parafilm M	Bems, Neenah
PCR tubes (0.2 ml)	Applied biosystems, Berlin
Petri dishes for bacterial culture	Sarstedt, Nümbrecht
Pipette (5 ml, 10 ml and 25 ml)	Sarstedt, Nümbrecht
PVDF membrane	VWR, Darmstadt
Syringe filters (0.2 µm and 0.45 µm)	Sarstedt, Nümbrecht
Transfection polypropylene tubes	TPP, Trasadingen

3.1.5 Equipments

Name	Manufacturer
Axiovert S 100 fluorescence microscope	Carl Zeiss MicroImaging GmbH, Jena
Bacterial incubator 07-26860	Binder, Turtlingen
Bacterial incubator/shaker Innova 44	New Brunswick Scientific, New Jersey
Bunsen burner	Usbeck, Radevormwald/type 1020
Cell incubators Excella ECO-1	New Brunswick Scientific, New Jersey
Centrifuge 5424, Rotor FA-45-24-11	Eppendorf, Hamburg
Centrifuge 5804R, Rotors A-4-44 and	Eppendorf, Hamburg

F45-30-11	
CO_2 cell incubators	New Brunswick Scientific,
Electroporator Genepulser Xcell	Bio-Rad, Munich
Electrophoresis power supply Power Source 250 V	VWR, Darmstadt
Freezer (-20 ºC)	Liebherr, Bulle
Freezer (-80 ºC)	GFL, Burgwedel
Galaxy mini centrifuge	VWR, Darmstadt
Gel electrophoresis chamber Mini	VWR, Darmstadt
HERAcell 240i CO_2 incubator	Thermo Fischer Scientific, Kandel
Ice machine AF100	Scotsman, Vernon Hills
Imaging system (Chemismart 51000)	Peqlab, Erlangen
INTEGRA Pipetboy	IBS Integrated Biosciences, Fernwald
Magnetic stirrer RH basic KT/C	IKA, Staufen
Microscope AE20	Motic, Wetzlar
Microwave oven (Clatronic700 W)	Severin GmbH, Germany
Nanodrop 1000	Peqlab, Erlangen
Nitrogen tank ARPEGE70	Air liquide, Düsseldorf
Orbital shaker 0S-10	PeqLab, Erlangen
pH-meter RHBKT/C WTW pH level 1	Inolab, Weilheim
Professional TRIO Thermocycler	Analytik Jena, Jena
Semidry membrane blotting machine	Peqlab
Sterile Laminar flow chambers	Bleymehl, Inden
Vortex Genie 2	Bender&Hobein AG, Zurich
Water bath shaker C76	New Brunswick Scientific, New Jersey

3.1.6 Software and programs

Name	Source
Adobe photoshop	Adobe Systems, Unterschleissheim
Axiovision v4.8/Zeiss microscopes	Carl Zeiss MicroImagi, Jena
Finch TV	Geospiza, Inc
GraphPad Prism 8.1.2	Graphpad Software Inc, La Jolla
Image J	NIH, Bethesda
pDRAW32	AcaClone software
Serial cloner	Serial basics

3.1.7 Antibiotics

Name	Manufacturer
Ampicillin	Roth, Karlsruhe
Chloramphenicol	Roth, Karlsruhe
Kanamycin sulphate	Roth, Karlsruhe
Penicillin	Roth, Karlsruhe
Streptomycin	Roth, Karlsruhe

3.1.8 Antibodies

Name	Source
Mouse anti-IBV antibody	Cornell University, NY, USA
Mouse anti-GFP monoclonal antibody	Cell signaling
Goat anti-mouse IgG-Alexa 488	Thermo Fisher
Goat anti-mouse IgG-Alexa 568	Thermo Fisher
Goat anti-rabbit IgG-Alexa 488	Thermo Fisher
Rabbit anti-HA antibody	Sigma-Aldrich, St Louis

3.1.9 Commercial kits for molecular biology

Name	Manufacturer
Cell Counting Kit	Merk, Darmstadt
Invisorb Spin Plasmid Mini Kit	Stratec Biomedical AG
GF-1 AmbiClean PCR/Gel Purification Kit	Vivantis, Malaysia
Monarch DNA Gel Extraction Kit	New England Biolabs, Ipswich
Monarch PCR & DNA Cleanup Kit (5 µg)	New England Biolabs, Ipswich
Plasmid Midi Kit	Qiagen, Hilden
RNeasy Plus Mini Kit	Qiagen, Hilden
RTP DNA-RNA Virus Mini Kit	Stratec Molecular, Berlin

3.1.10 Enzymes and markers

Name	Manufacturer
Enzyme	
Alkaline Phosphatase CIP	New England Biolabs, Ipswich
Ambion RNase I (100 U/µl)	Thermo Scientific, Darmstadt
ApaLI	New England Biolabs, Ipswich
BamHI-HF	New England Biolabs, Ipswich
BglII	New England Biolabs, Ipswich

ClaI	New England Biolabs, Ipswich
DpnI	New England Biolabs, Ipswich
EcoRI-HF	New England Biolabs, Ipswich
HindIII	New England Biolabs, Ipswich
KpnI	New England Biolabs, Ipswich
MluI	New England Biolabs, Ipswich
M-MLV reverse transcriptase	Promega, Mannheim
Phusion High-Fidelity DNA Polymerase	New England Biolabs, Ipswich
PrimeSTAR HS DNA Polymerase	Takara, Bio
PstI	New England Biolabs, Ipswich
PvuI-HF	New England Biolabs, Ipswich
RNasin Ribonuclease Inhibitors	Promega, Mannheim
T4 DNA ligase	New England Biolabs, Ipswich
Taq DNA Polymerase	PeqLab, Erlangen
Marker	
GeneRuler 1 kb Plus DNA Ladder	Thermo Scientific, Darmstadt

3.1.11 Bacteria and Cells

Name	Source
Bacteria	
Escherichia coli Top10	Invitrogen, Carlsbad
GS1783	Greg Smith, Northwestern University, Chicaco
Cells	
African green monkey kidney cell line (Vero)	ATCC CCL-81
Baby Hamster kidney cell line (BHK-21)	ATCC CCL-10
Chicken Embryo kidney cell (CEK)	Primary cell
DF-1	CRL-12203
Embryonated SPF eggs	VALO BioMedia

3.1.12 Viruses

Name	Species	Source
IBV Beaudette strain	Avian	Poultry Diseases, Freie Universität Berlin
IBV M41 strain	Avian	Cornell University, NY, USA

3.1.13 Plasmids

Name	Source
PsiCHECK-2	Addgene
pSMART-BAC	Addgene
pUC-19 vector	Addgene
pBluescript	Addgene
pECBAC vector	Addgene

3.1.14 Primers for cloning and sequencing

Name		**Sequence (5'-3')**
nsp4-EGFP-nsp5	F	TACTCCGCCACGTTACTCTATTGGTGTTAGTAGATTACAAAGTGGATTCAAAAAGTTAGTAGTGAGCAAGGGCGAGGA
	R	CAACAGCACTACTAGGAGAAACCAGTTTCTTAAAACCAGACTGCAGACGTGATACTCCGATCTTGTACAGCTCGTCCATGC
nsp5-EGFP-nsp6	F	GGAGTCTGTATTTAATCAGATTGGTGGTGTTAGATTACAAAGCAGTTTCGTTCGTAAGGCAGTGAGCAAGGGCGAGGA
	R	ACTCCAAAACCAAGATGTAGCTTTTCTTACAAAAGAAGACTGAAGACGTACTCCTCCTATCTTGTACAGCTCGTCCATGC
nsp6-EGFP-nsp7	F	AATTGGTGGTGACCGTGTGTTGCCTATTGCTACAGTTCAAGCAAAGCTTTCAGACGTTAAAGTGAGCAAGGGCGAGGA
	R	TAAAACAACAGTTGTACACTTTACATCACTCAATTTAGCCTGTACAGTTGCTATTGGTAGCTTGTACAGCTCGTCCATGC
nsp7-EGFP-nsp8	F	GTATTGTGATGACATACTTAAGAGGTCAACTGTATTACAAAGTGTAACACAGGAGTTTAGTGTGAGCAAGGGCGAGGA
	R	CAGCATAAGAGGGTATATGTGAGAATTCTTGAGTAACCGACTGAAGAACTGTACTTCGTTTCTTGTACAGCTCGTCCATGC
nsp8-EGFP-nsp9	F	GACTAGGAATGGGCATAATAAGGTTGATGTTGTTTTGCAAAACAACGAATTGATGCCtCAcGTGAGCAAGGGCGAGGA
	R	AGCCTTTGTTTTAACACCATGTGGCATAAGCTCATTATTCTGTAGTACTACGTCTACTTTCTTGTACAGCTCGTCCATGC
nsp9-EGFP-nsp10	F	TATGGTACTTGGTGCTATATCTAATGTTGTTGTCTTACAGAGCAAGGGCCACGAGACTGAAGTGAGCAAGGGCGAGGA
	R	TGCCAACAGCATCCACTTCCTCTGTTTCATGCCCTTTAGATTGAAGAACTACTACGTTGCTCTTGTACAGCTCGTCCATGC
nsp10-EGFP-nsp12	F	TCAGTGTGATTCACTTAGACAACCAAAATCTTCTGTTCAAAGTGTAGCAGGCGCTAGCGACGTGAGCAAGGGCGAGGA
	R	TTAAATAATTCTTATCAAAATCAGATGCTCCAGCAACTGACTGTACGCTACTCTTAGGCTGCTTGTACAGCTCGTCCATGC
nsp12-EGFP-nsp13	F	GTTCTATGAGAATATGTATAGAGCTCCTACGACTTTACAAAGTTGTGGAGTATGCGTTGTAGTGAGCAAGGGCGAGGA

	R	ATAGTTTGACTATTACAAACTACACAAACGCCACAAGACTGTAGTG TTGTTGGTGCACGCTTGTACAGCTCGTCCATGC
Nsp13-EGFP-Nsp14	F	TCTTAAGTTTACAGAGCTAGATAGTGAAACAAGTCTGCAAGGAACTG GCCTGTTCAAGATCGTGAGCAAGGGCGAGGA
	R	CACTAAATTCTTTGTTGCAAATTTTAAACAAACCTGTACCCTGAAGG CTAGTCTCGCTGTCCTTGTACAGCTCGTCCATGC
nsp14-EGFP-nsp15	F	TAACCCTTATAACTTATGGAAAAGTTTTTCAGCTCTCCAGAGCATTGA TAACATCGCATATGTGAGCAAGGGCGAGGA
	R	GACCACCCTTATACATATTATAAGCAATATTGTCGATAGATTGTAATGC ACTGAATGACTTCTTGTACAGCTCGTCCATGC
nsp15-EGFP-nsp16	F	TGAAGATGGCAGTATTAAAACATGTTATCCACAGCTTCAAAGCGCTT GGACATGCGGATACGTGAGCAAGGGCGAGGA
	R	ATAAAGTTCAGGCATATTATAACCACACGTCCATGCTGACTGCAATT GAGGGTAGCAAGTCTTGTACAGCTCGTCCATGC
N gene	F	TATATAGCTAGCCACCATGGCAAGCGGTAAAGCA
	R	TATATAGCTAGCTCTAACTCTATACTAGCCTATAAATTTTAAC
nsp13-nsp14	F	TTTAAAGCTAATGACACAGGCAAAAAG
	R	GAATTCACAGGCTCAAAATTATTGCCTATTG
nsp14-nsp15	F	CTAAAGCACCTCCAGGTG
	R	TTCTCTTTGCATATAGCTCAAACG
nsp15-nsp16	F	CAACTCTACCTACATCTGTGG
	R	TCTCTTACCAGTAACTTACCACAC

4. Methods

4.1 Cell culture

4.1.1 Continuous cell line culture

African green monkey kidney (Vero) and baby hamster kidney (BHK-21) cells were grown in complete cell growth medium (DMEM containing 10% FCS and 1% penicillin/streptomycin) at 37 °C and 5% CO_2. The continuous cell line, chicken fibroblast cells (DF-1), were propagated in DMEM medium supplemented with 10% FCS, 1% P/S, 1% Glutamine, and 2 mM pyruvate. When the cell confluence reaches to 90-100%, cells are split in the ratio of 1:3 or 1:5. Firstly, cell culture medium was removed by aspiration, and cells were rinsed gently with PBS. Then the pre-warmed trypsin-EDTA solution was added to completely cover the cell monolayer. Once cells appeared detached, complete growth medium was added to inactive trypsin. After that, the medium was dispersed by pipetting over the cell layer surface several times, and the cell suspension was then seeded onto new plates or dishes.

4.1.2 Primary chicken embryo kidney cell preparation

Primary chicken embryo kidney cells were prepared from 18-day-old SPF embryos. Briefly, the shell surface of an embryonated egg was sprayed with 70% ethanol and opened with sterile scissors. Then, the embryo was exposed and pulled out with sterile forces after the membrane was carefully removed. The embryo was placed in a sterile petri dish, and the parts, including head, feet, wings, and contents of the body cavity, were removed from the embryo. With the use of small forces and scissors, the kidney was gently and slowly dissected from the embryo and collected in a glass flask, followed by washing with PBS until the PBS solution looked clear. After that, the kidneys were shredded, minced into small pieces by scalpels, and treated with trypsin-EDTA solution for 15 minutes. Allow the large kidney tissues to settle to the bottom and, using a pipet, transfer the supernatant to a cell strainer placed on a tube containing complete cell culture medium. Centrifuge the cell suspension/culture medium mix for 10 min at 500 g at room temperature, discard the supernatant, and resuspend the cell pellet with an adequate amount of cell medium, followed by seeding in plates or dishes for further culture at 37 °C and 5% CO_2.

4.1.3 Cryopreservation and revival of cells

For cell cryopreservation, the 100% confluent cell monolayer grown in a 10 cm petri dish was washed with PBS and detached using the Trypsin-EDTA solution. Cells were collected and resuspended in complete growth medium containing 10% FCS and 10% DMSO. Cell aliquots were placed in the Mr. Frosty freezing container for at least 4 hours at -80 °C. Finally, the cells in cryotubes were transferred and stored in liquid nitrogen.

4.2 Construction of an infectious BAC clone carrying the complete genome of the Beaudette strain of IBV.

To establish the reverse genetics system for the IBV strain Beaudette, total RNA was extracted from IBV-infected DF-1 cells using the innuPREP Virus TS RNA Kit (Analytik Jena). The extracted RNA was reverse transcribed into cDNA using a reverse transcriptase kit (Promega). Six overlapping cDNA fragments (F1, F2a, F2b, F3a, F3b, and F4) spanning the complete genome of the strain Beaudette were amplified from the cDNA and cloned separately into the plasmid pUC18. The full-length genomic cDNA of IBV was then cloned sequentially from six subgenomic IBV fragments into a modified BAC vector by the two-step markerless "*en passant*" recombination system in *E. coli*. The IBV genome was placed under the control of the immediate-early promoter of the cytomegalovirus and flanked at its 3' end by the ribozyme of the hepatitis D ribozyme and the polyadenylation signal of the bovine growth hormone gene. The complete sequence of the pBeaudette BAC clone has been uploaded to Genbank (accession: MW847254).

4.3 Next generation sequencing (NGS) and data analysis.

The sequencing of the complete genomic sequences of Beaudette-FUB, replicase-EGFP viruses, and infectious BAC clones was performed on an Illumina MiSeq platform. The sequencing libraries were prepared from the total RNA isolated from the cell culture medium of infected DF-1 cells or BAC DNA using the NEBNext Ultra II RNA/DNA kits (NEB). The obtained sequencing reads were processed with Trimmonatic v.0.36 and mapped against the reference sequence of IBV (NC_001451.1), the IBV strain Beaudette, using Burrows-Wheeler aligner v.0.7.15. The single nucleotide polymorphisms (SNPs) and deletions were evaluated using FreeBayes v.1.1.0-333. Data were merged by position and mutation using R v.3.2.3. The SNPs were additionally assessed using the Geneious R11 software (Biomatters).

4.4 Engineering of mutant viruses

4.4.1 Primers design for mutagenesis

Primers used for generating mutants were designed based on the sequence of the Beaudette-FUB strain. To construct EGFP-replicase mutants, the EGFP ORF was inserted in each of the 11 putative cleavage sites of $3CL^{pro}$ in the replicase gene, between the coding sequences of two adjacent nonstructural proteins. To ensure efficient proteolytic cleavage, EGFP was flanked by identical 14 amino acid-long sequences designed by duplicating the insertion site. The eleven insertion fragments flanked by homologous arms of the target insertion place were amplified respectively with the primers listed in 3.1.14. Each pair of primers contains homologous sequences upstream and downstream of the target position and duplicate sequences, allowing the removal of the kanamycin selection marker. Finally, in total, 11 replicase-EGFP Beaudette mutants were generated (shown in **Table 1**) and verified by RFLP

analysis and sequencing of the target region.

Table 1. Thirteen replicase-EGFP Beaudette mutant viruses

No.	Name
1	pBeau-nsp4-EGFP-nsp5
2	pBeau-nsp5-EGFP-nsp6
3	pBeau-nsp6-EGFP-nsp7
4	pBeau-nsp7-EGFP-nsp8
5	pBeau-nsp8-EGFP-nsp9
6	pBeau-nsp9-EGFP-nsp10
7	pBeau-nsp10-EGFP-nsp12
8	pBeau-nsp12-EGFP-nsp13
9	pBeau-nsp13-EGFP-nsp14
10	pBeau-nsp14-EGFP-nsp15
11	pBeau-snp15-EGFP-nsp16

4.4.2 Preparation of recombination and electro-competent cells GS1783

In the process of preparing electro-competent cells, the *E. coli* strain GS1783 harboring pBeaudette was grown in LB with chloramphenicol at 32 °C until the OD_{600} reached 0.5-0.7. The GS1783 culture was immediately transferred to a water bath with a temperature of 42 ºC for 15 minutes at 220 rpm in order to induce the expression of the red recombinant system. Then, the bacteria culture was cooled down in an ice-cold water bath for 20 minutes with continuous shaking, washed with ice-cold 10% glycerol three times to get rid of the salts, and the pellet was resuspended in 10% glycerol. Finally, aliquots of the competent cell suspension were frozen in a -80 ºC fridge until further use or used fresh for electroporation.

4.4.3 Generation of EGFP or mScarlet replicase mutants

A technology called two-step-red-mediated recombination was utilized to insert a reporter gene (EGFP or mScarlet) in the replicase gene of Beaudette. Briefly, a plasmid containing EGFP/mScarlet-kanamycin was used as a template with a set of primers to produce the desired fragments. These PCR products were run on the DNA gel and purified using a gel purification kit. The freshly prepared GS1783 competent cell was electroporated with purified DNA fragments (approximately 100 ng) and recovered using 1 mL of SOC medium without antibiotics. After being placing in a shaker at 32 ºC for two hours, the bacterial culture was spread on kanamycin agar plates, followed by incubation at 32 ºC for another 48 hours. Kanamycin-resistant colonies were screened by restriction fragment length polymorphism (RFLP) analysis in comparison with the digestion pattern of the original BAC pBeaudette. The

digested BAC mutants were loaded on 0.8% agarose gel for overnight at 60 voltages. Afterwards, the overnight gel was stained with EB and visualized under UV light. The selected co-integrates were subjected to the removal of the positive selection marker (kanamycin cassette). The overnight culture harboring positive co-integrates was inoculated into 2 mL LB with chloramphenicol and shaken for 1-2 hours at 32 ºC and 220 rpm until the solution becomes faintly cloudy. Then, 2 mL of LB containing chloramphenicol and 1% L-arabinose was added to the tube and grown for another 1 hour at 32 ºC and 220 rpm to induce the expression of I-SceI. Then the culture was transferred immediately to a 42 ºC water bath shaker for half an hour to initiate the second step of Red-mediated recombination. Subsequently, bacteria were cultured at 32 ºC for 2-3 hours and diluted serially, followed by streaking on an agar plate with chloramphenicol and 1% L-arabinose for incubation at 32 ºC for two days. Replica plates, including one agar plate with chloramphenicol and kanamycin, the other with only chloramphenicol, were used to select kanamycin-sensitive clones, which were further screened by Sanger sequencing.

4.4.4 Extraction of BAC DNA (Mini preps)

A small amount of BAC DNA was extracted from bacterial cells by following the standard protocol based on alkaline lysis. In brief, 5 mL of overnight culture was centrifuged at maximal speed for 1 minute to pellet the bacteria. Then the bacterial cell pellet was resuspended in 250 µL of P1 buffer and mixed gently by inverting the tubes 6-8 times. Subsequently, the P2 lysis buffer was added to tubes, and the contents were mixed by carefully inverting the tubes 6-8 times to become clear and thicker. Then, a neutralization reaction occurs after adding P3 buffer, forming a white precipitate containing bacterial proteins and genomic DNA. By centrifugation at maximal speed for 10 minutes, the supernatant with a volume of 750 µL was collected in a new tube and mixed with ice-cold isopropanol, followed by centrifugation at full speed for 10 minutes to precipitate plasmid DNA. Next, the DNA pellet was washed twice with 70% ethanol and dissolved in 30 µL of elution buffer. The concentration and quality of the plasmid were determined using Nanodrop.

4.4.5 Extraction of BAC DNA (Midi preps)

Plasmid Midi kits manufactured by QIANGEN were used to extract a medium-scale amount of BAC DNA. The instructions are as follows: First, the overnight bacterial culture was harvested by centrifugation at 6,000 g for 15 minutes. The bacterial pellet was resuspended in 4 mL of Buffer P1, mixed thoroughly with an equal amount of Buffer P2 by vigorously inverting, and incubated at room temperature for 5 minutes. Then 4 mL of prechilled Buffer P3 was added and incubated on ice for 15 minutes. The mixture was then subjected to centrifugation at maximal speed for 30 minutes at 4 ºC. Subsequently, the supernatant was applied to a column that has been equilibrated in advance using Buffer QBT. By gravity flow, the column was washed with Buffer QC two times. Finally, the DNA was eluted in 5 mL of 65 ºC Buffer QF and

precipitated by adding 3.5 mL of isopropanol. After centrifugation at 15,000 g for 30 minutes, the supernatant was discarded, and the DNA pellet was washed with 70% ethanol. The air-dry pellet was dissolved eventually in a suitable volume of appropriate buffer, and its quantity was tested before use.

4.5 Construction of the plasmid expressing Beaudette N gene (pSiCHECK-2-N)

4.5.1 Beaudette RNA extraction

The instruction from QIANGEN RNeasy Mini kit was followed for purification total RNA. Briefly, the strain Beaudette infected cells in 100 mm petri dish were collected by scraping and subsequent centrifugation at low speed. Next, appropriate volume of Buffer RLT was added to the cell pellet, which was mixed thoroughly by vortexing to ensure that no cell clumps are visible. To homogenize the lysate, the lysate was pipetted into a QIAshredder spin column, followed by centrifugation at full speed for 2 minutes. Then 1 volume of 70% ethanol was added to the homogenized lysate and the mixture was loaded on a RNeasy spin column. The spin column membrane was washed with Buffer RW1 once and Buffer RPE twice sequentially. Then, the spin column was placed in a new collection tube (1.5 mL) and RNase-free water was added to elute the RNA.

4.5.2 Reverse transcription PCR (RT-PCR)

To synthesize single-stranded cDNA from total RNA, HighCapacity cDNA Reverse Transcription Kit was used according to manufacturer's instruction. Firstly, the 2×RT master mix was prepared in advance and the amount of each component was shown as follows:

Component	Volume (μL)
10×RT Buffer	2.0
25×dNTP Mix (100 mM)	0.8
10×RT Random Primers	2.0
Multiscribe Reverse Transcriptase	1.0
RNase Inhibitor	1.0
Nuclease-free H_2O	3.2
Total per reaction	10.0

At the next step, the 2×RT master mix was placed on ice and extracted RNA samples was added to each tube. The reverse transcription was performed in a thermal cycler by following the program shown below.

Step	Temperature (ºC)	Time (Min)
Step 1	25	10
Step 2	37	120

Step 3	85	5
Step 4	4	∞

For the PCR, the following reagents were mixed (left) and the synthesized cDNA was used as template to amplify the region of Beaudette N gene using the following PCR program (Right).

Components	Amount ((μL)
5×Pusion HF buffer	10.0
dNTP Mixture	4.0
Forward primer	1.0
Reverse primer	1.0
Template (Beau-cDNA)	1.0
PrimeSTAR polymerase	0.5
Sterile distilled water	32.5
Total	50.0

Step	Tm	Time	Cycles
1	98 ºC	5 min	1
2	98 ºC	10 s	35
	55 ºC	15 s	
	68 ºC	3 min	
3	68 ºC	5 min	1

4.5.3 Preparation of chemically competent bacterial cells

Chemically competent bacterial cells were prepared according to the standard protocol of calcium chloride ($CaCl_2$). On day 1, frozen glycerol stock of bacterial cells (Top10) was streak out onto an agar plate without antibiotics and grown at 37 ºC overnight. On day 2, a single bacterial colony was selected from the agar plate and grown in 5 mL of LB overnight in a 37 ºC shaker at 220 rpm. The next day, 1 mL of the starter overnight culture was inoculated into 100 mL fresh LB and incubated at 37 ºC with continuous shaking. During the incubation period, the OD_{600} should be monitored and measured carefully, especially when it gets above 0.2, as cells grow exponentially. When the optical density of the culture measured at a wavelength of 600 nm (OD_{600}) reaches 0.4-0.6, the cell cultures were immediately placed on ice for 10 min with occasional swirling to ensure even cooling. Subsequently, aliquots of bacterial culture were transferred to pre-chilled 50 mL falcons and centrifuged at 4000 rpm for 10 min at 4 ºC. The cell pellets were resuspended in 30 mL of ice-cold solution containing 20 mM $CaCl_2$ and 80 mM $MgCl_2$. After centrifugation at 4000 rpm for 10 min, the supernatant was removed and the cell pellet was resuspended in 2 mL ice-cold sterile 0.1 M $CaCl_2$, 15% glycerol. The cell suspension was aliquoted in pre-chilled 1.5 mL Eppendorf tubes and used for transformation directly or kept in -80 ºC until further use.

4.5.4 Ligation of psiCHECK-2 vector and Beaudette N gene

The isolated psiCheck-2 plasmid was digested with two restriction enzymes (NheI and XbaI) simultaneously, followed by CIP enzyme treatment and gel purification. In the meantime, the PCR product of Beaudette N gene was digested with NheI and purified. The linearized plasmid

(2.7 kb) and purified fragment (2.7 kb) were ligated together using T4 DNA ligase overnight at 16 ºC. On the second day, the ligation mixture was purified and transformed by heat shock method. Briefly, the ligation product psiCHECK2-N was added to a tube containing 50 µL thawed chemical competent cells (Top10) and incubated on ice for 30 minutes, followed by heat shock in a 42 ºC water bath for 40 s. Next, the tube was immediately placed on ice again for 1 minute. The competent cells were recovered in 800 µL of SOC medium with continuous shaking at 37 ºC for 1 hour. Afterwards, the cell and ligation mixture were plated on agar plate with Ampicillin resistance and put in incubator overnight at 37 ºC. Single colony was picked up and inoculated into LB for overnight culture in a 37 ºC shaker. Plasmids were isolated, screened by RFLP and finally sequenced with a series of primers. Equal volumes of the bacterial culture containing the correct clone confirmed by sequencing and 50% glycerol were mixed and stored at -80 ºC.

4.6 Virus recovery

One day before transfection, BHK-21 cells in growth medium without antibiotics was seeded on a 6-well plate to obtain cell monolayers with 90-95% confluence by the time of transfection. On the second day, the cell transfection was performed by following the protocol of Lipofectamine 2000. In brief, 5 µg of respective BAC mutant together with 1 µg of the psiCheck-2-N (Beau) were diluted in 250 µL of Opti-MEM medium and mixed carefully. Next, 10 µL of Lipofectamine 2000 was diluted in 250 µL of Opti-MEM medium and mixed by vortexing, followed by incubation at room temperature for 5 minutes. The diluted DNA was then combined with diluted Lipofectamine 2000 and incubated for 20 minutes at room temperature. During this incubation period, prepared BHK-21 cells were washed once with PBS and 1 mL of growth medium without antibiotics was added to each well. Then 500 µL of DNA/ Lipofectamine 2000 mixture was added drop-wise to each well and mixed by rocking the plate back and forth. After incubation for 6 hours, the transfection medium was removed. Cells were washed with PBS once and detached using 200 µL of trypsin–EDTA solution. To neutralize trypsin, 800 µL of growth medium was added. The cell suspension was reseeded over a confluent monolayer of DF-1 containing 1 mL of normal growth medium and incubated at 37 ºC for 48 hours. The supernatant was collected from each well, centrifuged at 2,000 × g for 5 min to get rid of cell debris, and used to infect susceptible cells cultured in 6-well plates. On day 2 post infection, cytopathic effect (CPE) was observed and confirmed by immunofluorescence assay (IF).

4.7 Virus titration

For virus titration, the plaque assay was performed on DF-1 cells in 6-well plates by following the standard protocol. 90-95% confluent monolayer of DF-1 cells were infected with serially ten-fold diluted virus. During the adsorption period of 1 hour, cells were incubated at 37 ºC with shaking every 15 minutes to distribute virus evenly. Afterwards, the inoculum was removed and overlaid with prepared Avicel overlay medium. After incubation at 37 ºC for 2-3 days, cells

were washed carefully with PBS to remove the overlay medium and fixed with 4% formaldehyde for 20 minutes with constant gentle shaking. After removing the fixative, cells are washed with PBS and Triton X-100 was added. To prevent non-specific of antigens and antibodies, 3% BSA in PBS was used as blocking buffer and incubated for 30 minutes at room temperature with gentle shaking. Subsequently, cells are stained with primary antibody (Mouse anti-IBV antibody) of dilution 1:500 and incubated for 45 minutes at room temperature. After washing cells three times with PBS, the secondary antibodies (Goat anti-mouse IgG-Alexa 568) with dilution 1:2000 was added and incubated for another 45 minutes at room temperature in the dark. After washing with PBS three times, plaques were observed and counted under the fluorescence microscope to determine the titer of virus stocks.

4.8 Characterization of Beaudette recombinant viruses

4.8.1 Multistep growth kinetics and plaque size assay

To assess the multi-step growth kinetics of virus, 100% confluent cell monolayers of DF-1 were infected with Beaudette virus or recombinant viruses at a MOI of 0.01. After 1 hour adsorption, the inoculum was replaced by 2 mL of fresh DMEM medium containing 1% glutamine and 2 mM pyruvate and placed in incubator at 37 ºC. The supernatant was collected at different time points post-infection (12, 24, 36 and 48 hours). After centrifugation, cell debris was removed and the harvested supernatants were stored in -80 ºC for further titration as described in 4.7.

To assess the spread of the recovered Beaudette virus, plaque assay was performed as described above. Images of 50 randomly selected plaques of each virus were taken and their plaque areas were determined using ImageJ software. The plaque diameters were calculated and normalized to the average plaque diameter of the wide type Beaudette virus.

4.8.2 SDS-PAGE and Western-blot

To detect the EGFP produced by recombinant viruses, 100% confluent cell monolayers in a 6-well plate were infected with different viruses. After 48 hours of infection, the cell medium was removed and cells were washed with PBS buffer once. Then infected cells were harvested and the cell pellet was lysed in RIPA buffer supplemented with protease inhibitor. After that, the lysed samples were centrifuged at 15,000 g at 4 °C for 5 min and supernatant was taken. The supernatant together with loading dye was boiled at 98°C for 2 minutes. Subsequently, proteins were separated by SDS-PAGE and transferred to PVDF membranes through semi-dry Western blotting. The membranes were then blocked by skimmed milk (5%) in PBS-T for 1 hour and incubated with the primary antibody (rabbit anti-GFP antibody, Cell signaling) with dilution 1:1000 overnight at 4 °C. After washing membranes with PBS-T three times, the HRP-conjugated secondary antibody with dilution 1:2000 was added, followed by incubation for 1 hour at room temperature. The chemiluminescence was detected and images were captured using ECL

4.8.3 EGFP stability analysis

To determine whether the EGFP insertion in replicase was inherited stably, recovered viruses expressing EGFP were passaged serially in DF-1 cells. The supernatant of each virus at passage 1, 5, 10, 15 and 20 (P1, P5, P10, and p20) were collected and used for plaque assay as described above. The percentage of viruses expressing EGFP was assessed by selection of 50 plaques followed by determination of EGFP expression. To analyze if the gene of EGFP stably integrated into viral replicase, reverse transcription PCR (RT-PCR) was performed using sets of primers shown in 3.1.14 to amplify the region surrounding the EGFP.

4.9 Cytotoxicity assay

The stock solutions of $3CL^{pro}$ inhibitor GC376 and ribonucleoside analog molnupiravir EIDD-2801 were prepared by dissolving in 100% dimethyl sulfoxide (DMSO). To determine the cytotoxicity of GC376 and EIDD-2801 to DF-1 cells, the Cell Counting Kit-8 (CCK-8) was used according to the standard protocol. Briefly, DF-1 cells were seeded in a 96-well plate and cultured in a CO_2 incubator at 37°C for 24 hours. The next day, 10 μL of various concentrations of the tested substances was added to the plate. After 24 hours of treatment, 10 μL of CCK-8 solution was added to each well of the plate and incubated for 1-4 hours. Then, the absorbance at 450 nm was measured by a microplate reader.

4.10 Antiviral assay

The antiviral effect of GC376 and EIDD-2801 on replication of one of the replicase-EGFP viruses, Beaudette Nsp13-EGFP-Nsp14 virus in DF-1 cells was determined by plaque assay and flow cytometry. In plaque assay, DF-1 cells with 100% confluence seeded in a 12-well plate were infected with Nsp13-EGFP-Nsp14 virus at an MOI of 0.01. After 1 h of incubation, the virus inoculum was replaced by overlay medium containing 0.6% Avicel and different concentrations of antiviral compounds. After 48 hours, plaques were counted and calculated as described above. To determine the inhibitory effect of antivirals by flow cytometry, confluent DF-1 cells in a 12-well plate were infected with Nsp13-EGFP-Nsp14 virus. After 1 h, the infected medium was removed and replaced with growth medium with various concentrations of antivirals. 48 hours later, cells were trypsinized and finally resuspended in PBS. The EGFP fluorescence was quantitated by flow cytometry. The EC_{50} values were determined by the nonlinear regression analysis using the dose-response (variable slope) equation using the GraphPad Prism 8.0 software (GraphPad Software).

4.11 Statistical analysis

Statistical analyses were done using the GraphPad Prism 8.0 software package (GraphPad). All applied statistical tests can be found in the respective figure legends. If $p \leqslant 0.05$, the results were considered significantly different. All experiments in which statistical tests were used, were repeated independently at least three times.

5. Results

5.1 Construction of an infectious BAC clone of IBV strain Beaudette-FUB

Infectious clones of many coronaviruses (e.g., SARS, MERS, TGEV, and PEDV) have been generated using bacterial artificial chromosomes (BACs) because viral sequences, especially in the replicase region cloned in BACs, are extremely stable, comparable to high-copy plasmids. In the BAC system, powerful and precise mutagenesis techniques could easily manipulate viral genes. Since there is no infectious BAC clone of the IBV strain Beaudette-FUB that was provided by the Institute of Poultry Diseases at the Free University of Berlin, Germany, available, our primary objective in this study was to clone the full-length genome of IBV strain Beaudette-FUB into a mini-F vector to generate an infectious BAC clone (Lv et al. 2020). The strategy we adopted here involved the assembly of the entire IBV genome into the BAC vector from multiple overlapping subgenomic fragments using red-mediated homologous recombination in *E. coli* in a stepwise manner (Tischer et al. 2010).

Before we started constructing the infectious BAC for Beaudette-FUB, we examined its replication ability in different cell lines. We found that it could grow on multiple cells, including CEC, Vero E6, and chicken fibroblast DF-1 cells. To obtain the sequence information of Beaudette-FUB, we extracted viral RNA from infected cells, as described above, and its complete genome was determined by Next Generation Sequencing (NGS) based on the Illumina MiSeq platform. We analyzed the sequencing data and found that its genome length is 27,608 nucleotides, and it had the highest similarity in genomic sequence with that of the reference sequence (NC_001451.1). These two strains had only 18 SNP differences, including 7 non-missense mutations, 9 missense mutations, and 2 SNPs, forming stop codons in the ORF5b region shown in **Table 2**.

Table 2. Sequence differences in the genomes of the reference sequence, parental Beaudette-FUB virus and the Beaudette-FUB variant eventually cloned in the pBeaudette BAC clone.

No.	Position	RefSeq	Beau-FUB	pBeau	Gene	Mutation
1	3,243	T	C	C	1ab	silent
2	3,428	C	A	A	1ab	A967D
3	4,239	C	T	T	1ab	silent
4	5,037	G	T	T	1ab	K1,503N
5	5,785	C	T	T	1ab	L1,753F
6	6,231	G	A	A	1ab	silent
7	7,293	A	C	C	1ab	silent
8	8,691	G	A	A	1ab	silent

9	10,754	T	C	C	1ab	V3,409A
10	19,089	A	G	G	1ab	I6,188V
11	20,480	G	A	A	spike	S38N
12	20,585	G	A	A	spike	G73D
13	20,731	T	A	A	spike	L122I
14	21,711	G	A	A	spike	silent
15	22,252	G	A	A	spike	G629R
16	24,275	A	T	T	sM	silent
17	25,770	T	A	A	5b	stop
18	25,771	T	A	A	5b	stop
19	5,625	A	A	T	1ab	silent
20	22,415	A	A	C	spike	silent
21	25,583	T	T	C	5a	silent

In the process of assembling the IBV genome into a BAC vector, the complete genome of IBV strain Beaudette-FUB was initially divided into four overlapping subgenomic fragments F1-F4 of 7 kb each. These four fragments were amplified by RT-PCR. Several studies have shown that sequences derived from replicase genes of IBV and other coronaviruses were unstable in bacteria and could not be cloned into a high-copy plasmid, such as pUC18. However, to test our luck, we attempted to clone four subgenomic fragments from F1 to F4 in the high-copy plasmid, pUC18 (**Figure 6**). We successfully cloned F1 and F4 but failed to clone F2 and F3 in pUC18, which is consistent with previous reports of the incompatibility of cloning IBV sequences into a high-copy plasmid. We still failed when trying to clone these two fragments (F2 and F3) into a low-copy plasmid. Next, we split F2 and F3 into two subgenomic overlapping fragments, each with a similar length of 3.5 kb, F2a and F2b, and F3a and F3b, respectively. Surprisingly, we were able to clone each of them into a high-copy plasmid, pUC18. The cloned subgenomic sequences were confirmed by sequencing. We found a total of 6 SNPs from the sequencing results compared to the reference sequence of IBV strain Beaudette-FUB. Of those, three were silent mutations, and three were missense mutations (**Table 2**). For these three missense SNPs, which caused amino acid changes on the protein level, we retained them as markers, which allowed us to distinguish between recovered and parental viruses. In the meantime, we also attempted to repair them in case we could not recover the Beaudette viruses from the infectious BAC clone with these SNPs.

Based on several plasmids containing subgenomic sequences of Beaudette-FUB, through six sequential red-mediated homologous recombination steps in *E. coli*, we assembled the full-length genome of IBV strain Beaudette-FUB into a BAC, which is referred to here as pBeaudette. To ensure that the infectious clone efficiently produces authentic nascent RNA molecules that have identical 5' and 3' ends as the parental IBV virus in eukaryotic cells, the complete Beaudette-FUB genome was flanked by the immediate-early promoter of human

cytomegalovirus (HCMV) at the 5' end. The poly(A) sequence, hepatitis delta virus (HDV) ribozyme, and a polyadenylation signal of the bovine growth hormone (BGH) gene were placed in order at its 3' end (**Figure 6**).

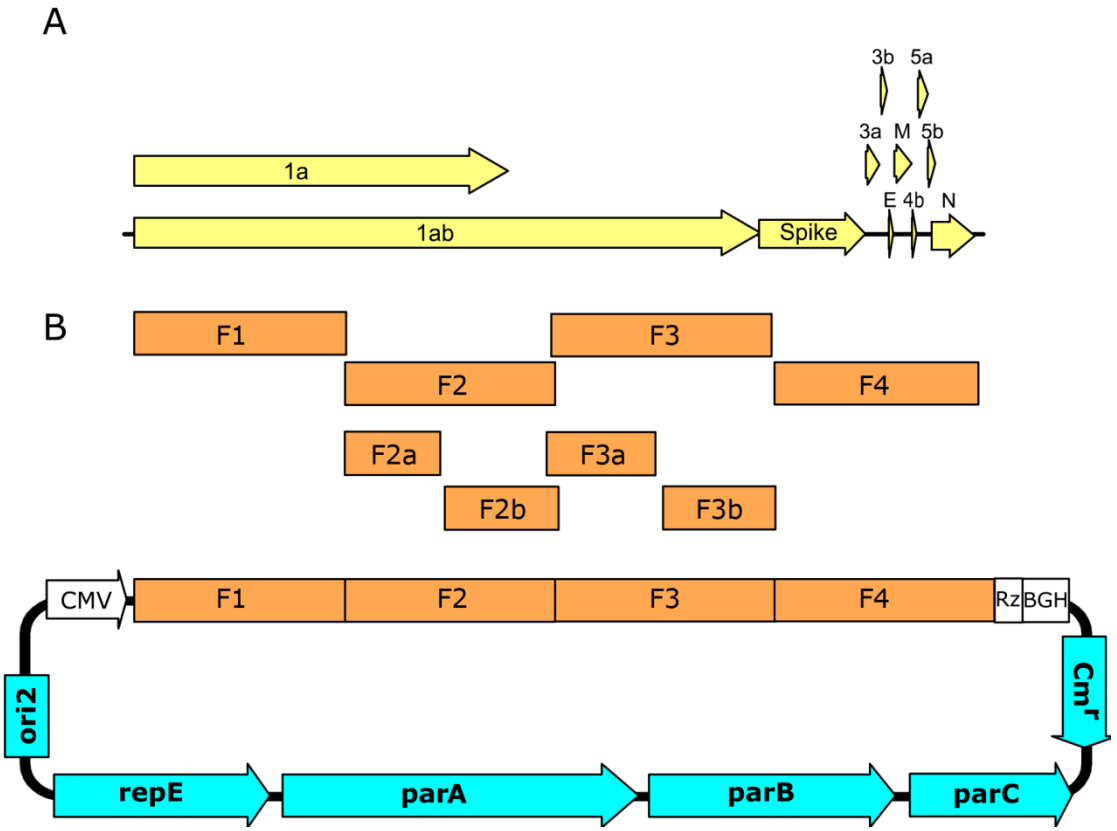

Figure 6. Organization of the IBV genome and structure of the infectious BAC clone of IBV, pBeaudette.

(A) Schematic of the IBV genome. The IBV genome is a single-stranded, positive-sense RNA molecule of about 28,000 nt. It encodes 11 canonical ORFs. The 5' end-terminal two-thirds of the genome encodes two large polyproteins 1a and 1ab that play important functions in the replication of the IBV genome. The genomic region located proximal to the 3' end encodes structural proteins, including the spike glycoprotein (S), the envelope protein (E), the membrane protein (M), and the nucleocapsid protein (N). The accessory genes 3a, 3b, 4b, 5a and 5b are interspersed amongst the structural genes.

(B) Structure and assembly of the infectious BAC clone of IBV. The IBV genome was divided into six overlapping subgenomic fragments (F1, F2a, F2b, F3a, F3b and F4) that were initially cloned in pUC18. The final BAC clone of IBV strain Beaudette-FUB (pBeaudette) was constructed via step-wise assembly by homologous recombination in *E. coli.* CMV – immediate-early promoter of human cytomegalovirus; Rz – ribozyme of hepatitis delta virus; BGH – polyadenylation signal of the bovine growth hormone gene; Cm r – chloramphenicol resistance gene; repE, parA, parB – partitioning genes, parC – the

centromere and ori2 – the replication origin of the BAC vector, which ensure that each daughter bacterial cell receives a copy of the BAC after cell division.

5.2 Recovery of Beaudette virus from the infectious BAC clone (pBeaudette)

Several studies have shown that the recovery efficiency of infectious viruses from coronavirus BAC could be significantly increased by the expression of exogenous nucleocapsid protein (N protein), but the reason is still unknown (Casais et al. 2001; Youn et al. 2005). Some people hypothesized that the N protein binds to the viral mRNA, stabilizing the RNA and protecting it from nuclease digestion. Thus, the mRNA is long enough to be recruited by the ribosomes and ensure efficient production of viral proteins. Since N protein is considered to enhance the recovery of virus from an infectious clone, we attempted to rescue infectious IBV in permissive DF-1 cells that were transfected with pBeaudette alone or in combination with the psiCHECK-2-N plasmid expressing N protein.

Recovery of the Beaudette virus, referred to here as rBeaudette, was achieved as described in 4.6. We found that recovery of infectious virus was successful regardless of the presence or absence of N protein, but apparently, providing N protein in transfection increased recovery efficiency by approximately 10-fold. Also, we recovered infectious viruses from the BAC clone with three SNPs that caused changes on the amino acid level, demonstrating that the three SNPs did not affect virus recovery.

By examining their growth properties, we conducted multi-step growth kinetics and plaque size assay, which showed that the parental virus and the rBeaudette exhibited identical growth kinetics and formed comparable plaque sizes on DF-1 cells (**Figure 7B**).

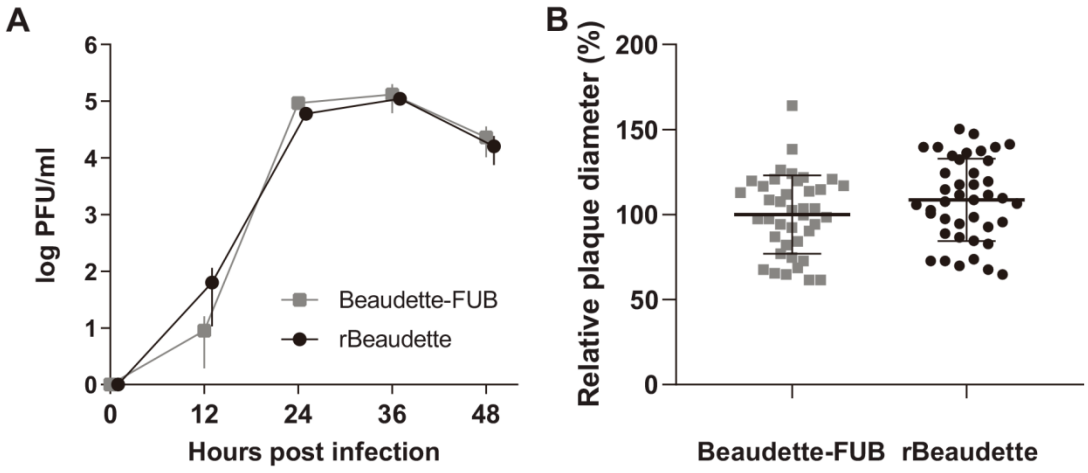

Figure 7: Replication of the parental and the recovered viruses *in vitro*.

(A) Multi-step growth kinetics of the parental Beaudette-FUB and the recovered rBeaudette virus. DF-1 cells were infected at an MOI of 0.01 and viral progeny was titered at indicated times after infection on DF-1 cells. Titers are shown as means of three independent experiments with standard deviations. ($p > 0.05$, Kruskal-Wallis H test).

(B) Plaque sizes of the parental Beaudette-FUB and the recovered rBeaudette virus. The box-plot displays the relative plaque diameter normalized against the average plaque diameters of the parental virus. p-values were calculated using unpaired t-test.

5.3 Generation of reporter viruses

Reporter viruses are widely used to study viral replication, transcription, and the screening of antiviral drugs. As a result, creating a reporter virus that stably expresses an enhanced green fluorescent protein (EGFP) or red fluorescent protein (mScarlet), allowing us to track the progression of viral infection and use it in antiviral drug screening, has become our second major goal.

5.3.1 Replacement of non-essential accessory genes with EGFP

For IBV, several recombinant mutants expressing the reporter genes (EGFP, firefly luciferase, or Renilla luciferase) have been constructed. The strategy for producing these EGFP reporter mutants involved replacing accessory genes with EGFP. However, it has been reported that EGFP mutants showed genetic stability only during the first 3-10 passages. Therefore, it is hard to generate a reporter virus that would tolerate the reporter gene in the IBV genome during serial passages (Youn et al. 2005; Shen et al. 2009; Bentley et al. 2013a; Bentley et al. 2013b).

Since it was suggested that the most genetically stable IBV recombinants could be produced when a heterologous gene replaced the IBV ORFs 3a and 3b, we initially attempted to construct EGFP reporter viruses by replacing the ORF3a or the putative ORF4b with an EGFP ORF. However, no infectious viruses could be recovered from the Beaudette BAC with the ORF3a deletion. For pBeau-△4b-EGFP, infectious viruses could be produced in permissive cells, but no green fluorescence could be detected in infected cells.

5.3.2 Insertion of EGFP into IBV replicase gene

Besides PL^{pro}, $3CL^{pro}$ is another protease that plays an important role in the cleavage of viral polyproteins. The cleavage sequence of IBV $3CL^{pro}$ was analyzed, and we found that it cleaves mainly at the consensus sequence LQ↓, but VQ↓ in two different places, including nsp6/nsp7 and nsp10 (GFL) /nsp 12 (RdRp) (**Figure 8**).

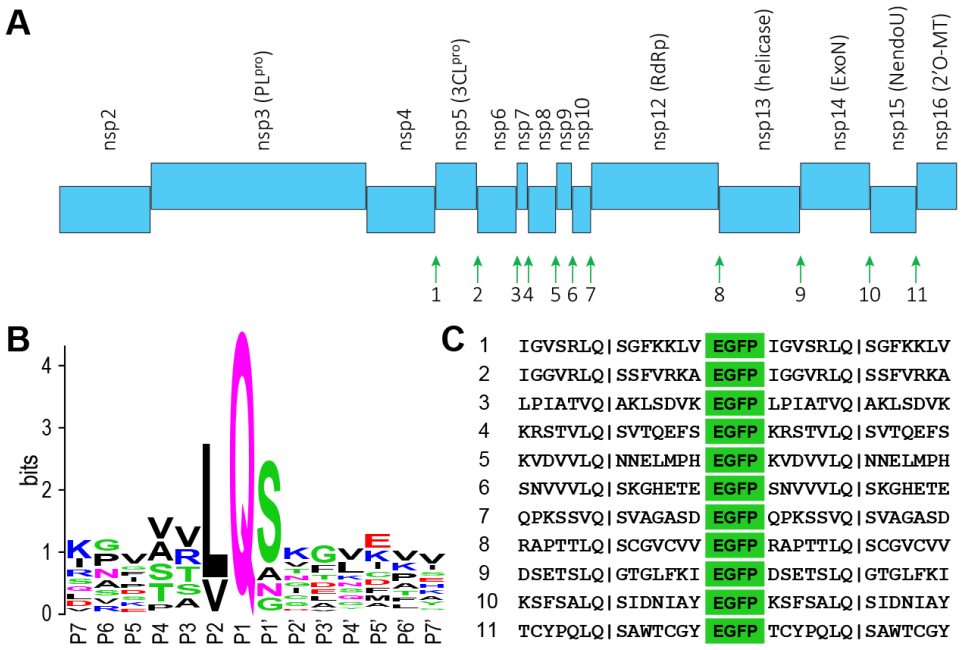

Figure 8: Design of replicase-EGFP Beaudette viruses.

(A) The replicase polyproteins 1a and 1ab are proteolytically processed by PL^{pro} and 3CL^{pro} which generate 14 different nonstructural proteins (blue boxes). The 11 putative cleavage sites of the 3CL^{pro} are indicated by arrow and they were selected for EGFP insertion.

(B) Analysis of the 3CL^{pro} cleavage sites in IBV genome shows that 3CL^{pro} has a very strong consensus around the cleavage site. The protease has a strong preference for leucine (L) at position P2, glutamine (Q) at position P1 and serine (S) or alanine (A) in position P1'.

(C) The reduplicated 14 amino acid-long sequences containing the native 3CL^{pro} cleavage sites (shown as vertical lines) flanked both termini of EGFP and allowed efficient proteolytic processing of the recombinant 1ab polyproteins.

In order to test whether reporter molecules that were inserted into the replicase gene ORF1 can be expressed and released from the replicase polyprotein by cleavage of 3CL^{pro}, through two-step-red-mediated recombination, we generated 11 different EGFP-reporter mutants in which a green fluorescent protein marker gene (EGFP) was inserted into 11 putative cleavage sites of 3CL^{pro} between coding sequences of two adjacent non-structural proteins. Additionally, the EGFP sequence was prolonged by 7 amino acids at both ends to enhance the recognition and cleavage efficiency of 3CL^{pro}. Together with 7 amino acids from adjacent viral sequences, the EGFP was flanked by an authentic recognition site of 3CL^{pro} with 14 amino acids in length at both ends. To prevent the EGFP sequence from being lost from the viral genome due to recombination between the duplicated sequences, two duplicated sequences flanking the EGFP coding sequences were designed to differ as much as possible in nucleotides.

Finally, 11 replicase-EGFP mutant viruses were successfully constructed, as described in 4.4.3. The positive constructs were confirmed by RFLP analysis, and the inserted region was further sequenced by Sanger sequencing. To validate whether replicase could tolerate the introduction of EGFP and whether these recombinant viruses could be recovered, BHK-21 cells cultured in a 6-well plate were co-transfected with psiCHECK-2-N and an individual replicase-EGFP construct. The supernatant was harvested and transferred to the monolayer of susceptible DF-1 cells after 48 hours post-transfection. We found that viruses with green fluorescence could be recovered from three different EGFP reporter mutant viruses, including Nsp13-EGFP-Nsp14, Nsp14-EGFP-Nsp15, and Nsp15-EGFP-Nsp16 (**Figure 9**).

Additionally, infectious viruses were produced from a recombinant clone containing the EGFP ORF between nsp4 and nsp5 (3CLpro), referred to as Nsp4-EGFP-Nsp5 (3CL^{pro}), but no green signal was detected in the infected cells. To further validate whether the identified EGFP insertion region in replicase could also tolerate foreign reporter proteins, a red fluorescent protein of different origins, mScarlet, has been inserted into the three newly identified locations, producing three replicase-mScarlet constructs. Again, all of these recombinant viruses were recovered with great success, and red fluorescence was detected in infected DF-1 cells (**Figure 10**).

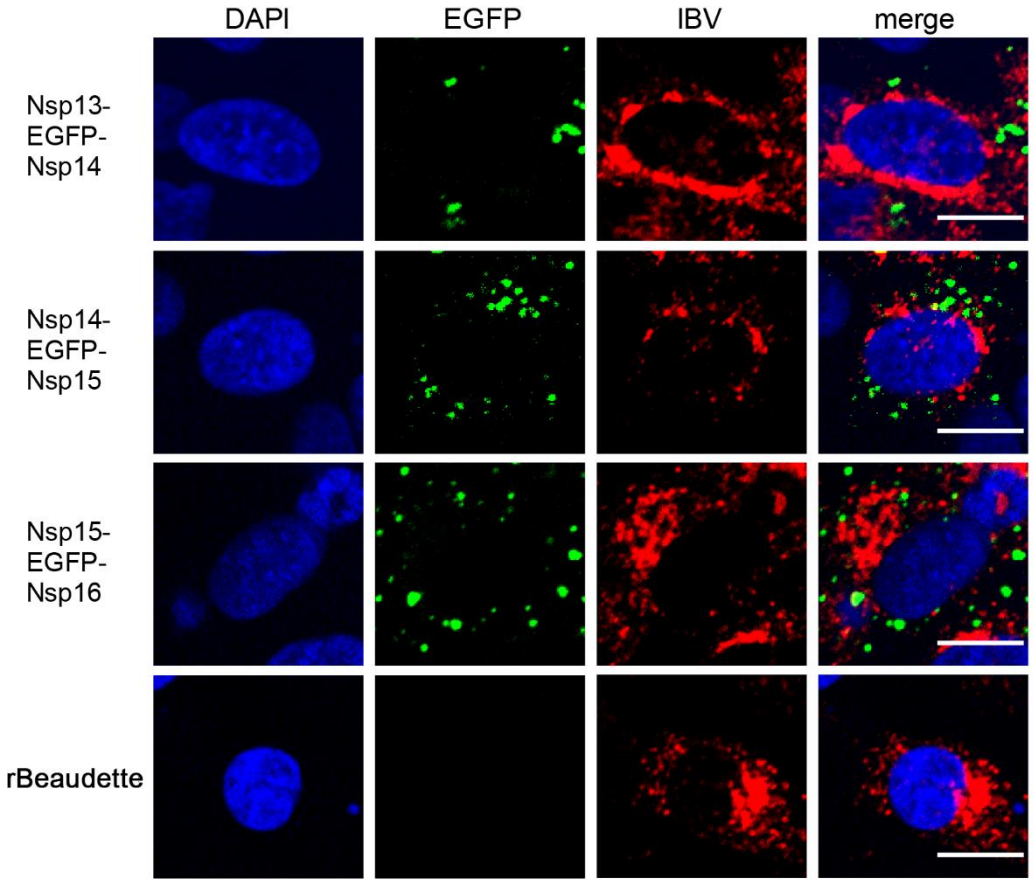

Figure 9：Production of EGFP in DF-1 cells infected with replicase-EGFP Beaudette viruses.

DF-1 cells were seeded onto glass coverslips and infected the indicated replicase-EGFP viruses. Cells were fixed 2 days after infection and viral proteins were detected with a mouse anti-IBV serum. Blue – DAPI, red – Beaudette antigens, green – EGFP. Heli – helicase, ExoN – exoribonuclease, NendoU – endoribonuclease, 2'-O-MT – ribose 2'-O-methyltransferase. Scale bar, 10 μm.

These findings confirmed that the Beaudette virus's replicase gene could tolerate heterologous sequences without interfering with viral viability or the production of essential replicase proteins.

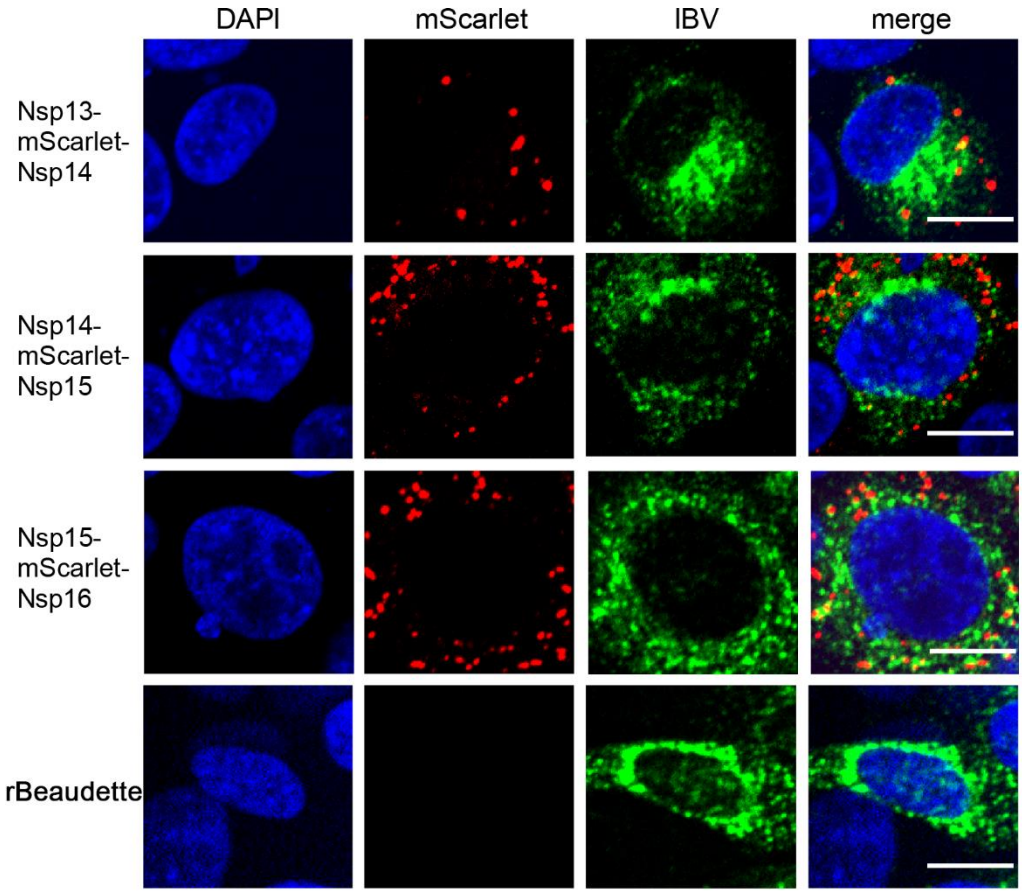

Figure 10. Production of mScarlet in DF-1 cells infected with recombinant replicase- mScarlet Beaudette viruses.

DF-1 cells were seeded onto glass coverslips and infected with the indicated replicase-mScarlet viruses. Heli – helicase, ExoN – exoribonuclease, NendoU–endoribonuclease, 2'-O-MT – ribose 2'-O-methyltransferase. Blue – DAPI, red – mScarlet, green – IBV antigens. Scale bar, 10 μm.

5.4 Growth properties of replicase-EGFP viruses *in vitro*

The effect of EGFP insertion within the viral replicase on virus replication was assessed by multiple-step growth kinetics. All three EGFP-reporter viruses replicated comparable to the Beaudette-FUB, indicating that viral replicase could tolerate additional reporter genes without impairing virus growth (**Figure 11**).

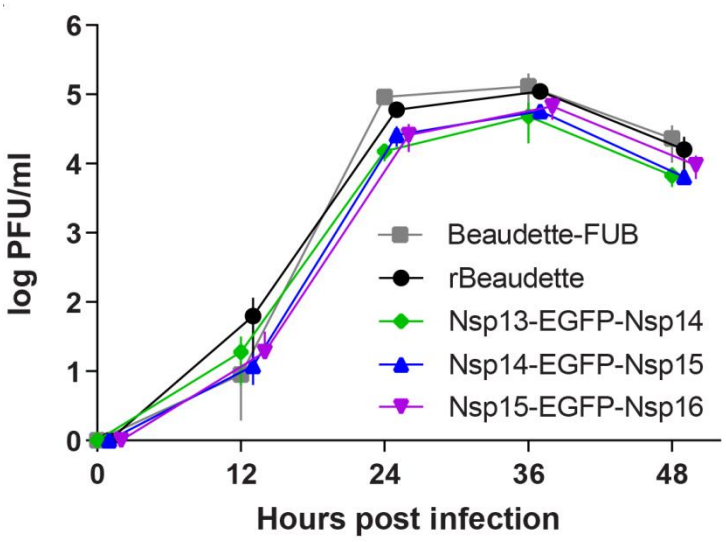

Figure 11. Characterization of replicase-EGFP viruses *in vitro*.

Multi-step growth kinetics of indicated viruses. DF-1 cells were infected with virus at MOI of 0.01 and viral progeny was titered at indicated h post infection. Data was shown as the mean of three independent experiments with standard deviations. ($p>0.05$, Kruskal-Wallis H test).

5.5 EGFP expression and processing in replicase-EGFP viruses

To determine if reporter EGFP was produced and processed from the viral replicase polyprotein by $3CL^{pro}$, DF-1 cells were infected with the rBeaudette as a negative control or three different replicase-EGFP viruses, respectively, and infected cell lysates were subjected to Western blotting by following the procedures described in 4.8.2. As expected, the EGFP protein was approximately 28 kDa in molecular weight and could be detected with a mouse anti-GFP monoclonal antibody (**Figure 12**), suggesting that the reporter molecule EGFP was expressed from the polyprotein and processed efficiently at the engineered cleavage sites instead of as fusions with adjacent non-structural proteins.

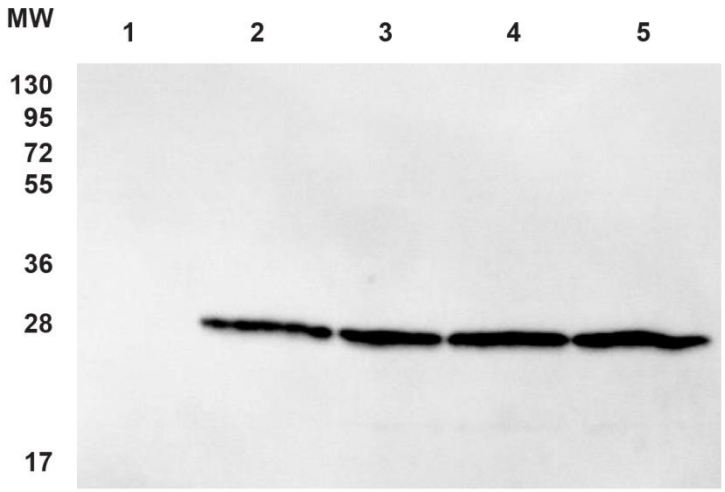

Figure 12. Expression and processing of EGFP in replicase-EGFP viruses.

DF-1 cells were either infected with replicase-EGFP viruses or transfected with a pEGFP-N1 plasmid as a positive control. The cell lysates were analysed by western blotting and detected with mouse anti-GFP monoclonal antibody. Lanes: 1 – rBeaudette; 2 – Nsp13-EGFP-Nsp14; 3 – Nsp14-EGFP-Nsp15; 4 – Nsp15-EGFP-Nsp16; 5 – cells transfected with the control plasmid pEGFP-N1.

5.6 Localization of EGFP in the replication organelles of IBV

As with other coronaviruses, RNA synthesis of IBV also occurs in the cytoplasm of host cells, in a network of interconnected double-membrane structures known as viral replication organelles (ROs) (Snijder et al. 2020). The ROs provide an optimal environment for viral RNA synthesis by concentrating viral replicative proteins and relevant host factors and spatially organizing different steps in the viral replication cycle. In addition, ROs can hide replication intermediates, which helps viruses escape innate immune defenses.

To test the localization of fluorescent proteins in infected cells, DF-1 cells seeded on coverslips were infected with either replicase-EGFP or replicase-mScarlet viruses. At 24 h post-infection, cells were fixed with 4% formalin, and dsRNA was stained with anti-dsRNA antibody J2. The images captured by the confocal microscopy showed that both dsRNA and fluorescence proteins were located in the cytoplasm of infected DF-1 cells. They colocalized in a small number of perinuclearly well-defined foci (**Figure 13AB**).

To compare the localization of replicase and plasmid-expressed EGFP in infected cells, DF-1 cells were transfected with a mCherry expression plasmid and, in the meantime, infected with Nsp13-EGFP-Nsp14 reporter viruses. We observed that the red fluorescence of mCherry was visible throughout the cells. In contrast, the green fluorescence was only present in small vesicles, indicating that in infected cells, replicase-expressed EGFP is restricted to specific

structures in the cytoplasm. (**Figure 13C**).

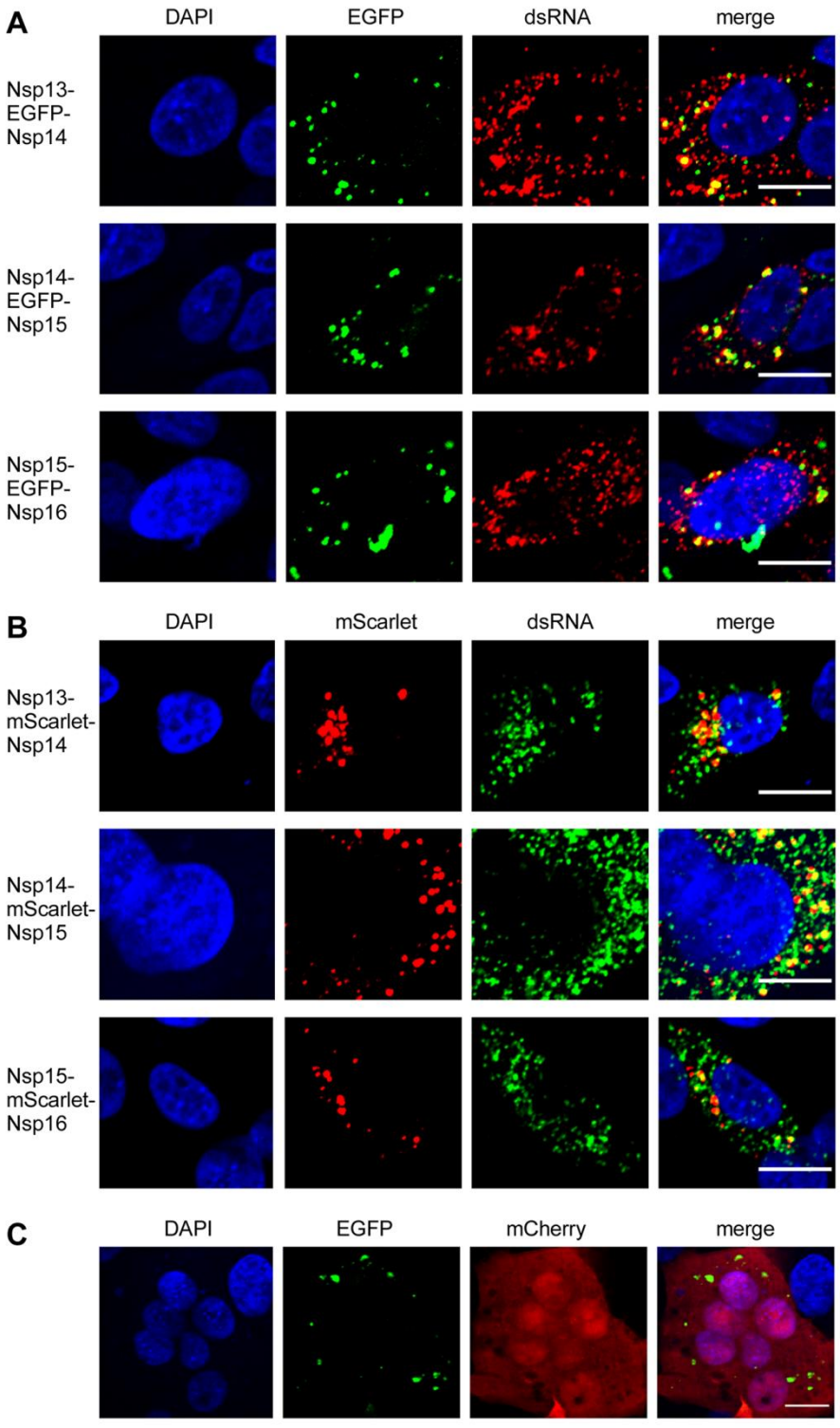

Figure 13. Intracellular location of dsRNA and reporter protein EGFP or mScarlet at 24 hours post-infection.

(A) Localization of EGFP and dsRNA in DF-1 cells infected with indicated replicase-EGFP Beaudette

viruses.

(B) Localization of mScarlet and dsRNA in DF-1 cells infected with indicated relicase-mScarlet Beaudette viruses.

(C) Subcellular localization of EGFP produced by Nsp13-EGFP-Nsp14 virus and mCherry produced by expression plasmid pmCherry in DF-1 cells. DF-1 cells were transiently transfected with the expression plasmid pmCherry and infected with Nsp13-EGFP-Nsp14 Beaudette virus. Scale bar, 10 μm.

Subsequently, the localization of EGFP and dsRNA in cells was determined at different time points after infection (6-12 hpi) with Nsp13-EGFP-Nsp14 viruses. We found that at the early stage of infection, dsRNA and EGFP colocalized in a small number of perinuclearly arranged spots (**Figure 14A**). Later in the infection, vesicles containing dsRNA or fluorescent proteins were dispersed throughout the cytoplasm. However, many structures still contained both dsRNA and fluorescent proteins, although a gradual decrease in the percentage of structures that contained both types of molecules was observed (**Figure 14C**).

The dsRNA has some limitations as a surrogate of RNA synthesis, as its presence is not always related to the site of active RNA synthesis. To confirm the colocalization of EGFP produced by replicase and the core components of the coronavirus replication machinery in DMVs, we added HA (YPYDVPDYA), 9 amino acids in length, to the N-terminus of nsp12, generating a modified Nsp13-EGFP-Nsp14 virus, which was referred to here as HA-Nsp12-EGFP. We successfully obtained the HA-Nsp12-EGFP virus, but the EGFP expression was lower than the parental virus, known as Nsp13-EGFP-Nsp14. To confirm the colocalization of EGFP and RdRp (nsp12), we infected DF-1 cells seeded on coverslips with the HA-Nsp12-EGFP virus. Infected cells were fixed at different time points post-infection, and RdRp with an HA-tag was detected using an anti-HA tag antibody (**Figure 14B**). We found that the colocalization percentage of EGFP and RdRp remained constant, above 95% (**Figure 14C**).

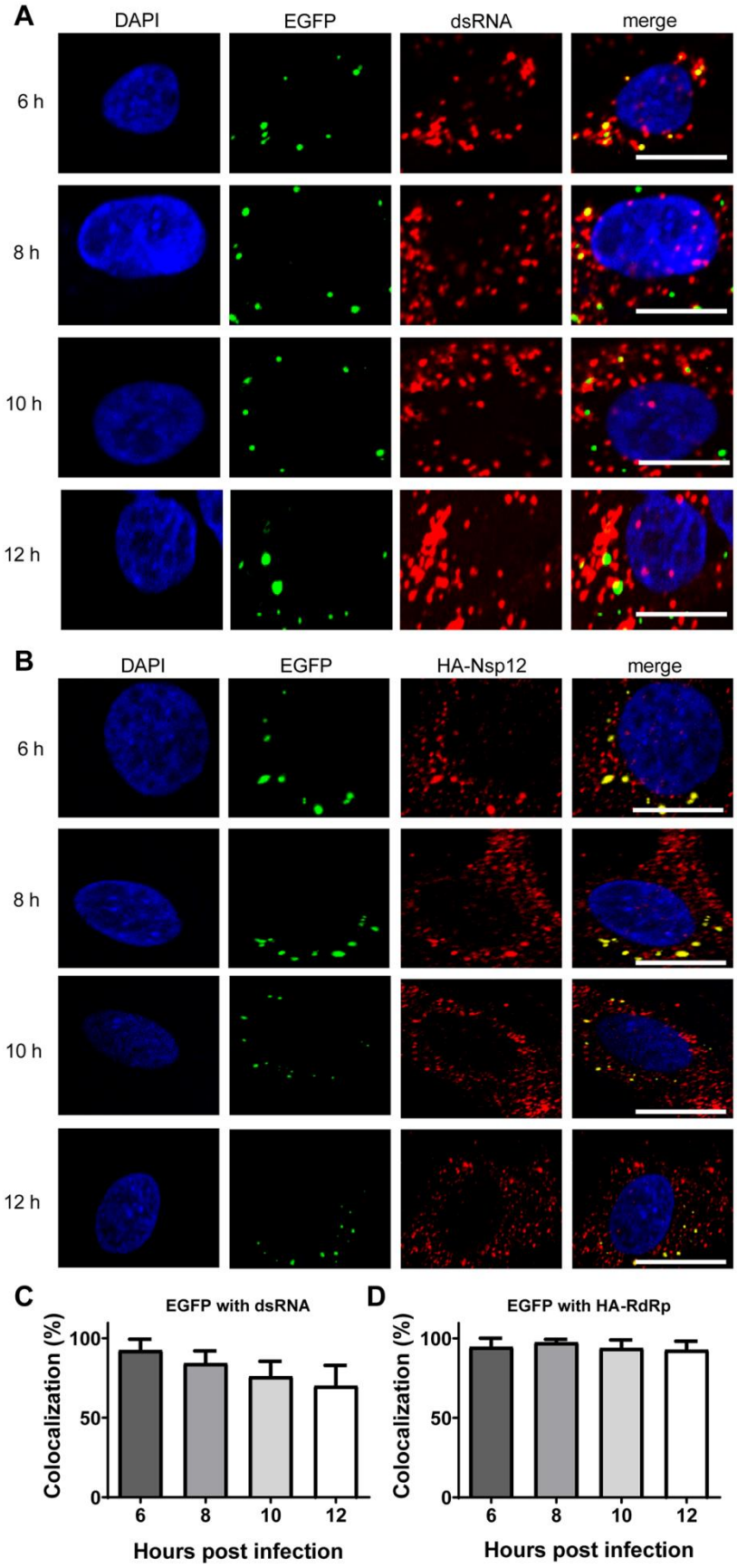

Figure 14. Colocalization of EGFP with dsRNA or HA-RdRp in DF-1 cells infected with Nsp13-

EGFP-Nsp14 Beaudette virus.

(A) Localization of EGFP with dsRNA in infected DF-1 cells at different time points after infection.

(B) Localization of EGFP with HA-tagged Nsp12 in infected DF-1 cells at different time points after infection.

(C, D) The percentage of colocalization of EGFP with dsRNA, and EGFP with HA-RdRp at different time points after infection in DF-1 cells. Scale bar, 10 μm.

5.7 Genetic stability of replicase-EGFP viruses during serial passage in cell culture

To test whether the replicase gene could stably express EGFP, we serially passaged three different replicase-EGFP viruses in DF-1 cells 20 times. The cell supernatant of each passage was harvested and centrifuged to remove the cell debris. The supernatants collected from P1, P5, P10, P15, and P20 were selected for plaque assay.

The EGFP in Nsp13-EGFP-Nsp14 was stably expressed after 20 serial passages (**Figure 15A**). In Nsp14-EGFP-Nsp15, the expression of EGFP was slightly affected at P5 and completely abrogated after 10 serial passages **(Figure 15A**). The first Nsp15-EGFP-Nsp16 variants without EGFP expression were detected after 15 serial passages, and after the 20th passage, no EGFP-expressed variants could be detected (**Figure 15A**).

To examine whether EGFP was stably integrated into viral replicase, we extracted viral RNA from respective viruses at different passages, including P1, P5, P10, P15, and P20, and amplified the corresponding region with the primers listed in 3.1.14 and further sequenced the targeted region by Sanger sequencing. In comparison with the plaque-based assay, the RT-PCR showed similar results. In the Nsp13-EGFP-Nsp14, the EGFP was stably integrated between Nsp13 and Nsp14 from P1 to P20 (**Figure 15B**). However, in Nsp14-EGFP-Nsp15 viruses, intact EGFP was detected only at P1, but partial viruses carried EGFP deletion at P5, and viruses lacking the introduced insertion completely outcompeted the original mutant virus after the 10th passage (**Figure 15B**). In contrast, the complete EGFP insertion of Nsp15-EGFP-Nsp16 was only intact until P10. Starting from P15, the EGFP-deficient virus population was detected, and the EGFP insertion was lost entirely at P20 (**Figure 15B**). From the sequencing data of the targeted region, we found that only the Nsp13-EGFP-Nsp14 virus had an intact insertion sequence. Viral variants, including Nsp14-EGFP-Nsp15 and Nsp15-EGFP-Nsp16, lost the ability to express EGFP and lacked the EGFP sequence. In Nsp14-EGFP-Nsp15 at P10, the entire EGFP and the engineered duplicate 3CL^{pro} cleavage site sequences were accurately deleted from its genome. However, in Nsp15-EGFP-Nsp16 at P20, only the EGFP ORF was deleted, and duplicated sequences were retained.

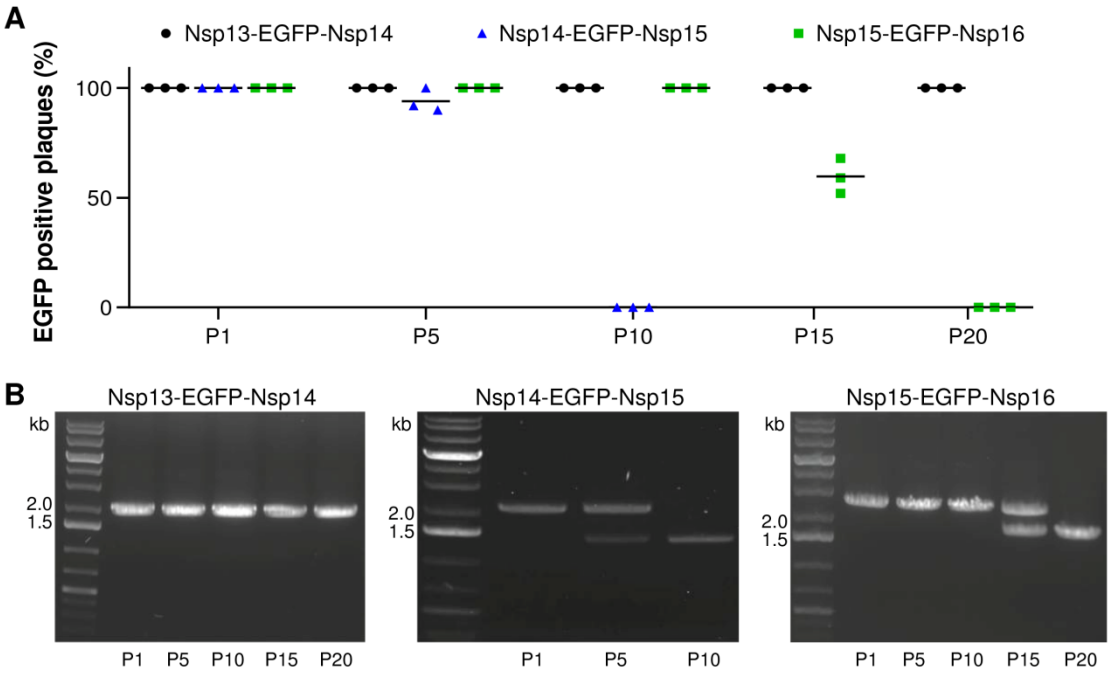

Figure 15. Genetic stability of recombinant replicase-EGFP Beaudette viruses after 20 serial passages in DF-1 cells.

(A) The recombinant replicase-EGFP Beaudette viruses were passaged 20 times in DF-1 cells. The supernatant of infected cells at P1, P5 P10, P15 and P20 was harvested and used for plaque assay. The percentage of viruses expressing EGFP was assessed by random selection of 50 plaques followed by determination of EGFP expression.

(B) The region with EGFP insertion was amplified with indicated set of primers and analyzed by sequencing. Amplicon of Nsp13-EGFP-Nsp14: with EGFP (1.9 kb), without EGFP (1.2 kb); amplicon of Nsp14-EGFP-NSP15: with EGFP (2 kb), without EGFP (1.3 kb); amplicon of Nap15-EGFP-Nsp16: with EGFP (2.5 kb), without EGFP (1.8 kb).

To investigate whether the insertion of EGFP into the replicase gene had any significant effect on virus growth, multi-step replication growth kinetics and plaque size assays were performed, as described above. Although the Nsp14-EGFP-Nsp15 virus lost the inserted EGFP ORF at P10, the growth capacity and plaque size of all three passaged mutants in DF-1 cells were comparable to those of the parental virus (**Figure 16**).

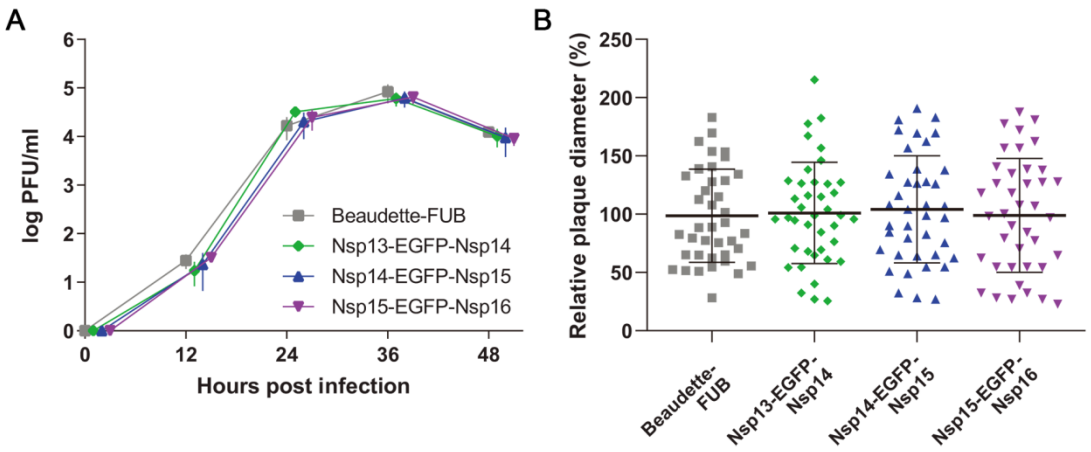

Figure 16. Growth properties of replicase-EGFP viruses from P10.

(A) Multi-step growth kinetics of parental Beaudette-FUB and three replicase-EGFP reporter viruses from 10th passage on DF-1 cells.

(B) Plaque sizes of the parental Beaudette-FUB and replicase-EGFP reporter viruses from the 10th passage on DF-1 cells.

To further confirm the sequencing data of engineered viruses from P10 obtained by RT-PCR and Sanger sequencing. We performed NGS, analyzed the sequencing data, and found that the genes of the parental and replicase-EGFP viruses were stable, except for inserted sequences in the Nsp14-EGFP-Nsp15 mutant viruses. In most Nsp14-EGFP-Nsp15 viruses of P10, the insertion sequences, consisting of the EGFP ORF and duplicated 3CL^{pro} cleavage site sequences, were removed entirely from the IBV genome. Furthermore, we found that the genetic diversity of all four virus populations was low. Only the Nsp14-EGFP-Nsp15, which ultimately lost the EGFP ORF by passage 10, accumulated 3 SNPs with a frequency greater than 10% (**Table 3**). At the same time, the recombinant Nsp13-EGFP-Nsp14 viruses were genetically stable after 20 serial passages in DF-1 cells. Only a small number of mutations were observed in the Nsp13-EGFP-Nsp14 population, suggesting that the insertion of EGFP between Nsp13 and Nsp14 did not affect the function of Nsp14, known as the RNA exonuclease, which plays a vital role in the proofreading of RNA. Since EGFP was inserted between nsps required for viral RNA processing, it would be valuable to characterize their enzymatic activities that could have been affected by the EGFP ORF insertion. We examined whether the EGFP ORF insertion affected genomic and subgenomic RNA synthesis by sequencing the viral RNA isolated from infected cells and cell culture medium by high-throughput sequencing. The analysis of the transcription profiles indicated that the insertion of heterologous sequences into the virus genomes did not affect genomic RNA and subgenomic RNA synthesis. The complete genomic RNA was detected, and subgenomic RNAs, encoding structural and accessory proteins, were also produced.

Table 3. SNPs detected in virus populations from 10th passages in DF-1 cells at a frequency greater than 10%

Virus	Nucleotide position	Genomic region	Mutation	Mutation (%)
nsp14-EGFP-nsp15	9,631	nsp5	A766C, S256R	16.9
nsp14-EGFP-nsp15	15,853	nsp13	G722T, C241F	14.9
nsp14-EGFP-nsp15	17,272	nsp14	C341T, A114V	30.1

5.8 Application of replicase-EGFP virus in antivirals screening

To determine whether our recombinant replicase-EGFP viruses can be applied in high-throughput screening of antiviral compounds, one of our EGFP reporter viruses, Nsp13-EGFP-Nsp14, was selected for evaluating the antiviral activity of two widely used inhibitors in coronaviruses, GC376 (3CL^{pro} inhibitor) and EIDD-2801 (Monupiravir, ribonucleoside analog). The inhibition was tested not only by flow cytometry but also by plaque size assay. As expected, the tested concentrations of GC376 or EIDD-2801 had no cytotoxicity on DF-1 cells (**Figure 17**), but fluorescence was significantly reduced or disappeared when higher concentrations of antivirals were applied (**Figure 17**). In our experiment, the half maximal effective concentrations (EC_{50}) of GC376 against IBV were 1.0 μM and 1.7 μM determined by plaque assays and flow cytometry, respectively. These results were in good agreement with the published EC_{50} values for IBV (0.58 μM). Likewise, the EC_{50} values of EIDD-2801 against IBV were 24 nM and 29 nM, also determined by plaque assays and flow cytometry, respectively. They were comparable to those reported for MERS-CoV (150 nM) and SARS-CoV-2 (80-300 nM). Overall, the results suggested the potential of our replicase-EGFP virus for large-scale screening of antiviral compounds.

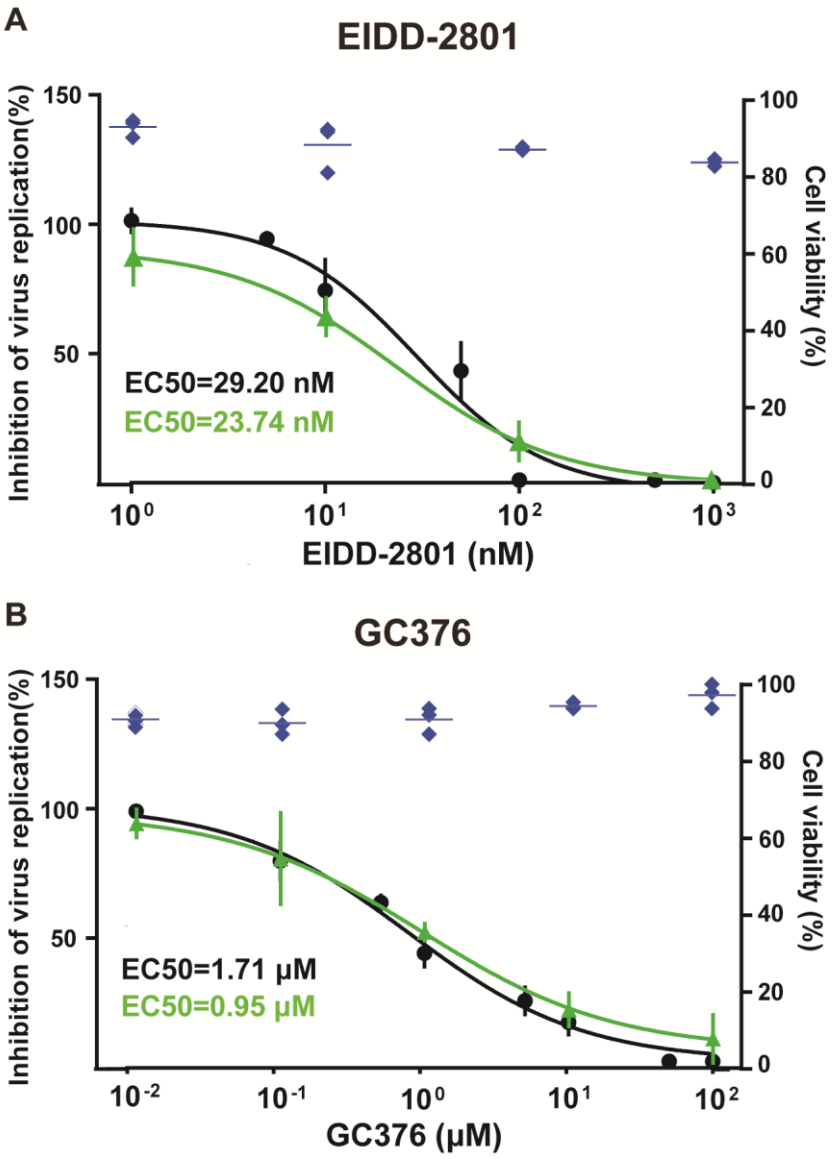

Figure 17. Inhibitory effect of EIDD-2801 and GC376 on the replication of reporter virus Nsp13-EGFP-Nsp14 in DF-1 cells.

The cytotoxicity and inhibitory effects of EIDD-2801 **(A)** or GC376 **(B)** on the replication of reporter virus Nsp13-EGFP-Nsp14 were determined in DF-1 cells. DF-1 cells were infected in triplicate with the reporter virus at an MOI of 0.01 in the presence of various amounts of EIDD-2801 (1, 5, 10, 50, 100, 500, or 1,000 nM) or GC376 (0.01, 0.1, 1, 10, or 100 μM). Replication of reporter virus was determined after 24 hours by quantifying EGFP production by flow cytometry (black dots) or plaque assay (green triangles). Cytotoxicity of EIDD-2801 and GC376 to DF-1 cells was determined in uninfected cells using a colorimetric assay (Cell Counting Kit 8; blue diamonds). Relative EGFP production is expressed as mean ± SD with nonlinear fit curve (n = 3). Cell viability was determined by comparison with DF-1 cells treated with vehicle (DMSO) only.

6. Discussion

6.1 Existing reverse genetics system of coronavirus

The availability of the reverse genetics system allows us to produce genetically modified viruses and investigate their molecular biology. Several reverse genetics systems for coronaviruses have been developed, including targeted RNA recombination, *in vitro* ligation of subgenomic fragments, vaccinia virus-based, and BAC or YAC-based reverse genetics systems.

The first established method for genetically manipulating coronavirus genomes is targeted RNA recombination, but it is limited to mutagenesis at the most 3'-proximal of the genomes. This method was used to create the reverse genetics system for the IBV strain H52. They recombined the spike glycoprotein from the mouse hepatitis virus (MHV) into the spike region of H52, which spread its cell tropism to mammalian cell lines. However, there are still some limitations to targeted RNA recombination, such as the difficulty in modifying the viral polymerase genes (Beurden et al. 2017).

The *in vitro* ligation of subgenomic fragments solves the problem that some regions in IBV replicase are unstable and potentially harmful to the host bacteria. Natural restriction sites were selected to avoid introducing additional modified sequences to the IBV genome. Continuous IBV genomic cDNAs were amplified, followed by digestion with restriction enzymes. Subsequently, the digested IBV cDNAs were ligated in one T4 ligase reaction. To recover viruses, a full-length cDNA containing the T7 or S6 promoter, located upstream of the IBV genome, was transcribed and electroporated into BHK-21 cells, along with an additional N gene transcript. However, finding appropriate restriction sites in the IBV genome is not always easy. Although Type IIS restriction enzymes that cleave outside their recognition sequences, such as BsmBI and BsaI, were employed to achieve ligation without introducing additional restriction enzyme sites, the procedure of ligating multiple DNA fragments is time-consuming, complicated, and labor-intensive (Zhou et al. 2013).

The reverse genetics system based on the vaccinia virus involves the construction of full-length IBV cDNA in a vaccinia virus vector. In this system, the step of *in vitro* ligation cannot be avoided, even though it only needs to be assembled once. Additionally, using commercial *in vitro* transcription kits to generate infectious RNA genomes is more expensive, and RNA instability always affects the recovery efficiency of viruses (Casais et al. 2001). Controlling mutagenesis of the coronavirus genome, which occurs via homologous recombination in eukaryotic cells, is also difficult.

The most cutting-edge way to rescue coronavirus is the BAC or YAC-based reverse genetics system, which has been developed for a variety of coronaviruses, including TGEV, SARS-CoV, FIPV, and MERS-CoV (Almazán et al. 2000; Almazán et al. 2006; Bálint et al. 2012; Scobey et

al. 2013).

In our study, we successfully established a reverse genetics system for the IBV strain Beaudette-FUB by homologous recombination in a BAC, allowing us to modify IBV genes regardless of where they are located in the viral genome. The virus sequences that have been cloned in BACs are extremely stable and can be easily and rapidly manipulated using well-established mutagenesis techniques of bacterial genome engineering, such as seamless "*en passant*" bacterial mutagenesis. In addition, viruses can be recovered directly by DNA transfection, and there is no need to transcribe DNA into RNA *in vitro*.

6.2 The role of nucleocapsid protein N in virus recovery

Since coronaviruses depend on N proteins for efficient genome replication, the presence of N proteins has significantly improved the efficiency of virus rescue (Yount et al. 2000). Some researchers found that virus recovery was only achieved by adding a eukaryotic plasmid expressing N protein (Casais et al. 2001) or the RNA transcript (Youn et al. 2005), indicating that IBV could not be recovered from either the vaccinia virus-based infectious clone (Casais et al. 2001) or the *in vitro* produced full-length IBV RNA transcript (Youn et al. 2005) without concurrent expression of N protein. According to our findings, the virus could be rescued without the N protein, but its efficiency was significantly higher when it was present.

6.3 IBV Beaudette mutants expressing reporter proteins from the replicase gene

When we started working on this project, we attempted to create an EGFP virus by replacing gene ORF3a or ORF4b with EGFP or inserting EGFP between ORFs M and 5a, known as the intergenic region. Nonetheless, all recombinant viruses were unrecoverable, with no or weak fluorescent proteins and genetic instability. As a result, we intended to test whether EGFP could be inserted into the replicase. As with other nonstructural proteins, EGFP was produced from the replicase gene and released through IBV main protease processing.

The replicase polyprotein was autocatalytically processed by two proteases, the PL^{pro} and the $3CL^{pro}$. Since there are more $3CL^{pro}$ than PL^{pro} cleavage sites in the IBV genome, and they are located at different sites of the ORF1ab gene, we thought that investigating which of the eleven $3CL^{pro}$ cleavage sites can tolerate the insertion of the foreign sequence would have a greater chance of success than exploring the PL^{pro} cleavage sites. In hindsight, to make the study more complete, we should have examined the insertion of EGFP ORF at the two PL^{pro} cleavage sites.

To determine whether the viral replicase gene could tolerate the foreign reporter gene, we inserted the reporter gene EGFP into each of the available $3CL^{pro}$ cleavage sites in the replicase gene. Analysis of cleavage site sequences in the coronavirus replicase gene revealed that the optimal cleavage site sequences differ distinctly among different coronaviruses. Furthermore, previous studies showed that the context of the cleavage site is closely related to the efficiency of cleavage. To ensure efficient cleavage between the

nonstructural and fluorescent proteins, we added 21-nt-long sequences to the 5’ and 3’ ends of the EGFP ORF, creating EGFP flanked by 14-aa-long $3CL^{pro}$ cleavage sites.

In our study, we found that viruses can be recovered from mutant constructs with EGFP or mScarlet ORFs inserted between the coding sequences of the nsps located at the outermost 3' end of the replicase gene, including helicase (nsp13), RNA exonuclease (nsp14), RNA endonuclease (nsp15), and RNA methyltransferase (nsp16), suggesting that IBV replicase can tolerate the introduction of foreign genetic material. However, we have no plausible explanation for why only the position located at the 3’ end of replicase gene 1 tolerates the insertion of reporter genes. We speculate that we could not recover most of the mutants because the insertion of the EGFP coding sequences before the ribosomal frameshifting element interferes with -1 ribosomal frameshifting and, thus, the production of RdRp, which is essential for viral replication. If this is true, the Nsp12-EGFP-Nsp13 mutant should be viable. Nevertheless, despite several additional attempts, we could not recover an infectious virus from such a DNA construct.

Because ribosomal frameshifting occurs at approximately 15-30% efficiency in various coronaviruses, proteins produced by ORF1b are less abundant than those produced by ORF1a. An alternative explanation for the inability to recover EGFP viruses carrying EGFP ORF inserted into ORF1a could be that higher EGFP production could be lethal to virus replication. We think more light can be shed on this problem by constructing similar mutants in different coronaviruses.

6.4 Genetic stability of the reporter virus after serial passage

Most studies constructed recombinant reporter viruses by replacing accessory genes or inserting reporter genes in the viral genome distal to the replicase, but none had desirable genetic stability to date. It has been investigated that reporter genes, such as EGFP or Renilla luciferase, can be expressed by replacing the ORF5 in the IBV infectious clone and that EGFP exhibited stability in chicken kidney cells until passage 8 (Shen et al. 2009). Similarly, a recombinant Beaudette virus with a reporter gene instead of the ORF5a gene grew on Vero cells at a 10-fold lower titer than the parental viruses. The genetic instability of EGFP was observed in Vero cells at passage 6 (Youn et al. 2005). When the EGFP ORF replaced the intergenic region, EGFP expression was abrogated in primary CK cells at passage 7 (Bentley et al. 2013a) and Vero cells at passage 5 (Shen et al. 2009). So far, the recombinant mutant with the firefly luciferase gene inserted into gene 3ab is the most genetically stable. Loss of EGFP was detectable at P15 in cell culture (Haan et al. 2005).

6.5 Colocalization of EGFP with dsRNA and RdRp

Coronavirus replication occurs in the cytoplasm, in an intricate reticulate double-membrane structure surrounding the nucleus known as viral replication organelles (Snijder et al. 2020). The core proteins of the replication and transcription complex (RTCs), newly synthesized

dsRNA, and nascent viral RNA were colocalized in a small number of perinuclearly arranged spots at the start of replication (Maier et al. 2013; Snijder et al. 2020). In the late stages of viral infection, foci containing dsRNA or virus replication machinery were distributed throughout the cytoplasm. In addition, the percentage of vesicles containing both of them decreased over time (Hagemeijer et al. 2012). Since fluorescent proteins were released from the replicase polyprotein by the cleavage of $3CL^{pro}$, it is reasonable to assume that they, like other replicase proteins, were present in a small number of well-defined vesicles during the early stages of replication. In our study, EGFP and dsRNA colocalized in small foci located perinuclearly, confirming our hypothesis. As the infection progressed, EGFP-containing vesicles became more widely distributed throughout the cytoplasm, while the percentage of EGFP and dsRNA colocalization decreased. However, the presence of dsRNA is not always associated with active RNA synthesis (Hagemeijer et al. 2012), so it is meaningful to give insight into the colocalization of EGFP and viral RdRp. Our finding indicated that EGFP always colocalized with RdRp throughout infection, with up to 95% colocalization.

6.6 Concluding remarks and outlook

During my Ph.D., we successfully constructed the infectious BAC clone of the IBV strain Beaudette-FUB, a cell-adapted strain that can propagate in a variety of cell lines, including DF-1 cells and BHK-cells. There is no need to prepare time-consuming and labor-intensive primary chicken embryonic kidney cells from 18-day-old embryonated eggs. The main disadvantage of using non-virulent IBV strains is that they cannot provide insights into the infection process in chickens because they do not cause a clinically relevant phenotype *in vivo*. As a result, we urgently need to establish a reverse genetics system for pathogenic stains, such as M41 and QX-like IBV strains, to identify virulence factors. We attempted to replace the Beaudette genome in pBeadeutte with the M41 genome by multiple "*en passant*" recombination in *E. coli* to produce an infectious BAC clone for pathogenic strain M41. Nevertheless, we failed to rescue viruses from this BAC. The reason for this should be studied further.

In addition, we identified three EGFP insertion positions in the replicase gene, which can tolerate foreign sequences in the IBV genome. It may be possible to produce heterologous proteins using IBV as an expression vector, allowing for the development of multivalent virus vaccines. Additionally, one EGFP-replicase virus, known as Nsp13-EGFP-Nsp14, which can stably express EGFP protein and has comparable growth properties to the parental virus, could be used as a fluorescent indicator at the early stage of infection. We used reporter viruses to successfully test two antiviral drugs using flow cytometry, so using Nsp13-EGFP-Nsp14 in antiviral screening appears promising.

Summary

Avian coronavirus, also known as infectious bronchitis virus (IBV), belongs to the genus *Gammacoronavirus* and is the causative agent of infectious bronchitis, a highly contagious respiratory disease in the poultry industry.

In virology studies, reverse genetics systems based on BACs are extremely valuable because they allow us to manipulate viral genes. In our study, we assembled the complete genome of the IBV strain Beaudette-FUB into an artificial bacterial chromosome (BAC), producing an infectious BAC clone. From this constructed IBV BAC clone, we successfully rescued infectious viruses with identical growth characteristics to the parental viruses. To establish genetically stable EGFP viruses, we then inserted the EGFP ORF into 11 putative cleavage sites of $3CL^{pro}$. Of these, we identified three insertion sites located at the outermost 3' end of the replicase gene– between the coding sequences of Nsp13 (helicase), Nsp14 (RNA exonuclease), Nsp15 (RNA endonuclease), and Nsp16 (RNA methyltransferase) could tolerate heterologous genes in the IBV genome. Additionally, we found that fluorescent proteins expressed by the replicase gene can be efficiently cleaved by the $3CL^{pro}$ and released from the replicase polyprotein. Furthermore, we also determined the genetic stability of these three EGFP-replicase viruses. Among them, the engineered Nsp13-EGFP-Nsp14 virus still exhibited high stability in DF-1 cells after 20 serial passages. The colocalization results showed that EGFP, together with dsRNA or RdRp, accumulated in the well-defined foci at the early stage of infection. When the infection progressed, EGFP proteins were produced and distributed throughout the cytoplasm.

Our studies have shown that the replicase-EGFP viruses could be used to study viral replication and transcription, to screen antiviral drugs on a large scale, to develop multivalent vaccines, and even that the potential positions could be applied to other coronaviruses.

Zusammenfassung

Entwicklung und Charakterisierung von Mutanten des Vogel-Coronavirus, die Reporterproteine des Replicase-Gens exprimieren

Das aviäre Coronavirus, bekannt als Infektiöses Bronchitisvirus (IBV), ist ein Virus der Gattung Gammacoronavirus, welches eine infektiöse Bronchitis, eine akute, hochansteckende Atemwegserkrankung bei Hühnern, verursacht.

Reverse-Genetik-Systeme sind äußerst wertvolle Werkzeuge in der Virologie, da diese eine zügige genetische Manipulation viraler Genome ermöglichen und so die angewandte und die Grundlagenforschung voranbringen. Hier berichten wir über die Konstruktion eines infektiösen Klons des IBV-Stammes Beaudette als künstliches Bakterienchromosom (BAC). Der konstruierte IBV-Klon in voller Länge ermöglichte die Rückgewinnung eines infektiösen Virus, das phänotypisch nicht vom Elternvirus zu unterscheiden war. Wir verwendeten den infektiösen IBV-Klon um zu untersuchen, ob EGFP, ein grün fluoreszierendes Protein, vom Replikase-Gen ORF1 produziert werden kann und autokatalytisch vom Replikase-Polyprotein durch Spaltung mittels 3CLpro, freigesetzt werden kann. Wir fanden heraus, dass IBV die Insertion des EGFP-ORF am 3'-Ende des Replicase-Gens toleriert - zwischen den kodierenden Sequenzen von Nsp13 (Helikase), Nsp14 (RNA-Exonuklease), Nsp15 (RNA-Endonuklease) und Nsp16 (RNA-Methyltransferase). Wir zeigen außerdem, dass EGFP effizient vom Replikase-Polyprotein gespalten wird und zusammen mit viraler RNA-Polymerase und doppelsträngiger RNA, einem Zwischenprodukt der IBV-Genomreplikation, in Doppelmembran-Vesikeln lokalisiert werden kann. Eines der gentechnisch hergestellten Reporter-EGFP-Viren, Nsp13-EGFP-Nsp14, blieb über 20 serielle Passagen hinweg in DF-1-Zellen genetisch stabil.

Wir zeigen, dass Reporter-EGFP-Viren zur Untersuchung der Virusreplikation in Wirtszellen, zum Beispiel zur Entdeckung antiviraler Arzneimittel und zur Entwicklung diagnostischer Tests, verwendet werden können. Diese Strategie kann genutzt werden, um IBV als Vektor zu verwenden, der andere heterologe Sequenzen exprimiert, oder um multivalente virale Impfstoffe zu entwickeln. Die Positionierung von fluoreszierenden ORFs innerhalb des Replikase-Gens kann zur fluoreszierenden Markierung von Stellen aktiver viraler Replikation verwendet werden und sollte auch auf andere Coronaviren anwendbar sein.

References

Albassam, M.A., Winterfield, R.W. and Thacker, H.L. 1986. Comparison of the nephropathogenicity of four strains of infectious bronchitis virus. *Avian Diseases* 30(3), p. 468. doi: 10.2307/1590408.

Alexander, D.J., Gough, R.E. and Pattison, M. 1978. A long-term study of the pathogenesis of infection of fowls with three strains of avian infectious bronchitis virus. *Research in Veterinary Science* 24(2), pp. 228–233. doi: 10.1016/s0034-5288(18)33077-7.

Almazán, F. et al. 2006. Construction of a severe acute respiratory syndrome coronavirus infectious cDNA clone and a replicon to study coronavirus RNA synthesis. *Journal of Virology* 80(21), pp. 10900–10906. doi: 10.1128/jvi.00385-06.

Almazán, F., González, J.M., Pénzes, Z., Izeta, A., Calvo, E., Plana-Durán, J. and Enjuanes, L. 2000. Engineering the largest RNA virus genome as an infectious bacterial artificial chromosome. *Proceedings of the National Academy of Sciences* 97(10), pp. 5516–5521. doi: 10.1073/pnas.97.10.5516.

Armesto, M., Cavanagh, D. and Britton, P. 2009. The replicase gene of avian coronavirus infectious bronchitis virus is a determinant of pathogenicity. *PLoS ONE* 4(10), p. e7384. doi: 10.1371/journal.pone.0007384.

Bálint, Á. et al. 2012. Molecular characterization of feline infectious peritonitis virus strain DF-2 and studies of the role of ORF3abc in viral cell tropism. *Journal of virology* 86(11), pp. 6258–67. doi: 10.1128/jvi.00189-12.

Beach, J.R. and Schalm, O.W. 1936. A filterable virus, distinct from that of laryngotracheitis, the cause of a respiratory disease of chicks. *Poultry Science* 15(3), pp. 199–206. doi: 10.3382/ps.0150199.

Becares, M., Pascual-Iglesias, A., Nogales, A., Sola, I., Enjuanes, L. and Zuñiga, S. 2015. Mutagenesis of coronavirus nsp14 reveals its potential role in modulation of the innate immune response. *Journal of virology* 90(11), pp. 5399–5414. doi: 10.1128/jvi.03259-15.

Bentley, K., Armesto, M. and Britton, P. 2013a. Infectious bronchitis virus as a vector for the expression of heterologous genes. *PLoS ONE* 8(6), p. e67875. doi: 10.1371/journal.pone.0067875.

Bentley, K., Keep, S.M., Armesto, M. and Britton, P. 2013b. Identification of a noncanonically transcribed subgenomic mRNA of infectious bronchitis virus and other *gammacoronaviruses*. *Journal of Virology* 87(4), pp. 2128–2136. doi: 10.1128/jvi.02967-12.

Beurden, S.J. van et al. 2017. A reverse genetics system for avian coronavirus infectious bronchitis virus based on targeted RNA recombination. *Virology Journal* 14(1), p. 109. doi: 10.1186/s12985-017-0775-8.

Bickerton, E., Maier, H.J., Stevenson-Leggett, P., Armesto, M. and Britton, P. 2018. The S2 subunit of infectious bronchitis virus Beaudette is a determinant of cellular tropism. *Journal of Virology* 92(19), pp. e01044-18. doi: 10.1128/jvi.01044-18.

Boursnell, M.E.G., Brown, T.D.K., Foulds, I.J., Green, P.F., Tomley, F.M. and Binns, M.M. 1987. Completion of the sequence of the genome of the coronavirus avian infectious bronchitis virus. *Journal of General Virology* 68(1), pp. 57–77. doi: 10.1099/0022-1317-68-1-57.

Bouvet, M. et al. 2014. Coronavirus Nsp10, a critical co-factor for activation of multiple replicative enzymes. *The Journal of Biological Chemistry* 289(37), pp. 25783–25796. doi: 10.1074/jbc.m114.577353.

Brierley, I., Boursnell, M.E., Binns, M.M., Bilimoria, B., Blok, V.C., Brown, T.D. and Inglis, S.C. 1987. An efficient ribosomal frame-shifting signal in the polymerase-encoding region of the coronavirus IBV. *The EMBO journal* 6(12), pp. 3779–85.

Britton, P., Armesto, M., Cavanagh, D. and Keep, S. 2012. Modification of the avian coronavirus infectious bronchitis virus for vaccine development. *Bioengineered* 3(2), pp. 114–119. doi: 10.4161/bbug.18983.

Britton, P., Evans, S., Dove, B., Davies, M., Casais, R. and Cavanagh, D. 2005. Generation of a recombinant avian coronavirus infectious bronchitis virus using transient dominant selection. *Journal of Virological Methods* 123(2), pp. 203–211. doi: 10.1016/j.jviromet.2004.09.017.

Britton, P., Green, P., Kottier, S., Mawditt, K.L., Penzes, Z., Cavanagh, D. and Skinner, M.A. 1996. Expression of bacteriophage T7 RNA polymerase in avian and mammalian cells by a recombinant fowlpox virus. *Journal of General Virology* 77(5), pp. 963–967. doi: 10.1099/0022-1317-77-5-963.

Carstens, E.B. and Ball, L.A. 2009. Ratification vote on taxonomic proposals to the International Committee on Taxonomy of Viruses (2008). *Archives of Virology* 154(7), pp. 1181–1188. doi: 10.1007/s00705-009-0400-2.

Casais, R., Davies, M., Cavanagh, D. and Britton, P. 2005. Gene 5 of the avian coronavirus infectious bronchitis virus is not essential for replication. *Journal of virology* 79(13), pp. 8065–78. doi: 10.1128/jvi.79.13.8065-8078.2005.

Casais, R., Dove, B., Cavanagh, D. and Britton, P. 2003. Recombinant avian infectious bronchitis virus expressing a heterologous spike gene demonstrates that the spike protein is a determinant of cell tropism. *Journal of virology* 77(16), pp. 9084–9. doi: 10.1128/jvi.77.16.9084-9089.2003.

Casais, R., Thiel, V., Siddell, S.G., Cavanagh, D. and Britton, P. 2001. Reverse genetics system for the avian coronavirus infectious bronchitis virus. *Journal of Virology* 75(24), pp. 12359–12369. doi: 10.1128/jvi.75.24.12359-12369.2001.

Case, J.B. et al. 2018. Murine hepatitis virus nsp14 exoribonuclease activity Is required for resistance to innate immunity. *Journal of Virology* 92(1). doi: 10.1128/jvi.01531-17.

Cavanagh, D. 2001. A nomenclature for avian coronavirus isolates and the question of species status. *Avian Pathology* 30(2), pp. 109–115. doi: 10.1080/03079450120044506.

Cavanagh, D. 2003. Severe acute respiratory syndrome vaccine development: experiences of vaccination against avian infectious bronchitis coronavirus. *Avian Pathology* 32(6), pp. 567–582. doi: 10.1080/03079450310001621198.

Cavanagh, D. 2007. Coronavirus avian infectious bronchitis virus. *Veterinary Research* 38(2), pp. 281–297. doi: 10.1051/vetres:2006055.

Cavanagh, D. et al. 2007. Manipulation of the infectious bronchitis coronavirus genome for vaccine development and analysis of the accessory proteins. *Vaccine* 25(30), pp. 5558–5562. doi: 10.1016/j.vaccine.2007.02.046.

Cavanagh, D., Davis, P.J. and Cook, J.K.A. 1992. Infectious bronchitis virus: Evidence for recombination within the Massachusetts serotype. *Avian Pathology* 21(3), pp. 401–408. doi: 10.1080/03079459208418858.

Cavanagh, D., Picault, J.-P., Gough, R.E., † M.H., Mawditt, K. and Britton, P. 2005. Variation in the spike protein of the 793/B type of infectious bronchitis virus, in the field and during alternate passage in chickens and embryonated eggs. *Avian Pathology* 34(1), pp. 20–25. doi: 10.1080/03079450400025414.

Chen, H.W., Huang, Y.P. and Wang, C.H. 2010. Identification of intertypic recombinant infectious bronchitis viruses from slaughtered chickens. *Poultry Science* 89(3), pp. 439–446. doi: 10.3382/ps.2009-00322.

Chen, S. et al. 2019. Feline infectious peritonitis virus Nsp5 inhibits type I interferon production by cleaving NEMO at multiple sites. *Viruses* 12(1), p. 43. doi: 10.3390/v12010043.

Chiem, K., Ye, C. and Martinez‐Sobrido, L. 2020. Generation of recombinant SARS‐CoV‐2 using a bacterial artificial chromosome. *Current Protocols in Microbiology* 59(1), p. e126. doi: 10.1002/cpmc.126.

Chomiak, T.W., Luginbuhl, R.E. and Jungherr, E.L. 1958. The propagation and cytopathogenic effect of an agg-adapted strain of infectious bronchitis virus in tissue culture. *Avian Diseases* 2(4), p. 456. doi: 10.2307/1587486.

Collisson, E.W., Pei, J., Dzielawa, J. and Seo, S.H. 2000. Cytotoxic T lymphocytes are critical in the control of infectious bronchitis virus in poultry. *Developmental & Comparative Immunology* 24(2–3), pp. 187–200. doi: 10.1016/s0145-305x(99)00072-5.

Cook, J.K.A. 1968. Duration of experimental infectious bronchitis in chickens. *Research in Veterinary Science* 9(6), pp. 506–514. doi: 10.1016/s0034-5288(18)34503-x.

Cook, J.K.A., Chesher, J., Baxendale, W., Greenwood, N., Huggins, M.B. and Orbell, S.J. 2001. Protection of chickens against renal damage caused by a nephropathogenic infectious bronchitis virus. *Avian Pathology* 30(4), pp. 423–426. doi: 10.1080/03079450120066421.

Cook, J.K.A., Orbell, S.J., Woods, M.A. and Huggins, M.B. 2010. Breadth of protection of the respiratory tract provided by different live-attenuated infectious bronchitis vaccines against challenge with infectious bronchitis viruses of heterologous serotypes. *Avian Pathology* 28(5), pp. 477–485. doi: 10.1080/03079459994506.

Coria, M.F. 1969. Intracellular avian infectious bronchitis virus: detection by fluorescent antibody techniques in nonavian kidney cell cultures. *Avian Diseases* 13(3), p. 540. doi: 10.2307/1588527.

Coria, M.F. and Ritchie, A.E. 1973. Serial passage of 3 strains of avian infectious bronchitis virus in african green monkey kidney cells (VERO). *Avian Diseases* 17(4), p. 697. doi: 10.2307/1589036.

Corse, E. and Machamer, C.E. 2003. The cytoplasmic tails of infectious bronchitis virus E and M proteins mediate their interaction. *Virology* 312(1), pp. 25–34. doi: 10.1016/s0042-6822(03)00175-2.

Cottam, E.M., Whelband, M.C. and Wileman, T. 2014. Coronavirus NSP6 restricts autophagosome expansion. *Autophagy* 10(8), pp. 1426–1441. doi: 10.4161/auto.29309.

Cumming, R.B. 1970. Studies on Australian Infectious Bronchitis Virus. IV. Apparent farm-to-farm airborne transmission of infectious bronchitis virus. *Avian Diseases* 14(1), p. 191. doi: 10.2307/1588572.

Cunningham, C.H., Spring, M.P. and Nazerian, K. 1972. Replication of avian infectious bronchitis virus in African Green Monkey Kidney Cell Line VERO. *Journal of General Virology* 16(3), pp. 423–427. doi: 10.1099/0022-1317-16-3-423.

Darbyshire, J.H., Rowell, J.G., Cook, J.K.A. and Peters, R.W. 1979. Taxonomic studies on strains of avian infectious bronchitis virus using neutralisation tests in tracheal organ cultures. *Archives of Virology* 61(3), pp. 227–238. doi: 10.1007/bf01318057.

Delmas, B. and Laude, H. 1990. Assembly of coronavirus spike protein into trimers and its role in epitope expression. *Journal of virology* 64(11), pp. 5367–75. doi: 10.1128/jvi.64.11.5367-5375.1990.

Deming, D.J., Graham, R.L., Denison, M.R. and Baric, R.S. 2006. MHV-A59 Orf1a replicase protein NSP7-NSP10 processing in replication. *The Nidoviruses* 581, pp. 101–104. doi: 10.1007/978-0-387-33012-9_17.

Deng, X. et al. 2017. Coronavirus nonstructural protein 15 mediates evasion of dsRNA sensors and limits apoptosis in macrophages. *Proceedings of the National Academy of Sciences* 114(21), pp. E4251–E4260. doi: 10.1073/pnas.1618310114.

Deng, X. et al. 2019. Coronavirus endoribonuclease activity in porcine epidemic diarrhea virus suppresses type I and type III interferon responses. *Journal of Virology* 93(8), pp. e02000-18. doi: 10.1128/jvi.02000-18.

DuBose, R.T. 1967. Adaptation of the Massachusetts strain of infectious bronchitis virus to turkey embryos. *Avian Diseases* 11(1), p. 28. doi: 10.2307/1588324.

Estevez, C., Villegas, P. and El-Attrache, J. 2003. A recombination event, induced *in Ovo*, between a low passage infectious bronchitis virus field isolate and a highly embryo adapted vaccine strain. *Avian Diseases* 47(4), pp. 1282–1290. doi: 10.1637/5919.

Farsang, A., Ros, C., Renström, L.H.M., Baule, C., Soós, T. and Belák, S. 2002. Molecular epizootiology of infectious bronchitis virus in Sweden indicating the involvement of a vaccine strain. *Avian Pathology* 31(3), pp. 229–236. doi: 10.1080/03079450220136530.

Fehr, A.R. et al. 2016. The conserved coronavirus macrodomain promotes virulence and suppresses the innate immune response during severe acute respiratory syndrome coronavirus infection. *mBio* 7(6), pp. e01721-16. doi: 10.1128/mbio.01721-16.

Fehr, A.R. 2019. Bacterial artificial chromosome-based lambda red recombination with the i-scei homing endonuclease for genetic alteration of MERS-CoV. *MERS Coronavirus* 2099, pp. 53–68. doi: 10.1007/978-1-0716-0211-9_5.

Fehr, A.R., Athmer, J., Channappanavar, R., Phillips, J.M., Meyerholz, D.K. and Perlman, S. 2014. The nsp3 macrodomain promotes virulence in mice with coronavirus-induced encephalitis. *Journal of virology* 89(3), pp. 1523–36. doi: 10.1128/jvi.02596-14.

Fischer, F., Stegen, C.F., Masters, P.S. and Samsonoff, W.A. 1998. Analysis of constructed E gene mutants of mouse hepatitis virus confirms a pivotal role for E protein in coronavirus assembly. *Journal of virology* 72(10), pp. 7885–94. doi: 10.1128/jvi.72.10.7885-7894.1998.

Godet, M., L'Haridon, R., Vautherot, J.-F. and Laude, H. 1992. TGEV corona virus ORF4 encodes a membrane protein that is incorporated into virions. *Virology* 188(2), pp. 666–675. doi: 10.1016/0042-6822(92)90521-p.

González, J.M., Gomez-Puertas, P., Cavanagh, D., Gorbalenya, A.E. and Enjuanes, L. 2003. A comparative sequence analysis to revise the current taxonomy of the family Coronaviridae. *Archives of Virology* 148(11), pp. 2207–2235. doi: 10.1007/s00705-003-0162-1.

Gorbalenya, A.E. 2001. Big nidovirus genome. When count and order of domains matter. *Advances in experimental medicine and biology* 494, pp. 1–17.

Gorbalenya, A.E., Koonin, E.V., Donchenko, A.P. and Blinov, V.M. 1989. Coronavirus genome: prediction of putative functional domains in the non-structural polyprotein by comparative amino acid sequence analysis. *Nucleic Acids Research* 17(12), pp. 4847–4861. doi: 10.1093/nar/17.12.4847.

Graepel, K.W., Lu, X., Case, J.B., Sexton, N.R., Smith, E.C. and Denison, M.R. 2017. Proofreading-deficient coronaviruses adapt for increased fitness over long-term passage without reversion of exoribonuclease-inactivating mutations. *mBio* 8(6), pp. e01503-17. doi: 10.1128/mbio.01503-17.

Graham, R.L., Becker, M.M., Eckerle, L.D., Bolles, M., Denison, M.R. and Baric, R.S. 2012. A live, impaired-fidelity coronavirus vaccine protects in an aged, immunocompromised mouse model of lethal disease. *Nature Medicine* 18(12), pp. 1820–1826. doi: 10.1038/nm.2972.

Graham, R.L., Sims, A.C., Brockway, S.M., Baric, R.S. and Denison, M.R. 2005. The nsp2 replicase proteins of murine hepatitis virus and severe acute respiratory syndrome coronavirus are dispensable for viral replication. *Journal of Virology* 79(21), pp. 13399–13411. doi: 10.1128/jvi.79.21.13399-13411.2005.

Haan, C.A.M. de, Haijema, B.J., Boss, D., Heuts, F.W.H. and Rottier, P.J.M. 2005. Coronaviruses as vectors: stability of foreign gene expression. *Journal of virology* 79(20), pp. 12742–51. doi: 10.1128/jvi.79.20.12742-12751.2005.

Haas, J., Park, E.-C. and Seed, B. 1996. Codon usage limitation in the expression of HIV-1 envelope glycoprotein. *Current Biology* 6(3), pp. 315–324. doi: 10.1016/s0960-9822(02)00482-7.

Hagemeijer, M.C., Vonk, A.M., Monastyrska, I., Rottier, P.J.M. and Haan, C.A.M. de 2012. Visualizing coronavirus RNA synthesis in time by using click chemistry. *Journal of virology* 86(10), pp. 5808–16. doi: 10.1128/jvi.07207-11.

Hemert, M.J. van, Worm, S.H.E. van den, Knoops, K., Mommaas, A.M., Gorbalenya, A.E. and Snijder, E.J. 2008. SARS-coronavirus replication/transcription complexes are membrane-protected and need a host factor for activity *in vitro*. *PLoS Pathogens* 4(5), p. e1000054. doi: 10.1371/journal.ppat.1000054.

Hewson, K., Robertson, T., Steer, P., Devlin, J., Noormohammadi, A. and Ignjatovic, J. 2014. Assessment of the potential relationship between egg quality and infectious bronchitis virus

infection in Australian layer flocks. *Australian Veterinary Journal* 92(4), pp. 132–138. doi: 10.1111/avj.12156.

Hodgson, T., Britton, P. and Cavanagh, D. 2005. Neither the RNA nor the proteins of open reading frames 3a and 3b of the coronavirus infectious bronchitis virus are essential for replication. *Journal of virology* 80(1), pp. 296–305. doi: 10.1128/jvi.80.1.296-305.2006.

Hogue, B.G. and Machamer, C.E. 2007. *Nidoviruses*., pp. 179–200. doi: 10.1128/9781555815790.ch12.

Hopkins, S.R. and Yoder, H.W. 1982. Influence of infectious bronchitis strains and vaccines on the incidence of mycoplasma synoviae airsacculitis. *Avian Diseases* 26(4), p. 741. doi: 10.2307/1589860.

Hou, Y., Meulia, T., Gao, X., Saif, L.J. and Wang, Q. 2019. Deletion of both the tyrosine-based endocytosis signal and the endoplasmic reticulum retrieval signal in the cytoplasmic tail of spike protein attenuates porcine epidemic diarrhea virus in pigs. *Journal of Virology* 93(2), pp. e01758-18. doi: 10.1128/jvi.01758-18.

Hurst, K.R., Kuo, L., Koetzner, C.A., Ye, R., Hsue, B. and Masters, P.S. 2005. A major determinant for membrane protein interaction localizes to the carboxy-terminal domain of the mouse coronavirus nucleocapsid protein. *Journal of Virology* 79(21), pp. 13285–13297. doi: 10.1128/jvi.79.21.13285-13297.2005.

Ignjatovic, J., Ashton, D.F., Reece, R., Scott, P. and Hooper, P. 2002. Pathogenicity of australian strains of avian infectious bronchitis virus. *Journal of Comparative Pathology* 126(2–3), pp. 115–123. doi: 10.1053/jcpa.2001.0528.

Ignjatovic, J. and Galli, L. 1994. The S1 glycoprotein but not the N or M proteins of avian infectious bronchitis virus induces protection in vaccinated chickens. *Archives of Virology* 138(1–2), pp. 117–134. doi: 10.1007/bf01310043.

Ignjatovic, J. and McWaters, P.G. 1991. Monoclonal antibodies to three structural proteins of avian infectious bronchitis virus: characterization of epitopes and antigenic differentiation of Australian strains. *Journal of General Virology* 72(12), pp. 2915–2922. doi: 10.1099/0022-1317-72-12-2915.

Jackwood, M.W. 1999. Current and future recombinant viral vaccines for poultry. *Advances in Veterinary Medicine* 41, pp. 517–522. doi: 10.1016/s0065-3519(99)80038-x.

Jackwood, M.W. et al. 2010. Emergence of a group 3 coronavirus through recombination. *Virology* 398(1), pp. 98–108. doi: 10.1016/j.virol.2009.11.044.

Jackwood, M.W., Yousef, N.M. and Hilt, D.A. 1997. Further development and use of a molecular serotype identification test for infectious bronchitis virus. *Avian diseases* 41(1), pp. 105–10.

Jengarn, J., Wongthida, P., Wanasen, N., Frantz, P.N., Wanitchang, A. and Jongkaewwattana, A. 2015. Genetic manipulation of porcine epidemic diarrhoea virus recovered from a full-length infectious cDNA clone. *Journal of General Virology* 96(8), pp. 2206–2218. doi: 10.1099/vir.0.000184.

Jia, W., Karaca, K., Parrish, C.R. and Naqi, S.A. 1995. A novel variant of avian infectious bronchitis virus resulting from recombination among three different strains. *Archives of Virology* 140(2), pp. 259–271. doi: 10.1007/bf01309861.

Jimenez-Guardeño, J.M., Nieto-Torres, J.L., DeDiego, M.L., Regla-Nava, J.A., Fernandez-Delgado, R., Castaño-Rodriguez, C. and Enjuanes, L. 2014. The PDZ-binding motif of severe acute respiratory syndrome coronavirus envelope protein is a determinant of viral pathogenesis. *PLoS Pathogens* 10(8), p. e1004320. doi: 10.1371/journal.ppat.1004320.

Jo, S., Kim, S., Shin, D.H. and Kim, M.-S. 2019. Inhibition of SARS-CoV 3CL protease by flavonoids. *Journal of Enzyme Inhibition and Medicinal Chemistry* 35(1), pp. 145–151. doi: 10.1080/14756366.2019.1690480.

Johnson, M.A., Pooley, C., Ignjatovic, J. and Tyack, S.G. 2003. A recombinant fowl adenovirus expressing the S1 gene of infectious bronchitis virus protects against challenge with infectious bronchitis virus. *Vaccine* 21(21–22), pp. 2730–2736. doi: 10.1016/s0264-410x(03)00227-5.

Jr, J.G., Weisman, Y., Ladman, B.S. and Meir, R. 2005. S1 gene characteristics and efficacy of vaccination against infectious bronchitis virus field isolates from the United States and Israel (1996 to 2000). *Avian Pathology* 34(3), pp. 194–203. doi: 10.1080/03079450500096539.

Klumperman, J., Locker, J.K., Meijer, A., Horzinek, M.C., Geuze, H.J. and Rottier, P.J. 1994. Coronavirus M proteins accumulate in the Golgi complex beyond the site of virion budding. *Journal of Virology* 68(10), pp. 6523–6534. doi: 10.1128/jvi.68.10.6523-6534.1994.

Koch, G., Hartog, L., Kant, A. and Roozelaar, D.J. van 1990. Antigenic domains on the peplomer protein of avian infectious bronchitis virus: correlation with biological functions. *Journal of General Virology* 71(9), pp. 1929–1935. doi: 10.1099/0022-1317-71-9-1929.

Koch, G. and Kant, A. 1990. Nucleotide and amino acid sequence of the S1 subunit of the spike glycoprotein of avian infectious bronchitis virus, strain D3896. *Nucleic Acids Research* 18(10), pp. 3063–3064. doi: 10.1093/nar/18.10.3063.

KOTTIER, S.A., CAVANAGH, D. and BRITTON, P. 1995. Experimental evidence of recombination in coronavirus infectious bronchitis virus. *Virology* 213(2), pp. 569–580. doi: 10.1006/viro.1995.0029.

Kuo, S.-M., Wang, C.-H., Hou, M.-H., Huang, Y.-P., Kao, H.-W. and Su, H.-L. 2010. Evolution of infectious bronchitis virus in Taiwan: Characterisation of RNA recombination in the nucleocapsid gene. *Veterinary Microbiology* 144(3), pp. 293–302. doi: 10.1016/j.vetmic.2010.02.027.

Kusters, J.G., Jager, E.J., Niesters, H.G.M. and Zeijst, B.A.M. van der 1990. Sequence evidence for RNA recombination in field isolates of avian coronavirus infectious bronchitis virus. *Vaccine* 8(6), pp. 605–608. doi: 10.1016/0264-410x(90)90018-h.

L, M., K, M. and DJN, T. 1968. Virology: *Coronaviruses*. *Nature* 220(5168), pp. 650–650. doi: 10.1038/220650b0.

Ladman, B.S., Pope, C.R., Ziegler, A.F., Swieczkowski, T., Callahan, C.J.M., Davison, S. and Gelb, J. 2002. Protection of chickens after live and inactivated virus vaccination against challenge with nephropathogenic infectious bronchitis virus PA/Wolgemuth/98. *Avian diseases* 46(4), pp. 938–44. doi: 10.1637/0005-2086(2002)046[0938:pocala]2.0.co;2.

Lai, M.M.C. and Cavanagh, D. 1997. The molecular biology of coronaviruses. *Advances in Virus Research* 48, pp. 1–100. doi: 10.1016/s0065-3527(08)60286-9.

Lambrechts, C., Pensaert, M. and Ducatelle, R. 1993. Challenge experiments to evaluate cross‐protection induced at the trachea and kidney level by vaccine strains and Belgian nephropathogenic isolates of avian infectious bronchitis virus. *Avian Pathology* 22(3), pp. 577–590. doi: 10.1080/03079459308418945.

Lee, C.-W. and Jackwood, M.W. 2000. Evidence of genetic diversity generated by recombination among avian coronavirus IBV. *Archives of Virology* 145(10), pp. 2135–2148. doi: 10.1007/s007050070044.

Lee, H.J. et al. 2010. Characterization of a novel live attenuated infectious bronchitis virus vaccine candidate derived from a Korean nephropathogenic strain. *Vaccine* 28(16), pp. 2887–2894. doi: 10.1016/j.vaccine.2010.01.062.

Lei, J., Kusov, Y. and Hilgenfeld, R. 2018. Nsp3 of coronaviruses: Structures and functions of a large multi-domain protein. *Antiviral Research* 149, pp. 58–74. doi: 10.1016/j.antiviral.2017.11.001.

Li, H. and Yang, H. 2001. Sequence analysis of nephropathogenic infectious bronchitis virus strains of the Massachusetts genotype in Beijing. *Avian Pathology* 30(5), pp. 535–541. doi: 10.1080/03079450120078734.

Lim, K.P. and Liu, D.X. 2001. The missing link in coronavirus assembly retention of the avian coronavirus infectious bronchitis virus envelope protein in the pre-Golgi compartments and physical interaction between the envelope and membrane proteins. *Journal of Biological Chemistry* 276(20), pp. 17515–17523. doi: 10.1074/jbc.m009731200.

Liu, D.X. and Inglis, S.C. 1991. Association of the infectious bronchitis virus 3c protein with the virion envelope. *Virology* 185(2), pp. 911–917. doi: 10.1016/0042-6822(91)90572-s.

Liu, S. and Kong, X. 2004. A new genotype of nephropathogenic infectious bronchitis virus circulating in vaccinated and non-vaccinated flocks in China. *Avian Pathology* 33(3), pp. 321–327. doi: 10.1080/0307945042000220697.

Lokugamage, K.G., Narayanan, K., Nakagawa, K., Terasaki, K., Ramirez, S.I., Tseng, C.-T.K. and Makino, S. 2015. Middle east respiratory syndrome coronavirus nsp1 inhibits host gene expression by selectively targeting mrnas transcribed in the nucleus while sparing mrnas of cytoplasmic origin. *Journal of virology* 89(21), pp. 10970–81. doi: 10.1128/jvi.01352-15.

Lukert, P.D. 1965. Comparative sensitivities of embryonating chicken's eggs and primary chicken embryo kidney and liver cell cultures to infectious bronchitis virus. *Avian Diseases* 9(2), p. 308. doi: 10.2307/1588016.

Lukert, P.D. 1966. Immunofluorescence of avian infectious bronchitis virus in primary chicken embryo kidney, liver, lung, and fibroblast cell cultures. *Archiv für die gesamte Virusforschung* 19(3), pp. 265–272. doi: 10.1007/bf01241849.

Luo, Z. and Weiss, S.R. 1998. Roles in cell-to-cell fusion of two conserved hydrophobic regions in the murine coronavirus spike protein. *Virology* 244(2), pp. 483–494. doi: 10.1006/viro.1998.9121.

Lv, C. et al. 2020. Construction of an infectious bronchitis virus vaccine strain carrying chimeric S1 gene of a virulent isolate and its pathogenicity analysis. *Applied Microbiology and Biotechnology* 104(19), pp. 8427–8437. doi: 10.1007/s00253-020-10834-2.

Machamer, C.E., Mentone, S.A., Rose, J.K. and Farquhar, M.G. 1990. The E1 glycoprotein of an avian coronavirus is targeted to the cis Golgi complex. *Proceedings of the National Academy of Sciences* 87(18), pp. 6944–6948. doi: 10.1073/pnas.87.18.6944.

Maeda, J., Maeda, A. and Makino, S. 1999. Release of coronavirus e protein in membrane vesicles from virus-infected cells and e protein-expressing cells. *Virology* 263(2), pp. 265–272. doi: 10.1006/viro.1999.9955.

Maier, H.J. et al. 2013. Infectious bronchitis virus generates spherules from zippered endoplasmic reticulum membranes. *mBio* 4(5), pp. e00801-13. doi: 10.1128/mbio.00801-13.

Mardani, K., Noormohammadi, A.H., Ignjatovic, J. and Browning, G.F. 2010. Naturally occurring recombination between distant strains of infectious bronchitis virus. *Archives of Virology* 155(10), pp. 1581–1586. doi: 10.1007/s00705-010-0731-z.

Masters, P.S. 1999. Reverse Genetics of The Largest RNA Viruses. *Advances in Virus Research* 53, pp. 245–264. doi: 10.1016/s0065-3527(08)60351-6.

Masters, P.S. and Rottier, P.J.M. 2005. Coronavirus reverse genetics by targeted rna recombination. *Coronavirus Replication and Reverse Genetics* 287, pp. 133–159. doi: 10.1007/3-540-26765-4_5.

McKinley, E.T., Hilt, D.A. and Jackwood, M.W. 2008. Avian coronavirus infectious bronchitis attenuated live vaccines undergo selection of subpopulations and mutations following vaccination. *Vaccine* 26(10), pp. 1274–1284. doi: 10.1016/j.vaccine.2008.01.006.

Mielech, A.M. et al. 2015. Murine coronavirus ubiquitin-like domain is important for papain-like protease stability and viral pathogenesis. *Journal of virology* 89(9), pp. 4907–17. doi: 10.1128/jvi.00338-15.

Mo, M. et al. 2012. Complete genome sequences of two chinese virulent avian coronavirus infectious bronchitis virus variants. *Journal of Virology* 86(19), pp. 10903–10904. doi: 10.1128/jvi.01895-12.

Muneer, M.A., Newman, J.A., Halvorson, D.A., Sivanandan, V. and Coon, C.N. 1987. Effects of avian infectious bronchitis virus (arkansas strain) on vaccinated laying chickens. *Avian Diseases* 31(4), p. 820. doi: 10.2307/1591038.

Pasternak, A.O., Spaan, W.J.M. and Snijder, E.J. 2006. Nidovirus transcription: how to make sense...? *The Journal of general virology* 87(Pt 6), pp. 1403–1421. doi: 10.1099/vir.0.81611-0.

Patterson, S. and Bingham, R.W. 1976. Electron microscope observations on the entry of avian infectious bronchitis virus into susceptible cells. *Archives of Virology* 52(3), pp. 191–200. doi: 10.1007/bf01348016.

Polo, S., Ketner, G., Levis, R. and Falgout, B. 1997. Infectious RNA transcripts from full-length dengue virus type 2 cDNA clones made in yeast. *Journal of virology* 71(7), pp. 5366–74. doi: 10.1128/jvi.71.7.5366-5374.1997.

Raj, G.D. and Jones, R.C. 2007. Infectious bronchitis virus: Immunopathogenesis of infection in the chicken. *Avian Pathology* 26(4), pp. 677–706. doi: 10.1080/03079459708419246.

Rice, C.M., Levis, R., Strauss, J.H. and Huang, H.V. 1987. Production of infectious RNA transcripts from Sindbis virus cDNA clones: mapping of lethal mutations, rescue of a temperature-sensitive marker, and in vitro mutagenesis to generate defined mutants. *Journal of virology* 61(12), pp. 3809–19. doi: 10.1128/jvi.61.12.3809-3819.1987.

Sakai, Y., Kawachi, K., Terada, Y., Omori, H., Matsuura, Y. and Kamitani, W. 2017. Two-amino acids change in the nsp4 of SARS coronavirus abolishes viral replication. *Virology* 510, pp. 165–174. doi: 10.1016/j.virol.2017.07.019.

Sawicki, S.G., Sawicki, D.L. and Siddell, S.G. 2007. A Contemporary View of Coronavirus Transcription. *Journal of Virology* 81(1), pp. 20–29. doi: 10.1128/jvi.01358-06.

Schalk, A.F. 1931. An apparently new respiratory disease of baby chicks. *J. Am. Vet. Med. Assoc.* 78, pp. 413–423.

Schultze, B., Cavanagh, D. and Herrler, G. 1992. Neuraminidase treatment of avian infectious bronchitis coronavirus reveals a hemagglutinating activity that is dependent on sialic acid-containing receptors on erythrocytes. *Virology* 189(2), pp. 792–794. doi: 10.1016/0042-6822(92)90608-r.

Scobey, T. et al. 2013. Reverse genetics with a full-length infectious cDNA of the Middle East respiratory syndrome coronavirus. *Proceedings of the National Academy of Sciences* 110(40), pp. 16157–16162. doi: 10.1073/pnas.1311542110.

Senanayake, S.D. and Brian, D.A. 1999. Translation from the 5′ Untranslated Region (UTR) of mRNA 1 Is Repressed, but That from the 5′ UTR of mRNA 7 Is Stimulated in Coronavirus-Infected Cells. *Journal of Virology* 73(10), pp. 8003–8009. doi: 10.1128/jvi.73.10.8003-8009.1999.

Seo, S.H. and Collisson, E.W. 1997. Specific cytotoxic T lymphocytes are involved in in vivo clearance of infectious bronchitis virus. *Journal of virology* 71(7), pp. 5173–7. doi: 10.1128/jvi.71.7.5173-5177.1997.

Sevoian, M. and Levine, P.P. 1957. Effects of infectious bronchitis on the reproductive tracts, egg production, and egg quality of laying chickens. *Avian Diseases* 1(2), p. 136. doi: 10.2307/1587727.

Shen, H., Fang, S.G., Chen, B., Chen, G., Tay, F.P.L. and Liu, D.X. 2009. Towards construction of viral vectors based on avian coronavirus infectious bronchitis virus for gene delivery and vaccine development. *Journal of Virological Methods* 160(1–2), pp. 48–56. doi: 10.1016/j.jviromet.2009.04.023.

Shen, Z. et al. 2017. Structural basis for the inhibition of host gene expression by porcine epidemic diarrhea virus nsp1. *Journal of virology* 92(5). doi: 10.1128/jvi.01896-17.

Shen, Z. et al. 2019. A conserved region of nonstructural protein 1 from alphacoronaviruses inhibits host gene expression and is critical for viral virulence. *Journal of Biological Chemistry* 294(37), pp. 13606–13618. doi: 10.1074/jbc.ra119.009713.

Smith, A.R., Boursnell, M.E.G., Binns, M.M., Brown, T.D.K. and Inglis, S.C. 1990. Identification of a new membrane-associated polypeptide specified by the coronavirus infectious bronchitis virus. *Journal of General Virology* 71(1), pp. 3–11. doi: 10.1099/0022-1317-71-1-3.

Smith, E.C., Case, J.B., Blanc, H., Isakov, O., Shomron, N., Vignuzzi, M. and Denison, M.R. 2015. Mutations in coronavirus nonstructural protein 10 decrease virus replication fidelity. *Journal of Virology* 89(12), pp. 6418–6426. doi: 10.1128/jvi.00110-15.

Snijder, E.J. et al. 2020. A unifying structural and functional model of the coronavirus replication organelle: Tracking down RNA synthesis. *PLoS Biology* 18(6), p. e3000715. doi: 10.1371/journal.pbio.3000715.

Sparks, J.S., Lu, X. and Denison, M.R. 2007. Genetic analysis of Murine hepatitis virus nsp4 in virus replication. *Journal of virology* 81(22), pp. 12554–63. doi: 10.1128/jvi.01257-07.

Tan, B., Wang, H., Shang, L. and Yang, T. 2009. Coadministration of chicken GM-CSF with a DNA vaccine expressing infectious bronchitis virus (IBV) S1 glycoprotein enhances the specific immune response and protects against IBV infection. *Archives of Virology* 154(7), pp. 1117–1124. doi: 10.1007/s00705-009-0424-7.

Tang, M., Wang, H., Zhou, S. and Tian, G. 2008. Enhancement of the immunogenicity of an infectious bronchitis virus DNA vaccine by a bicistronic plasmid encoding nucleocapsid protein and interleukin-2. *Journal of Virological Methods* 149(1), pp. 42–48. doi: 10.1016/j.jviromet.2008.01.017.

Tarpey, I. et al. 2006. Safety and efficacy of an infectious bronchitis virus used for chicken embryo vaccination. *Vaccine* 24(47), pp. 6830–6838. doi: 10.1016/j.vaccine.2006.06.040.

Thao, T.T.N. et al. 2020. Rapid reconstruction of SARS-CoV-2 using a synthetic genomics platform. *Nature* 582(7813), pp. 561–565. doi: 10.1038/s41586-020-2294-9.

Thiel, V., Herold, J., Schelle, B. and Siddell, S.G. 2001. Infectious RNA transcribed in vitro from a cDNA copy of the human coronavirus genome cloned in vaccinia virus. *Journal of General Virology* 82(6), pp. 1273–1281. doi: 10.1099/0022-1317-82-6-1273.

Thor, S.W., Hilt, D.A., Kissinger, J.C., Paterson, A.H. and Jackwood, M.W. 2011. Recombination in avian gamma-coronavirus infectious bronchitis virus. *Viruses* 3(9), pp. 1777–1799. doi: 10.3390/v3091777.

Tischer, B.K., Smith, G.A. and Osterrieder, N. 2010. En passant mutagenesis: a two step markerless red recombination system. *Methods in molecular biology (Clifton, N.J.)* 634, pp. 421–30. doi: 10.1007/978-1-60761-652-8_30.

Tomar, S. et al. 2015. Ligand-induced dimerization of middle east respiratory syndrome (MERS) coronavirus nsp5 protease (3CLpro) implications for nsp5 regulation and the development of antivirals. *Journal of Biological Chemistry* 290(32), pp. 19403–19422. doi: 10.1074/jbc.m115.651463.

Toro, H., Zhao, W., Breedlove, C., Zhang, Z., Santen, V. van and Yu, Q. 2014. Infectious bronchitis virus S2 expressed from recombinant virus confers broad protection against challenge. *Avian Diseases* 58(1), pp. 83–89. doi: 10.1637/10641-081613-reg.1.

Tseng, Y.-T., Wang, S.-M., Huang, K.-J., Lee, A.I.-R., Chiang, C.-C. and Wang, C.-T. 2010. Self-assembly of severe acute respiratory syndrome coronavirus membrane protein. *The Journal of Biological Chemistry* 285(17), pp. 12862–12872. doi: 10.1074/jbc.m109.030270.

Vagnozzi, A., Garca, M., Riblet, S.M. and Zavala, G. 2010. Protection induced by infectious laryngotracheitis virus vaccines alone and combined with Newcastle disease virus and/or infectious bronchitis virus vaccines. *Avian Diseases* 54(4), pp. 1210–1219. doi: 10.1637/9362-040710-reg.1.

Vennema, H., Godeke, G.J., Rossen, J.W., Voorhout, W.F., Horzinek, M.C., Opstelten, D.J. and Rottier, P.J. 1996. Nucleocapsid‐independent assembly of coronavirus‐like particles by co‐expression of viral envelope protein genes. *The EMBO Journal* 15(8), pp. 2020–2028. doi: 10.1002/j.1460-2075.1996.tb00553.x.

Wang, D. et al. 2015. Porcine epidemic diarrhea virus 3c-like protease regulates its interferon antagonism by cleaving NEMO. *Journal of virology* 90(4), pp. 2090–101. doi: 10.1128/jvi.02514-15.

Wang, L. et al. 2018. Porcine transmissible gastroenteritis virus nonstructural protein 2 contributes to inflammation via NF-κB activation. *Virulence* 9(1), pp. 1685–1698. doi: 10.1080/21505594.2018.1536632.

Wang, L., Junker, D. and Collisson, E.W. 1993. Evidence of natural recombination within the s1 gens of infectious bronchitis virus. *Virology* 192(2), pp. 710–716. doi: 10.1006/viro.1993.1093.

Wang, L., Xu, Y. and Collisson, E.W. 1997. Experimental confirmation of recombination upstream of the S1 hypervariable region of infectious bronchitis virus. *Virus Research* 49(2), pp. 139–145. doi: 10.1016/s0168-1702(97)01466-4.

Wang, Y. et al. 2019. Porcine transmissible gastroenteritis virus inhibits NF-κB activity via nonstructural protein 3 to evade host immune system. *Virology Journal* 16(1), p. 97. doi: 10.1186/s12985-019-1206-9.

Wit, J.J. (Sjaak) de, Cook, J.K.A. and Heijden, H.M.J.F. van der 2011. Infectious bronchitis virus variants: a review of the history, current situation and control measures. *Avian Pathology* 40(3), pp. 223–235. doi: 10.1080/03079457.2011.566260.

Yamshchikov, V., Mishin, V. and Cominelli, F. 2001. A new strategy in design of (+)rna virus infectious clones enabling their stable propagation in *E. coli*. *Virology* 281(2), pp. 272–280. doi: 10.1006/viro.2000.0793.

YANG, T. et al. 2009. The protective immune response against infectious bronchitis virus induced by multi-epitope based peptide vaccines. *Bioscience, Biotechnology, and Biochemistry* 73(7), pp. 1500–1504. doi: 10.1271/bbb.80864.

Yong, C.Y., Ong, H.K., Yeap, S.K., Ho, K.L. and Tan, W.S. 2019. Recent advances in the vaccine development against middle east respiratory syndrome-coronavirus. *Frontiers in Microbiology* 10, p. 1781. doi: 10.3389/fmicb.2019.01781.

Youn, S., Leibowitz, J.L. and Collisson, E.W. 2005. In vitro assembled, recombinant infectious bronchitis viruses demonstrate that the 5a open reading frame is not essential for replication. *Virology* 332(1), pp. 206–215. doi: 10.1016/j.virol.2004.10.045.

Yount, B., Curtis, K.M. and Baric, R.S. 2000. Strategy for systematic assembly of large RNA and DNA genomes: transmissible gastroenteritis virus model. *Journal of Virology* 74(22), pp. 10600–10611. doi: 10.1128/jvi.74.22.10600-10611.2000.

Zelus, B.D., Schickli, J.H., Blau, D.M., Weiss, S.R. and Holmes, K.V. 2003. Conformational changes in the Spike glycoprotein of murine coronavirus are induced at 37°C either by soluble murine CEACAM1 receptors or by pH 8. *Journal of Virology* 77(2), pp. 830–840. doi: 10.1128/jvi.77.2.830-840.2003.

Zhang, Q., Shi, K. and Yoo, D. 2016. Suppression of type I interferon production by porcine epidemic diarrhea virus and degradation of CREB-binding protein by nsp1. *Virology* 489, pp. 252–268. doi: 10.1016/j.virol.2015.12.010.

Zhang, R. et al. 2015. The nsp1, nsp13, and M proteins contribute to the hepatotropism of murine coronavirus JHM.WU. *Journal of Virology* 89(7), pp. 3598–3609. doi: 10.1128/jvi.03535-14.

Zhou, Y.S. et al. 2013. Establishment of reverse genetics system for infectious bronchitis virus attenuated vaccine strain H120. *Veterinary Microbiology* 162(1), pp. 53–61. doi: 10.1016/j.vetmic.2012.08.013.

Zhu, X. et al. 2017. Porcine Deltacoronavirus nsp5 antagonizes type I interferon signaling by cleaving STAT2. *Journal of Virology* 91(10). doi: 10.1128/jvi.00003-17.

Ziebuhr, J., Snijder, E.J. and Gorbalenya, A.E. 2000. Virus-encoded proteinases and proteolytic processing in the *Nidovirales*. *Journal of General Virology* 81(4), pp. 853–879. doi: 10.1099/0022-1317-81-4-853.

Publications

Xing, N., Wang, Z., Wang, J., Nascimiento, M., Jongkaewwattana, A., Trimpert, J., Osterrieder, N., Kunec, D. *Engineering and characterization of Avian coronavirus mutants expressing fluorescent reporter proteins from the replicase gene*. Journal of Virology. 2022

Na Xing., Thomas Höfler., Mariana Nascimento., Georgina Camps Paradell., Dino P. McMahon., Dusan Kunec., Nikolaus Osterrieder., Hans H. Cheng., Cari Hearn., Jakob Trimpert. *Fast forwarding evolution - Accelerated adaptation in a proofreading deficient hypermutator herpesvirus*. Virus Evolution. 2022

Lin, X., Fu, B., Xiong, Y., **Xing, N**., Xue, W., Guo, D., Zaky, M.Y., Pavani, K.C., Kunec, D., and Trimpert, J.J.b. *Unconventional secretion of unglycosylated ORF8 is critical for the cytokine storm during SARS-CoV-2 infection.* (Under review)

Shytaj, I.L., Fares, M., Gallucci, L., Lucic, B., Tolba, M.M., Zimmermann, L., Adler, J.M., **Xing, N.,** Bushe, J., and Gruber, A.D.J.M. *The FDA-Approved drug Cobicistat synergizes with Remdesivir to inhibit SARS-CoV-2 replication in Vitro and decreases viral titers and disease progression in syrian hamsters.* mBio. 2022. 13(2): e0370521.

Wu, H., **Xing, N**., Meng, K., Fu, B., Xue, W., Dong, P., Tang, W., Xiao, Y., Liu, G., Luo, H.J.C.h., et al. *Nucleocapsid mutations R203K/G204R increase the infectivity, fitness, and virulence of SARS-CoV-2.* Cell Host & Microbe. 2021. 29 (12):1788-1801.e6.

Yang, J., Lin, X., **Xing, N.,** Zhang, Z., Zhang, H., Wu, H., Xue, W. *Structure-based discovery of novel nonpeptide inhibitors targeting SARS-CoV-2 M^{pro}.* Journal of Chemical Information and Modeling. 2021. 61(8):3917-3926.

Lin, X., Fu, B., Yin, S., Li, Z., Liu, H., Zhang, H., **Xing, N.,** Wang, Y., Xue, W., and Xiong, Y.J.I. *ORF8 contributes to cytokine storm during SARS-CoV-2 infection by activating IL-17 pathway*. iScience. 2021. 24(4):102293.

Acknowledgements

First and foremost, I would like to thank my supervisor, Prof. Dr. Nikolaus Osterrieder, who gave me the opportunity to work in his lab. Through my PhD, he always gave me precious suggestions and guidance. I learned a lot from him, not only his knowledge but also his rigorous attitude towards science. Without his help, the completion of this thesis would not have been possible.

I would like to express my deep gratitude to Dr. Dusan Kunec, who is always there when I have problems with my research. At the early stage of my PhD, my project did not make any progress. I felt really bad about myself and even thought of giving up, but he always encouraged me and continuously supported me with valuable advice and discussions. He is a man full of wisdom and humor, and the experience of working with him will become the most precious asset of my life.

I also want to thank Prof. Dr. Benedikt Kaufer and Prof. Dr. Michael Viet for their valuable and constructive suggestions during the course of my PhD program at FU.

I greatly appreciate the help from all the members of the Institute of Virology. Special thanks to Dr. Jakob Trimpert for his help and guidance during my PhD study. Thanks to our technician, Mrs. Annett Neubert, not only for her assistance in the lab but also for the positive energy and happiness she brings to us. Thanks to Dr. Nicole Groenke and Mariana Nascimento for help with NGS sequencing. Thanks to Thomas, Daria, Julia, Renato, the secretary Kia, and some others.

I am particularly grateful to my Chinese friends who have been with me as family members during these years: Bodan, De, Minze, Xiaorong, Xu, Xuejiao, and Yu.

Most importantly, I would like to express my sincere gratitude to my parents for their endless love and unconditional support. Particularly, my heartfelt gratitude goes to my beloved husband, Congkai, for his accompaniment, support, encouragement, and understanding. The unforgettable moment of my life is the birth of our daughter Muyao Claire, who brings me lots of happiness and luck. I am happy that my husband can take my hands and spend the rest of his life with me, witnessing the growth of our daughter together.

Last but not least, I am grateful to the China Scholarship Council (CSC) for the financial support.

Finanzierungsquellen

Die Arbeiten wurden finanziell unterstützt durch CSC Stipendium.

Interessenskonflikte

Im Rahmen dieser Arbeit bestehen keine Interessenskonflikte durch Zuwendungen Dritter.

Selbständigkeitserklärung

Hiermit bestätige ich, dass ich die vorliegende Arbeit selbständig angefertigt habe. Ich versichere, dass ich ausschließlich die angegebenen Quellen und Hilfen Anspruch genommen habe.

Berlin, am 21.11.2022

Na Xing